Iowa Research Online
The University of Iowa's Institutional Repository

University of Iowa
Iowa Research Online

Theses and Dissertations

2010

Functional analysis of an alternative Replication Protein A complex containing RPA4

Aaron Charles Mason
University of Iowa

Copyright 2010 Aaron Charles Mason

This dissertation is available at Iowa Research Online: http://ir.uiowa.edu/etd/1020

Recommended Citation

Mason, Aaron Charles. "Functional analysis of an alternative Replication Protein A complex containing RPA4." PhD (Doctor of Philosophy) thesis, University of Iowa, 2010.
http://ir.uiowa.edu/etd/1020.

Follow this and additional works at: http://ir.uiowa.edu/etd

Part of the Biochemistry Commons

FUNCTIONAL ANALYSIS OF AN ALTERNATIVE REPLICATION PROTEIN A COMPLEX CONTAINING RPA4

by

Aaron Charles Mason

An Abstract

Of a thesis submitted in partial fulfillment
of the requirements for the Doctor of
Philosophy degree in Biochemistry
in the Graduate College of
The University of Iowa

May 2010

Thesis Supervisor: Professor Marc S. Wold

ABSTRACT

Replication Protein A (RPA), the eukaryotic single-stranded DNA-binding complex, is essential for multiple processes in cellular DNA metabolism including, but not limited to, DNA replication, DNA repair and recombination. The 'canonical' RPA is composed of three subunits (RPA1, RPA2, and RPA3). In addition to the three canonical subunits, there is a human homolog to the RPA2 subunit, termed RPA4, which can substitute for RPA2 in complex formation. The resulting RPA complex has been termed 'alternative' RPA (aRPA). The normal function of aRPA is not known; however, previous studies have shown that it does not support S-phase progression *in vivo*. The goal of this thesis was to characterize the function of aRPA in DNA replication, DNA repair and recombination and profile its expression in human tissues.

The studies presented in this thesis show that the aRPA complex has solution and DNA binding properties indistinguishable from the canonical RPA complex as determined by gel mobility shift assays. However, aRPA was unable to support DNA replication and inhibited canonical RPA function in a cell-free simian virus 40 system. aRPA inhibited both initiation and elongation of DNA synthesis in the SV40 system. Two regions of RPA4, the putative L34 loop and the C-terminal winged helix domain, were responsible for inhibiting SV40 DNA replication.

The mechanism of SV40 DNA replication inhibition during initiation and elongation was characterized using assays for DNA polymerase α and DNA polymerase δ. aRPA was shown to have reduced interaction with DNA polymerase α and was not able to efficiently stimulate DNA synthesis by DNA polymerase α on aRPA coated single-stranded DNA. However, aRPA stimulated DNA synthesis by DNA polymerase δ in the presence of PCNA and RFC even though a reduced interaction was observed between aRPA and polymerase δ.

The role of aRPA in DNA repair was also investigated. aRPA interacted with both Rad52 and Rad51 but had a reduced interaction with Rad51. However, aRPA was still able to stimulate Rad51-dependent strand exchange. aRPA also supported the dual incision/excision reaction of nucleotide excision repair. aRPA was less efficient in nucleotide excision repair than canonical RPA and this reduction was attributed to reduced interactions with the repair factor XPA. In contrast, aRPA exhibited higher affinity for damaged DNA than canonical RPA.

The expression of *RPA4* and *RPA2* was determined by quantitative PCR in established cell lines, human normal tissues and human tumor tissue. *RPA4* was shown to be expressed in all normal tissues examined but the level of expression was tissue specific. Additionally, *RPA4* expression was decreased in all tumor tissues examined and was at the limit of detection in established cell lines. Taken together, the results presented in this thesis suggest that aRPA is a 'non-proliferative' form of RPA that functions to maintain the genomic stability of non-dividing cells.

Abstract Approved: ______________________________
Thesis Supervisor

____
Title and Department

____
Date

FUNCTIONAL ANALYSIS OF AN ALTERNATIVE REPLICATION PROTEIN A COMPLEX CONTAINING RPA4

by

Aaron Charles Mason

A thesis submitted in partial fulfillment
of the requirements for the Doctor of
Philosophy degree in Biochemistry
in the Graduate College of
The University of Iowa

May 2010

Thesis Supervisor: Professor Marc S. Wold

Graduate College
The University of Iowa
Iowa City, Iowa

CERTIFICATE OF APPROVAL

PH.D. THESIS

This is to certify that the Ph.D. thesis of

Aaron Charles Mason

has been approved by the Examining Committee
for the thesis requirement for the Doctor of Philosophy
degree in Biochemistry at the May 2010 graduation.

Thesis Committee: ______________________________
Adrian Elcock, Thesis Chair

____
Kris A. DeMali

____
M. Todd Washington

____
Daniel L. Weeks

____
Amnon Kohen

To my wife and son

ACKNOWLEDGMENTS

This thesis would not have been possible without the support of many people. I am grateful to my thesis advisor, Dr. Marc S. Wold. He has given me encouragement, supervision and support from my first days working in his lab as an undergraduate to my final days as a graduate student. Personally, I am grateful to Marc for his support and understanding during the two months my son spent in the hospital. He made a difficult situation easier to handle. I would like to thank members of Wold Lab for their useful discussions and critical interpretation of data. I am also grateful for the lab of Dr. Todd Washington for their thoughtful discussion during joint lab meetings and allowing me use of their equipment.

I would also like to thank many labs for their willingness to collaborate and provide reagents. I am grateful to Dr. Aziz Sancar and Dr. Mike Kemp (University of North Carolina), Dr. Daniel Simmons (University of Delaware), Dr. Gloria Borgstahl (University of Nebraska Medical Center), Dr. Stephen Kowalczkowski (University of California, Davis), Dr. Yoshihiro Matsumoto (Fox Chase Cancer Center) and Dr. Yuli Masuda (Hiroshime University).

Last but not least, I would like express my love and gratitude to my family for their understanding and endless love. Nothing makes the thoughts of a bad experiment disappear quicker than a hug from your wife and son.

TABLE OF CONTENTS

LIST OF TABLES vii

LIST OF FIGURES viii

LIST OF ABBREVIATIONS x

CHAPTER 1 INTRODUCTION 1

- General RPA Background 1
    - Structure 2
    - Interactions with ssDNA 3
    - Protein-protein Interactions 4
- RPA in Replication 5
- RPA in Recombination 6
- RPA in DNA Repair 7
- RPA in DNA Damage Response 9
- RPA4 and the alternative RPA complex 10
- Outline 13

CHAPTER 2 AN ALTERNATIVE FORM OF REPLICATION PROTEIN A PREVENTS VIRAL REPLICATION IN VITRO 24

- Abstract 24
- Introduction 24
- Materials and Methods 25
    - Materials 25
    - Construction of aRPA and aRPA Hybrid Expression Plasmids 25
    - Protein Expression and Purification 26
    - Trimer Formation 26
    - DNA Binding Assays 26
    - SV40 Replication and Elongation Assays 27
- Results 28
    - RPA4 Forms a Stable, Functional ssDNA-Binding Complex 28
    - aRPA Function in SV40 Replication 31
    - Mechanism of aRPA Inhibition of SV40 Replication 33
    - Structural Basis of RPA4 Inhibition 35
    - Construction of a Dominant Negative Form of RPA2 36
- Discussion 37

CHAPTER 3 AN ALTERNATIVE FORM OF RPA EXPRESSED IN NORMAL HUMAN TISSUES SUPPORTS DNA REPAIR 55

- Abstract 55
- Introduction 55
- Materials and Methods 57
    - Protein Purification 57
    - Quantitative PCR 57
    - Enzyme-Linked Immunosorbent Assay (ELISA) 58
    - Excision Repair Assay 58
    - Immunoblotting 59

DNA Strand Exchange Assay 59
Results..60
RPA4 mRNA is Found in Normal Human Tissues 60
aRPA Supports Rad51 Dependent Strand Exchange 61
aRPA Substitutes for RPA in Nucleotide Excision Repair 62
aRPA Does Not Stably Bind XPA 64
Other Functions of aRPA in Nucleotide Excision Repair.......................65
Discussion..66

CHAPTER 4 FUNCTIONS OF ALTERNATIVE REPLICATION PROTEIN A IN INITIATION AND ELONGATION...80

Abstract...80
Introduction..80
Experimental Procedures..83
Plasmids...83
Protein Purification...83
Enzyme-Linked Immunosorbent Assay 85
Pol α Extension Assay..86
Pol δ Extension on Singly Primed ssM13mp18 Assay 87
Results..87
Effect of aRPA on pol α...87
Mechanism of pol α Inhibition by aRPA...90
Effect of aRPA on the Synthesis of RNA-DNA Primers.........................91
Effect of aRPA on pol δ DNA synthesis 91
Discussion..93

CHAPTER 5 SUMMARY AND PERSPECTIVE.......................................113

Summary...113
Perspective..114
Replication...115
DNA Repair...118
Regulation by Phosphorylation 119
Therapeutic Potential...121
RPA4 Evolution...122

APPENDIX A DEFINING CONFORMATIONAL CHANGES OF RPA AFTER PHOSPHORYLATION OF THE N-TERMINUS OF RPA2 129

Introduction..129
Materials and Methods 130
Materials..130
Plasmids...130
ReAsH and FlAsH Protein Labeling 130
Fluorescence Resonance Energy Transfer Assay.................................131
Protein Expression and Purification 131
Nuclear Magneict Resonance Spectroscopy 131
Results..132
Discussion..136

APPENDIX B DEFINING THE DOMAINS OF RPA THAT INTERACT WITH DIFFERENT DNA STRUCTURES FOUND IN ESSENTIAL CELLULAR PROCESSES 164

Introduction...164
Materials and Methods 165
    DNA Substrates 165
    Protein...165
    Fluorescence Assay 166
    Photochemical Crosslinking Assay 166
    Factor X_a Digestion 166
    Matrix Assisted Laser Desorption Ionization Time of Flight 167
    Liquid Chromatography – Tandem Mass Spectroscopy 167
Results...167
Discussion...169

REFERENCES 184

LIST OF TABLES

Table 3-1: Source of FirstChoice® Total Human RNA used for quantitative PCR..........70

Table A-1: Nomenclature of RPA proteins with FlAsH/ReAsH recognition sequence. 137

LIST OF FIGURES

Figure 1-1: Schematic of structural and functional domains of RPA and aRPA..............14

Figure 1-2: Structure of RPA high-affinity DNA-binding domains. 16

Figure 1-3: Proteins known to interact with RPA. 18

Figure 1-4: Schematic representation of RPA function in different cellular processes. 20

Figure 1-5: Alignment of human RPA2 and RPA4 from five mammalian species...........22

Figure 2-1: Properties of aRPA complex. 41

Figure 2-2: Trimer Formation. 43

Figure 2-3: Structural Models of RPA2 and RPA4. 45

Figure 2-4: DNA binding properties of RPA complexes. 47

Figure 2-5: SV40 DNA replication with various forms of RPA.......................................49

Figure 2-6: Function in elongation and Tag interactions. 51

Figure 2-7: Schematic showing observed properties for RPA2, RPA4 and RPA2 hybrids. 53

Figure 3-1: Quantitative PCR of *RPA4* and *RPA2* mRNA from different tissues. 72

Figure 3-2: aRPA interacts with Rad51 and Rad52 and stimulates strand exchange. 74

Figure 3-3: aRPA supports nucleotide excision repair. 76

Figure 3-4: aRPA has altered interactions with XPA. 78

Figure 4-1: The effect of RPA and aRPA on pol α when polymerase is pre-mixed with the DNA substrate. 97

Figure 4-2: The effect on pol α when either RPA or aRPA are pre-bound to the DNA substrate. 99

Figure 4-3: Titration of RPA and aRPA in pol α extension assay. 101

Figure 4-4: Interactions with replication proteins. 103

Figure 4-5: Mechanism of pol α inhibition. 105

Figure 4-6: RPA2-RPA4 hybrids in pol α extension assays. 107

Figure 4-7: Pol δ synthesis on singly-primed single-stranded M13mp18 template. 109

Figure 4-8: Salt dependence of pol δ activity. 111

Figure 5-1: Effects of RPA/aRPA/hSSB1/*E. coli* SSB on TopBP1-dependent activation of ATR kinase activity in the presence of ssDNA...................125

Figure 5-2: Predicted sites of RPA2 and RPA4 phosphorylation..................................127

Figure A-1: Detection of FlAsH labeled RPA1 and RPA2 subunits. 138

Figure A-2: FRET analysis of heterolabeled RPA mutants in cell lysates. 140

Figure A-3: Detection of purified RPA mutants labeled with FlAsH.............................142

Figure A-4: FRET analysis of purified RPA mutants..144

Figure A-5: Proteolysis of RPA does not decrease subunit interactions. 146

Figure A-6: Inter-molecular interactions between the phosphorylation mimetic, phosphorylation domain and DBDs of RPA1. 148

Figure A-7: Purified RPA2/3 and RPA-FAB. 150

Figure A-8: HSQC of ^{15}N labeled RPA2/3. 152

Figure A-9: HSQC of ^{15}N labeled RPA2/3Asp. 154

Figure A-10: Overlay of RPA2/3 and RPA2/3Asp HSPC spectra. 156

Figure A-11: DBD F causes peaks shifts in a distinct region of the RPA2/3Asp HSQC spectra. 158

Figure A-12: TROSY spectrum of ^{15}N labeled RPA-FAB. 160

Figure A-13: Changes in TROSY spectra of RPA-FAB caused by phosphorylation mimetic peptide. 162

Figure B-1: DNA substrates..170

Figure B-2: RPA dependent changes in 2-AP fluorescence. 172

Figure B-3: Factor X_a digestion of RPA-X_a..174

Figure B-4: Photochemical crosslinking of RPA to ssDNA..176

Figure B-5: Photochemical crosslinking of RPA to partially duplex DNA substrates. 178

Figure B-6: MALDI-TOF MS analysis of RPA-X_a..180

Figure B-7: MALDI-TOF MS analysis of RPA-X_a crosslinked to DNA. 182

LIST OF ABBREVIATIONS

aRPA	alternative RPA
AS-Ex	ammonium sulfate-fractionated extract
ATM	ataxia telangiectasia mutated
ATR	ataxia telangiectasia mutated and Rad3 related
BER	Base Excision Repair
BSA	Bovine Serum Albumin
Cdk2	cyclin dependent kinase 2
CHK1	checkpoint kinase-1
CHK2	checkpoint kinase-2
CMG	Cdc45, MCM2-7, GINS
DBD	DNA binding domain
dCTP	Deoxycytidine Triphosphate
DDK	Cdc7-Dbf4
DNA-PKcs	DNA-dependent protein kinase, catalytic subunit
dNTPs	Deoxynucleotide Triphosphate
ELISA	Enzyme-Linked Immunosorbent Assay
FAB	C-terminal deletion of RPA1
FBB	Filter Binding Buffer
FlAsH	Fluorescein Arsenical Helix binder
FRET	Fluorescence Resonance Energy Transfer
HSQC	Heteronuclear Single Quantum Correlation
JM	joint molecules
LC/MS/MS	liquid chromatography – tandem mass spectrometry
MALDI-TOF MS	matrix-assisted laser desorption/ionization – time of flight mass spectrometry

MBP	maltose binding protein
MMR	Mismatch Repair
MRN	MRE11, RAD50, NBS1
NC	nicked circled
NER	Nucleotide Excision Repair
NMR	Nuclear Magnetic Resonance
nt	nucleotide
OB-fold	oligonucleotide/oligosaccharide binding fold
ORC	Origin Recognition Complex
PBS	phosphate buffered saline
PCNA	Proliferating Cell Nuclear Antigen
PMSF	phenylmethylsulfonyl fluoride
Pol α	DNA polymerase α
Pol δ	DNA polymerase δ
Pol ε	DNA polymerase ε
Pre-RC	pre-replication complex
ReAsH	Resorufin Arsenical Helix binder
RFC	Replication Factor C
RPA	Replication Protein A
RPA1	70 kilodalton subunit of RPA
RPA2	32 kilodalton subunit of RPA
RPA3	14 kilodalton subunit of RPA
RPA4	34 kilodalton subunit of RPA
S-CDK	S-phase cyclin dependent kinase
ssDNA	single-stranded deoxyribonucleic acid
SV40	Simian Virus 40
Tag	SV40 large T antigen

Tet	tetracycline
TOPBP1	topoisomerase-binding protein-1
Topo I	topoisomerase I
TROSY	transverse relaxation optimized spectroscopy
UV	ultraviolet
2-AP	2-aminopurine
9-1-1 complex	RAD9-RAD1-HUS1

CHAPTER 1

INTRODUCTION

General RPA Background

Single-stranded DNA is perhaps one of the most ubiquitous and important biological intermediate structures formed throughout the life of cells. Once formed, it must be protected from unwanted attack by endonucleases and it must be maintained for multiple biological processes to be carried out. Proteins that protect ssDNA do so by binding to it nonspecifically with high affinity. In eukaryotes, Replication Protein A (RPA) is the main single-stranded DNA (ssDNA) binding protein [1]. Consistent with the importance of ssDNA, RPA is required for almost all aspects of cellular DNA metabolism. This is reflected by the abundance of the protein in human cells. It has been estimated that there are $3 \times 10^4 – 2 \times 10^5$ molecules of RPA per cell in transformed human cells with proteins levels remaining constant throughout the cell cycle [2-4].

RPA is essential for cell viability [1], and viable missense mutations in RPA subunits can lead to defects in DNA repair pathways or show increased chromosome instability. For example, a missense change in a high affinity DNA-binding domain (DBD) was demonstrated to cause a high rate of chromosome re-arrangement and lymphoid tumor development in heterozygous mice [5]. RPA has also been shown to have increased expression in colon and breast cancers [6, 7]. High RPA levels in cancer cells are also correlated with poor overall patient survival [6, 7], which is consistent with RPA having a role in efficient cell proliferation.

RPA was originally identified as an essential component for simian virus 40 (SV40) DNA replication [8-10]. Since its discovery, it is now known to be essential for chromosomal DNA replication, repair and recombination and play an important role in the cellular response to DNA damage [11-17]. Not only does RPA function to protect the ssDNA but it also appears to actively coordinate the sequential assembly and disassembly of DNA processing proteins on ssDNA [18]. This coordination is through specific physical interactions with other essential proteins in DNA metabolism and most often dependent on RPA binding to ssDNA [18, 19].

Structure

RPA is a stable heterotrimeric complex of 70, 32 and 14 kDa subunits termed RPA1, RPA2 and RPA3, respectively (Figure 1-1) [1]. The heterotrimeric structure of the RPA family differs from all other known ssDNA binding proteins which are either monomers or homo-oligomers [20, 21]. Within the three subunits of RPA are six structurally conserved DNA binding domains composed of an oligonucleotide/oligosaccharide binding fold (OB-fold) [1, 19]. The OB-fold consists of five beta-strands that form a closed beta-barrel that includes an alpha helix between strands three and four [22]. This fold is found in many proteins that bind ssDNA or oligosaccharides. The six DBDs found in RPA have been identified by a combination of sequence analysis and structural studies [23-26]. These DBDs, designated A-F, are all essential for RPA function and participate in DNA binding, protein-protein interactions and inter-domain interactions [1]. There are four DBDs in RPA1 and one each in RPA2 and RPA3. These DBDs have different functions: there is evidence that they interact with DNA with different affinity and differentially with various proteins involved in DNA metabolism [1, 18]. The structures of the individual domains are known but the structure of the trimeric RPA complex remains elusive.

RPA1 is composed of four OB-fold domains (DBD A-C and F) (Figure 1-1). The N-terminal end, DBD F, has been shown to interact with multiple proteins and to bind DNA weakly [1]. DBD F is connected to DBD A through a ~60 amino acid flexible linker. DBDs A and B form the high affinity ssDNA binding core [25, 27]. At the C-terminus of RPA1 is a zinc finger containing OB-fold domain, DBD C. This domain contributes to ssDNA binding as a deletion of DBD C or mutation of the four cysteine residues in the zinc finger motif reduces the binding affinity by one order of magnitude [28]. DBD C has also been implicated to interact specifically with some forms of damaged ssDNA [28]. The C-terminal α-helix is required for the formation of the RPA complex[29, 30].

The 32-kDa subunit of RPA (RPA2) is composed of three distinct functional domains with the middle domain being DBD D, which has weak ssDNA binding activity(Figure 1-1) [31, 32]. The N-terminal domain contains a phosphorylation domain that exists in an extended, flexible conformation and is the major site of phosphorylation on RPA [33-35]. The C-terminal domain is a winged helix domain that interacts with several proteins involved in DNA metabolism [18].

The 14 kDa subunit of RPA (RPA3) termed DBD E has been shown to bind weakly and preferentially to telomeric DNA(Figure 1-1) [36]. The C-terminal region of RPA3 is important for trimerization [35]. The RPA trimerization core includes DBD C, DBD D, and DBD E and is mediated by three C-terminal α-helices, one from each DBD [37, 38]. RPA3 can also form a stable dimer with RPA2 *in vitro* but the significance of the subcomplex *in vivo* is unknown [35].

Interactions with ssDNA

RPA binds to ssDNA tightly with reported association constants ranging from $10^{8} – 10^{11}\ M^{-1}$, depending on conditions used [1, 19]. RPA binds nonspecifically to ssDNA but has approximately a 50-fold preference for binding sequences rich in pyrimidines [39]. Similarly, human RPA has been shown to strongly prefer binding to the pyrimidine-rich strand of the SV40 origin of replication [40]. Binding to ssDNA occurs in a 5’ to 3’ direction with RPA1 binding first at the 5’ end followed by RPA2 binding at the 3’ end of the ssDNA [41, 42]. The current model of RPA binding to ssDNA is a three-step process. First, DBD A and DBD B of RPA1 bind to a short stretch of ssDNA 8-10 nt in length. Second, DBD C binds increasing the binding site to 12-23 nt in length.

Third, DBD D of RPA2 binds at the 3' end of the ssDNA and possibly DBD F binds at the 5' end of the ssDNA, which increases the occluded binding site to ~30 nt [18].

DBD A and DBD B comprise the high affinity binding core of the RPA complex and both are necessary and sufficient for high-affinity binding of the RPA complex [43]. The crystal structure of this DNA binding core (RPA70-AB) has been solved both in the absence (Figure 1-2A) and presence (Figure 1-2B) of ssDNA giving insight into the interactions and conformational changes that occur upon binding ssDNA [44]. In the absence of ssDNA, both DBD A and DBD B have a similar OB-fold but they are in different orientations relative to each other. The ability of the two domains to move independently has been attributed to the short linker connecting the two domains. When RPA70-AB was crystallized in the presence of dC_8 the two domains align to partially wrap around the ssDNA [44]. Additionally, there are two loops at the top of each DBD that close in around the ssDNA. RPA makes a combination of polar and non-polar interactions with the ssDNA. Extensive hydrogen bonding is observed between amino acid side chains of RPA and either the bases or the phosphate backbone of the ssDNA. Two aromatic residues in each DNA binding domain base stack with bases of the DNA and are highly conserved throughout all single-stranded binding proteins.

Protein-protein Interactions

RPA is essential to many processes of DNA metabolism and functions not only by binding to ssDNA but also by interacting with multiple proteins involved in each process. A majority of the interaction sites have been mapped on RPA and are localized at a few domains. DBD F, DBD A and DBD B of RPA1 and the winged helix domain of RPA2 are the main interaction sites and most of these interactions have been shown to be functionally important to a specific process of DNA metabolism (Figure 1-3) [18, 19]. With the exception of DBD F, most of the interactions are located on the side of the protein that does not directly interact with DNA. Specific interactions will be discussed in the following sections.

RPA in Replication

RPA was first identified as an essential component for simian virus 40 DNA replication (Figure 1-4A). SV40 is a small double-stranded papova virus that normally infects primate cells [45]. DNA containing the SV40 origin of replication is replicated by proteins of the host cell with the exception of one viral protein, SV40 large T-antigen (Tag). During initiation of SV40 DNA replication the coordination of Tag, RPA, topoisomerase I (Topo I) and DNA polymerase α (pol α) are required [46]. Tag assembles as a double hexamer on the origin sequence and bidirectionally unwinds the dsDNA in an ATP dependent manner [45]. RPA is required for the Tag unwinding reaction but there is little specificity for RPA since *E. coli* SSB also supports this reaction [47]. Topo I releases the torsional stress induced by the helicase activity of Tag. Following origin unwinding, pol α is recruited by RPA and primers are synthesized [48, 49]. The pol α-RPA interaction is species specific as this reaction will not occur with any single-stranded binding protein unlike the Tag unwinding reaction [50]. Additionally, RPA increases the stability of pol α on the DNA and reduces the overall misincorporation of rate of pol α [51].

Following primer synthesis by pol α, a polymerase switch occurs where pol α is removed from the primer-template junction and one of the replicative polymerases, DNA polymerase δ (pol δ) and DNA polymerase ε (pol ε) are loaded depending if it is leading or lagging strand [52]. RPA plays a crucial role during this switching process. Once the primer is extended to a length of ~30 nucleotides by pol α, Replication Factor C (RFC) contacts RPA disrupting interaction between pol α and RPA [53]. This causes pol α to dissociate from the primer-template junction. RFC binds the junction and loads the sliding clamp, Proliferating Cell Nuclear Antigen (PCNA), while still interacting with

RPA. Pol δ then competes with RFC for binding to RPA, which causes RFC to be replaced by pol δ at the primer-template junction [53]. Pol δ then couples to PCNA and processive DNA synthesis is started. The polymerase switch is not only used early on during DNA replication, but is used continually during lagging strand synthesis.

RPA is not only required for initiation of DNA replication and the polymerase switch but also for elongation [54]. During elongation synthesis, RPA binds to the exposed ssDNA on both the leading and lagging strand. Even though the high affinity binding of RPA to ssDNA is necessary for elongation, it is not sufficient to promote efficient DNA synthesis. Studies using mutant forms of RPA that bound ssDNA with high affinity but could not interact with other essential protein components showed a drastic reduction in SV40 DNA synthesis during elongation indicating RPA-protein interactions are also required [54]. The current model suggests that RPA is a common touch-point for multiple proteins during DNA replication and the coordinated action of these proteins is based on a competitive interaction with RPA [18].

Since the discovery that RPA was essential for SV40 DNA replication, it has also been shown to have a similar role in chromosomal DNA replication as RPA associates with sites of DNA synthesis during S-phase [55]. RPA is not part of the pre-replicative complex but associates after the replisome is activated by S-phase cyclin dependent kinases and Dbf4/Cdc7 [56, 57]. Once activated, the origin is unwound by the presumed helicase complex (CMG; Cdc45, MCM, GINS) generating ssDNA to which RPA binds and is thought to help recruit pol α [58, 59].

RPA in Recombination

Homologous recombination is a process that involves genetic exchange between two DNA molecules that share an extended region of nearly identical sequence. In eukaryotes, homologous recombination is involved in the repair of double-strand breaks, meiosis and immunoglobulin switching. Recombination depends on proteins in the

Rad52 epistasis group, including Rad51 and Rad52, and RPA (Figure1-4B) [60]. Following the generation of a double strand break, the 5' ends of the break are resected by the MRE11-RAD50-NBS1 (MRN) complex aided by the CtIP-BRCA1-BARD1 complex, which creates ssDNA tails with a 3'-hydroxyl end. RPA binds and removes secondary structure from these ssDNA tails. BRCA1 interacts with RPA and recruits BRCA2, which facilitates the loading of Rad51. Rad51 forms filaments on ssDNA and initiates strand exchange facilitated by Rad55 and Rad57, which also recruit Rad52 and Rad54 [60-62]. These proteins promote ATP-dependent homologous DNA pairing and strand exchange. RPA interacts with both Rad51 and Rad52 [63-65]. Following strand invasion into a homologous sequence, a D-loop intermediate is formed, the 3'-end of the invading strand is extended by a polymerase and the template duplex DNA is unwound by RecQ-like helicases, BLM and WRN [60, 66]. RPA interacts with both of these helicases and has been shown to increase the processivity of BLM and WRN [67-69]. Homologous recombination can result in crossing-over but noncrossing-over appears to be favored for repair of double-strand breaks.

RPA in DNA Repair

In addition to repair of double-strand breaks that are resolved by homologous recombination, RPA is required for other repair process: nucleotide excision repair, base excision, and mismatch repair.

Nucleotide excision repair (NER) is the main mechanism in humans for the removal of helix-distorting lesions from DNA induced by agents such as ultraviolet (UV) light from the sun [70-72]. This multi-component excision repair reaction requires six core repair factors that recognize the lesion-containing DNA and make dual incisions bracketing the base adduct to remove (excise) the damaged base(s) as a 24-32 nucleotide-long oligonucleotide (Figure 1-4C). The resulting gap is filled and sealed by replicative DNA polymerases and ligases. Importantly, the nucleotide excision repair activity (excision nuclease) has been reconstituted *in vitro* with purified proteins [73-75], thus providing mechanistic insight into excision repair and allowing the characterization of the specific roles of the six minimal essential factors in the excision reaction.

One of the six core excision repair factors is RPA [73]. RPA is thought to participate in multiple steps in excision repair [70, 71, 76]. It appears to play an important role in damage recognition because of its higher affinity for damaged DNA than undamaged DNA [76, 77]. Both RPA1 and RPA2 subunits also bind to the core repair factor XPA [78-81] though only the RPA1-XPA interaction appears essential for excision repair and survival of UV-irradiated cells [80, 82]. RPA and XPA act cooperatively in DNA damage recognition [78, 81, 83], and the presence of RPA in the various "preincision complexes" [83, 84] that can be detected on damaged DNA prior to lesion removal provides additional evidence for a role of RPA in promoting or stabilizing the proper assembly of the excision nuclease. Formation of these complexes may be promoted by the strand separation activity of RPA [85]. In addition, RPA participates in the dual incision by stimulating the XPF-ERCC1 endonuclease [42, 86, 87]. Lastly, RPA has been implicated in the coordination of DNA synthesis after removal of DNA lesions [88].

Base excision repair (BER) is the predominate DNA damage repair pathway for non-bulky single-base lesions such as 3-methyladenine, 8-oxoguanine, abasic sites and uracil [89]. The damaged DNA is removed by a family of enzymes called DNA *N*-glycosylases, which recognize non-bulky single-base lesions and excise the damaged DNA base by cleavage of the *N*-glycosidic bond between the 2'-deoxyribose and the damaged base [90]. All organisms contain multiple glycosylases that recognize and remove specific kinds of DNA damage. RPA has been shown to interact with uracil-DNA glycosylase, which removes uracil from DNA [91]. Additionally, RPA stimulates long patch base excision repair where not only the damaged base is excised but 2-13 nt are also removed and subsequently replaced [92].

DNA mismatch repair (MMR) is a repair pathway that corrects base-base mismatches and insertions/deletions generated during DNA replication and recombination. Key proteins required for human MMR include MutSα/β (DNA mismatch/damage recognition), MutLα/β/γ (endonuclease and termination mismatch-provoked repair) and ExoI (mismatch excision) along with proteins required for repair synthesis (pol δ, PCNA, RFC) [93]. RPA is involved in all stages of MMR: it binds to nicked heteroduplex DNA before MutSα and MutLα, stimulates mismatch-provoked excision, protects the ssDNA-gapped region generated during excision and facilitates DNA resynthesis [94, 95].

RPA in DNA Damage Response

When cells are challenged by DNA damage, a coordinated response to DNA damage is required to maintain cellular viability and prevent disease. The DNA damage response is a complex signal transduction pathway that coordinates cell cycle transitions, DNA repair and apoptosis. The signaling cascade consists of sensor, mediator/transducer and effector proteins and is mediated by post-translational modification such as phosphorylation and acetylation [96, 97]. The major regulators of the DNA damage response are the phosphoinositide 3-kinase-related protein kinases, which include ataxia telangiectasia mutated (ATM), ATM and RAD3-related (ATR) and DNA-dependent protein kinase catalytic subunit (DNA-PKcs) (Figure1-4D). These kinases phosphorylate Ser or Thr residues that are followed by Gln and promote cell cycle arrest and DNA repair[96]. Specifically, ATM is activated in response to double strand breaks activating the downstream checkpoint kinase-2 (CHK2) [98]. ATR is activated during S-phase to (1) regulate replication origin firing, (2) repair stalled replication forks, (3) prevent premature onset of mitosis and (4) activates checkpoint kinase-1 (CHK1) along with other downstream effectors[96]. DNA-PKcs, along with Ku70/80, recognizes double-strand breaks for repair by non-homologous end joining [99].

It is not surprising that RPA is also involved in the DNA damage response. For ATR to be activated damaged DNA must first be recognized. As it turns out, the types of DNA damage that trigger ATR activation all contain stretches of ssDNA that are coated with RPA [100]. This recruits ATR to the sites of DNA damage via a physical interaction between ATRIP, a subunit of the ATR complex, and RPA. However, this is not sufficient to activate ATR but it does recruit RAD9-RAD1-HUS1/RAD17-RFC2-5 (9-1-1 complex/clamp loader), which is similar to PCNA and RFC [101]. Once the 9-1-1 complex is loaded on the primer-template junction the ATR activator, topoisomerase-binding protein-1 (TOPBP1), is recruited. TOPBP1 then activates ATR leading to phosphorylation of downstream effectors.

How RPA functions in the ATM pathway is less clear. RPA has been shown to interact with the MRE11-RAD50-NBS1 complex, which functions as a double-strand break sensor upstream of ATM by binding to and unwinding the exposed dsDNA ends [102]. Interestingly, the unwinding of the DNA ends by MRN is essential for ATM activation, which suggests RPA binding and stabilizing the newly generated ssDNA. Even though RPA plays a crucial role in the DNA damage response, there is evidence that both the ATR and ATM pathways can be activated in the absence of RPA [96, 103].

RPA4 and the alternative RPA complex

RPA is a highly conserved complex, as all eukaryotes contain homologs of each of the three RPA subunits [1]. Until recently, only one copy of the RPA complex was thought to be present in eukaryotes. However, in higher plants (characterized in *Oryza sativa* and *Arabdosis thaliana*) there are multiple copies of RPA1 and RPA2 giving rise to at least three different complexes all sharing a common RPA3 subunit [104-106]. Not only are there multiple RPA complexes but they each function in different capacities and are spatially segregated. For example in *O. sativa*, A type RPA is found in the chloroplast where as B and C type RPAs are nuclear [106]. Even though B and C type are both found in the nucleus, they do not have overlapping functions as one is specific to repair/recombination and the other to replication/transcription [107]. In addition to plants, some protists (*e.g.*, *Cryptosporidium parvum*) have two RPA1 subunits that together with RPA2 and RPA3 form two different RPA complexes [108]. The two different RPA complexes have not been fully characterized but evidence suggests that they each have a unique role in the life cycle of the parasite.

In contrast, only a single alternative form of RPA2, called RPA4, has been identified in humans (Figure 1-1) [109]. RPA4 was originally identified as a protein that interacts with RPA1 in a yeast two-hybrid screen [109]. The RPA4 subunit sequence is 63% similar to RPA2. Comparison of the sequences of RPA4 and RPA2 suggest that the two genes have a similar domain organization (Figure 1-5) [110]. RPA4 appears to contain a putative core DNA binding domain (termed DBD G) flanked by a putative N-terminal phosphorylation domain and a C-terminus containing a putative winged-helix domain (Figure 1-1) [111]. The phosphorylation domain of RPA2 is phosphorylated in a cell cycle dependent manner by cyclin dependent kinase 2 (Cdk2) at two sites and is also hyper-phosphorylated in response to DNA damage at up to seven additional sites [33]. RPA4 retains five of these nine sites of phosphorylation with only one of them being a Cdk2 site. RPA4 also has an additional four serines in the putative phosphorylation domain.

The *RPA4* gene is located on the X chromosome at position q21.33. Interestingly, *RPA4* is intronless, suggesting it arose from a viral- or retrotransposon-mediated gene duplication event. *RPA4* also lies in the intron of a known coding gene. This gene codes for a protein called diaphanous 2, which is a formin-related actin-binding protein [112]. Expression of *RPA4* has not been well characterized, but available data indicates that *RPA4* is expressed in different tissues than diaphanous 2, suggesting it is independently regulated (http://genome.ucsc.edu and http://www-bimas.cit.nih.gov/cards).

A protein coding *RPA4*-related sequence is commonly found in primates: complete coding sequences have been identified in human, chimpanzee, orangutan, rhesus monkey and marmoset [111]. Horse also contains a complete coding sequence. When other mammalian genomes were queried, either a partial *RPA4* sequence was identified or a *RPA4* pseudogene was located at the equivalent location on the X chromosome.

Initial characterization of RPA4 by Keshav *et al.*, indicated that either RPA2 or RPA4, but not both simultaneously, interact with RPA1 and RPA3 to form a complex, which has since been termed alternative RPA (aRPA) (Figure 1-1) [109]. Additionally, when RPA4 was transcribed/translated *in vitro* with RPA1 and RPA3, the complex was retained on ssDNA cellulose, suggesting the alternative RPA complex has ssDNA-binding ability. Using immuno-blotting techniques, RPA4 was shown to be expressed in placenta and colon tissue but was either not detected or expressed at low levels in most established cell lines examined [109].

To study the function of RPA4 *in vivo*, the Wold Lab carried out knockdown and replacement studies in HeLa cells [111]. Levels of RPA2 were depleted using small interfering RNA and exogenous RPA4 was transiently expressed from a plasmid using a cytomegalovirus promoter. By examining the cell cycle distribution of RPA2 knockdown and RPA4 expression we showed that RPA4 could rescue the RPA2 knockdown phenotype but resulted in an increase of cells in S-phase and an accumulation in G2/M. Further investigation showed that RPA4 did not support S-phase progression. However, RPA4 did localize to site of DNA damage suggesting that RPA4 and by inference, aRPA, could support some of the processes that require RPA. These initial studies on RPA4 suggest that aRPA has different functions than RPA. Therefore, understanding RPA4's function could lead to a better understanding of the mechanisms that lead to abnormal cell proliferation and cancer. However, further biochemical analysis was required to understand the function of RPA4 and aRPA.

Outline

This dissertation describes my studies characterizing the function of the alternative RPA complex that contains RPA4. Chapter 2 describes the purification and biochemical characterization of aRPA and its role in SV40 DNA replication. Chapter 3 describes the expression of *RPA4* and *RPA2* in human tissues and the role of aRPA in nucleotide excision repair and homologous recombination using *in vitro* assays. Chapter 4 describes the effect of aRPA on pol α and pol δ DNA synthesis using synthetic DNA substrates. Chapter 5 summarizes my findings and places them into a broader context. Chapters 2-4 represent manuscripts that have either been published (Chapters 2 and 3) or have been submitted for publication (Chapter 4) and have been modified to conform to the format required for University of Iowa Doctoral Thesis.

Figure 1-1: Schematic of structural and functional domains of RPA and aRPA.

Replication Protein A is composed of RPA1 (green), RPA2 (blue) and RPA3 (red) and alternative Replication Protein A (aRPA) is composed of RPA1, RPA4 (orange) and RPA3. RPA1 is composed of 4 DBDs designated A, B, C and F. RPA2 is composed of an N-terminal phosphorylation domain (designated by P), a central DBD (DBD D) and a C-terminal winged helix domain. RPA3 is solely composed of DBD E. RPA4 is composed of an N-terminal putative phosphorylation domain (designated by P), a central DBD (DBD G) and a C-terminal winged helix domain based on sequence similarity to RPA2. Known functions of each domain are indicated with bars (ssDNA binding: purple, protein-protein interactions: orange, subunit interactions: light blue).

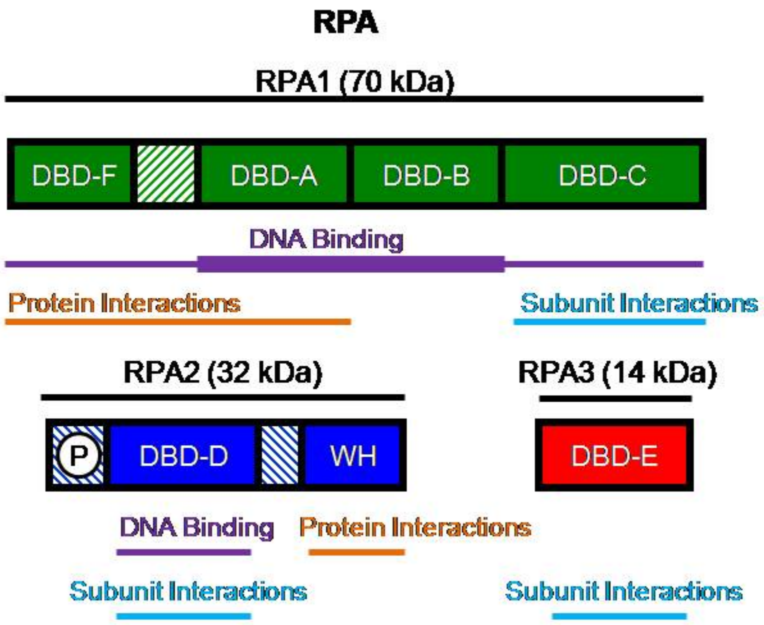
RPA
RPA1 (70 kDa)
DBD-F
DBD-A
DBD-B
DBD-C
DNA Binding
Protein Interactions
Subunit Interactions
RPA2 (32 kDa)
RPA3 (14 kDa)
P
DBD-D
WH
DBD-E
DNA Binding
Protein Interactions
Subunit Interactions
Subunit Interactions

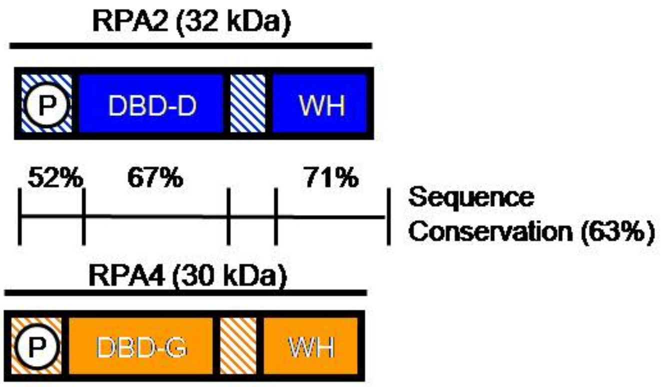
RPA2 (32 kDa)
P
DBD-D
WH
52%
67%
71%
Sequence Conservation (63%)
RPA4 (30 kDa)
P
DBD-G
WH

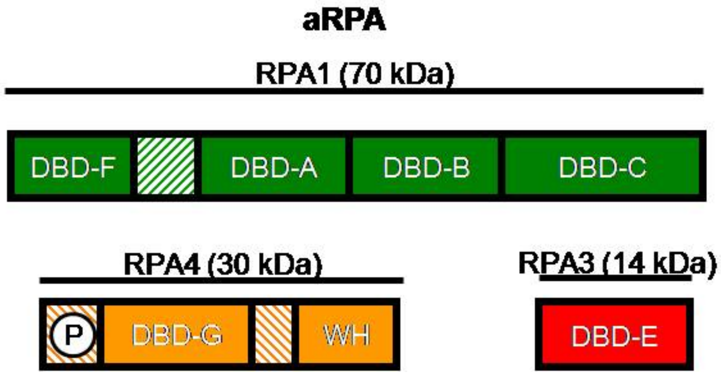
aRPA
RPA1 (70 kDa)
DBD-F
DBD-A
DBD-B
DBD-C
RPA4 (30 kDa)
RPA3 (14 kDa)
P
DBD-G
WH
DBD-E

Figure 1-2: Structure of RPA high-affinity DNA-binding domains.

Ribbon diagram of DBD A and DBD B colored in blue (β-strands), red (α helices) and green (random coil). (A) The structure of DBD A and DBD B of RPA1 (residues 181-422; pdb 1FGU). (B) The structure of DBD A and DBD B of RPA1 (residues 181-422; pdb 1JMC) bound to dC_8 (purple). Top – front view. Bottom – side view. [25].

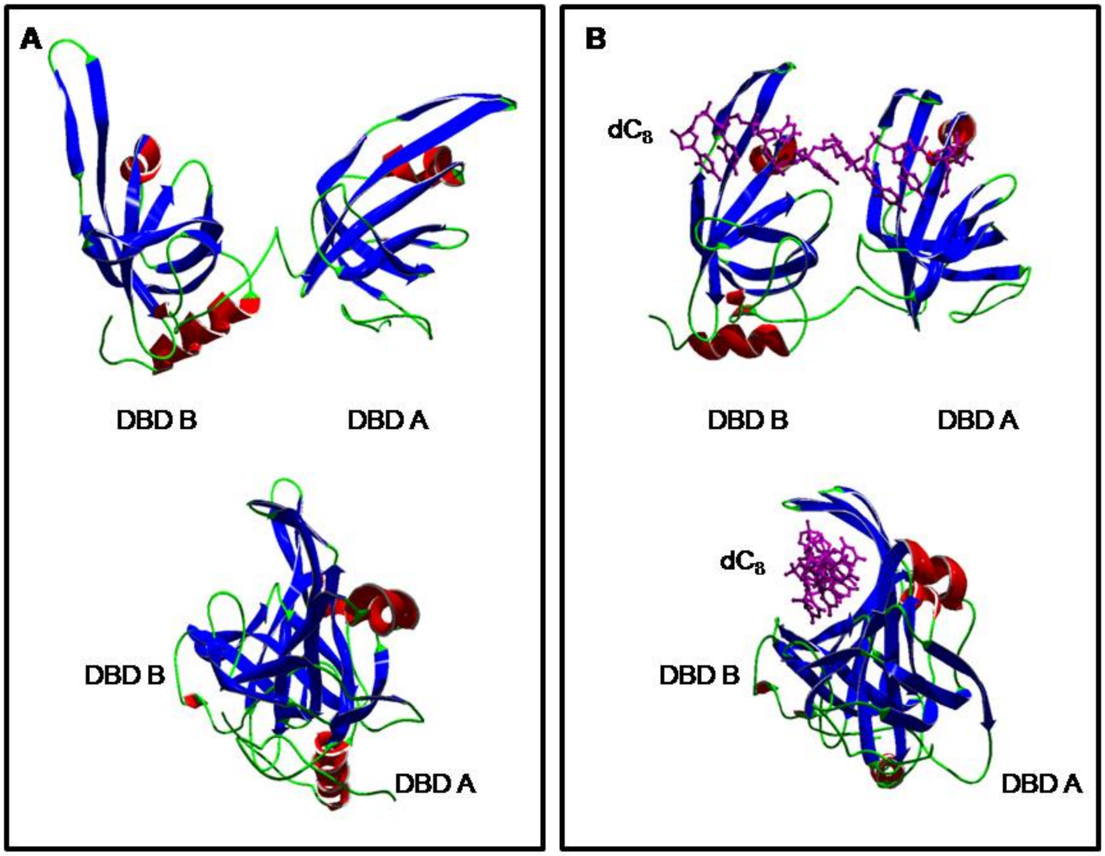
A
DBD B
DBD A
DBD B
DBD A
B
dC$_8$
DBD B
DBD A
dC$_8$
DBD B
DBD A

Figure 1-3: Proteins known to interact with RPA.

Select proteins known to interact with RPA in various processes of DNA metabolism. Sites of interaction on RPA are indicated with bars. Proteins that function in DNA replication (black), DNA repair (red), recombination (blue) and DNA damage response (green) are differentiated by the color of the line.

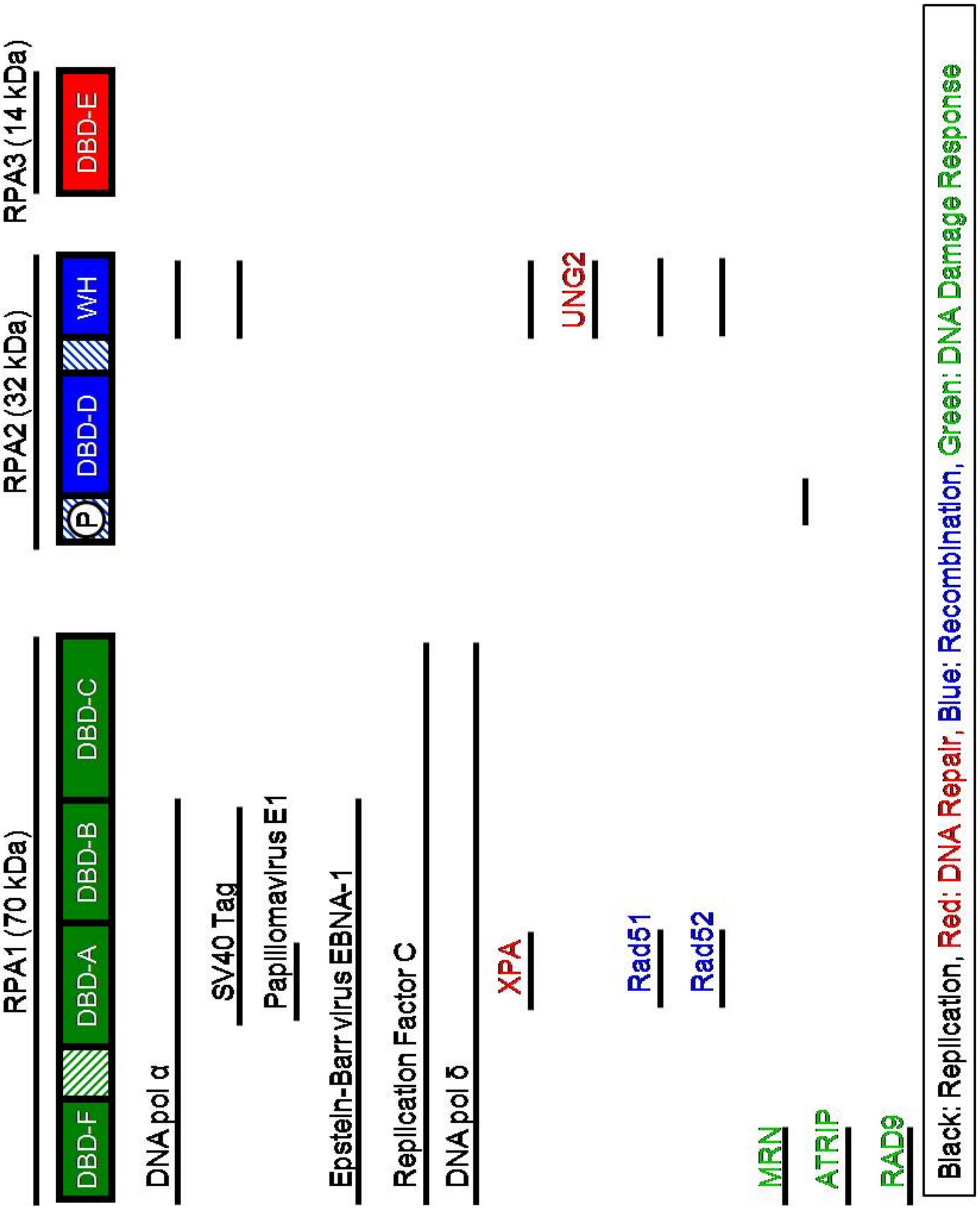
RPA1 (70 kDa)
DBD-F
DBD-A
DBD-B
DBD-C
RPA2 (32 kDa)
P
DBD-D
WH
RPA3 (14 kDa)
DBD-E
DNA pol α
SV40 Tag
Papillomavirus E1
Epstein-Barr virus EBNA-1
Replication Factor C
DNA pol δ
XPA
UNG2
Rad51
Rad52
MRN
ATRIP
RAD9
Black: Replication, Red: DNA Repair, Blue: Recombination, Green: DNA Damage Response

Figure 1-4: Schematic representation of RPA function in different cellular processes.

(A) RPA in DNA replication. Eukaryotic replication fork showing select proteins required for leading and lagging strand DNA synthesis. (B) RPA in homologous recombination used in repair of double-strand breaks, which involves exchange of genetic material between the damaged DNA strand and a similar region of DNA on the sister chromosome. (C) RPA in nucleotide excision repair. RPA functions in DNA damage recognition, recruitment and coordination of additional proteins and DNA repair synthesis. (D) RPA in DNA damage response. RPA is one of several key proteins that initiate the activation of the DNA damage checkpoints, leading to cell cycle arrest, DNA repair, senescence or apoptosis. Figure modified from Humphreys and Wold [113].

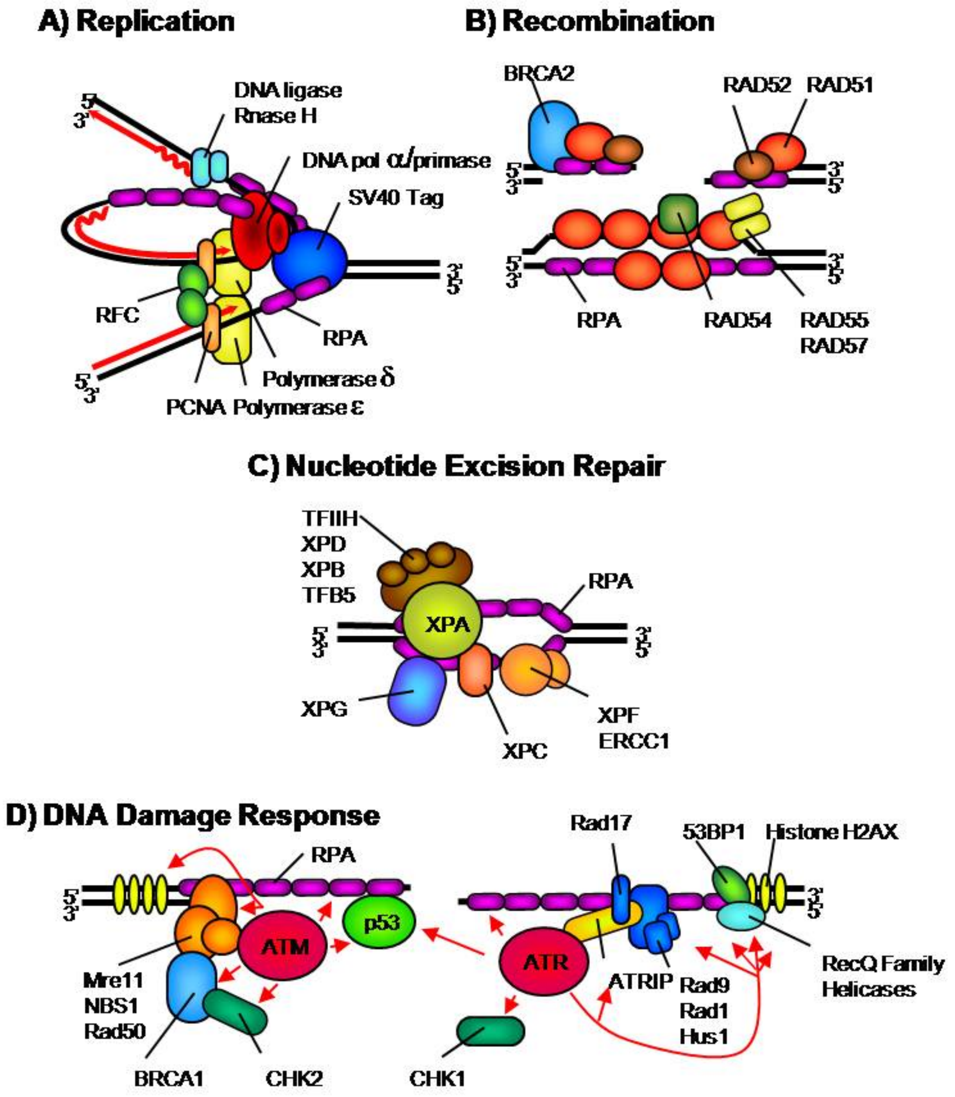
A) Replication
5'
3'
DNA ligase
Rnase H
DNA pol α/primase
SV40 Tag
3'
5'
RFC
RPA
Polymerase δ
5'
3'
PCNA
Polymerase ε
B) Recombination
BRCA2
RAD52
RAD51
5'
3'
3'
5'
5'
3'
3'
5'
RPA
RAD54
RAD55
RAD57
C) Nucleotide Excision Repair
TFIIH
XPD
XPB
TFB5
RPA
XPA
5'
3'
3'
5'
XPG
XPC
XPF
ERCC1
D) DNA Damage Response
RPA
5'
3'
ATM
p53
Mre11
NBS1
Rad50
BRCA1
CHK2
Rad17
53BP1
Histone H2AX
3'
5'
ATR
ATRIP
Rad9
Rad1
Hus1
RecQ Family
Helicases
CHK1

Figure 1-5: Alignment of human RPA2 and RPA4 from five mammalian species.

RPA4 and RPA2 protein sequences are from *Homo sapiens* (Hosa) and the predicted sequences from *Pan troglodytes* (Patr), *Pongo abelii* (Poab), *Macaca mullata* (Mamu) and *Equus caballus* (Eqca). Alignment was performed by TCOFFEE [114]: identical (*), conserved (:) and semiconserved (.) residues are denoted below each alignment by TCOFFEE. The putative phosphorylation domains are denoted with lowercase letter, DNA binding domains with uppercase letters and winged helix domain with uppercase italics. Figure modified from Haring *et* al. [111].

```
Hosa.RPA2   mwnsgfesygsssy--ggaggytqspggfgspapsqaekksraraQHIVPCTISQLLSAT
Hosa.RPA4   msksgfgsygsisaadgasggsdqlcer-d-atpaiktqrpkvriQDVVPCNVNQLLSST
Patr.RPA4   msksgfgsygsisaadgasggsdqqcer-d-atpamktqrpkvriQDVVPCNVNQLLSST
Poab.RPA4   msksgfgsygsisaadgasggsdplcer-d-aapaiktqrpkvriQDVVPCNVNQLLSST
Caja.RPA4   msksgfgsygsisaasgasggsdqpser-g-aapvvktqrprvriQNIVPCNVYQLLSST
Mamu.RPA4   msnsgfgsygsisaadggsggsdqlcer-d-aapaiktqrpkvriQDVVPCNVNQLLSST
Eqca.RPA4   mskngfgsygsisaaggasggndqpsqg-ggtapatklfrsraliQEIIPCSVNQLLTST
            * :.** **** *   *.:**        . .:*     :.:.  *.::**.: ***::*
Hosa.RPA2   LVDEVFRIGNVEISQVTIVGIIRHAEKAPTNIVYKIDDMTAAPMDVRQWVDTDDTSSENT
Hosa.RPA4   VFDPVFKVRGIIVSQVSIVGVIRGAEKASNHICYKIDDMTAKPIEARQWFGREKVKQ-VT
Patr.RPA4   VFDPVFKVRGIIVSQVSIVGVIRGAEKASNHICYKIDDMTAKPIEVRQWFGREKVKQ-VT
Poab.RPA4   VFDTVFKIRGIIVSQVSIVGVIRGADKASNHICYKIDDMTAKPIEARQWFGREKVKQ-VT
Caja.RPA4   VLDTVFKVRGITVSQVSVVGVIREAEKASNHICYKIDDMTAKPIEARQWFGREKVKQ-LT
Mamu.RPA4   VFDTVFKVRGIIVSQVSIVGVIRGAEKASNHICYKIDDMTAKPIEARQWFGREKVKQ-VT
Eqca.RPA4   LVDDVFQIRGVEVSQVSIVGIIRQAEMAPNYVLYKIDDMTTKPIEVRQWVSNEKAKQGVT
            :.* **:: .: :***::**:** *: *.. : *******: *::.***.. :....  *
Hosa.RPA2   VVPPETYVKVAGHLRSFQNKKSLVAFKIMPLEDMNEFTTHILEVINAHMVLSKANSQPSA
HOSA.RPA4   PLSVGVYVKVFGILKCPTGTKSLEVLKIHVLEDMNEFTVHILETVNAHMMLDKARRDTTV
PATR.RPA4   PLSVGVYVKVFGILKCPTGTKSLEVLKIHVLEDMNEFTVHILETVNAHMMLDKARRDTTV
POAB.RPA4   PLTVGVYVKVFGILKCPTGTKSLEVLKIHVLEDMNEFTVHILETVNAHMMLDKACRDTTV
CAJA.RPA4   PLSVGLYVKVFGILKCPAGTKSLEVLKIYVLEDMNEFTVHILETVSAHMMLYKARGDTTL
MAMU.RPA4   PLSVGAYVKVFGILKCPTGTKTLEVLKIHVLEDMNEFTVHILETVNAHMMLDKARRDTTV
EQCA.RPA4   LLPVGVYVKVFGTLKCSAGVKCLEVLNIRVLESMNEFTAHVLETGHAHMMLPKAYQLAPV
             :.   **** * *:.  . * * .::*  **.*****.*:**.  ***:* **   ..
HOSA.RPA2   GRAPISNPGMSEAGNFGGNSFMPANGLTVAQNQVLNLIKACPRPEGLNFQDLKNQLKHMS
HOSA.RPA4   ESVPVSPSEVNDAGDNDE------SHRNFIQDEVLRLIHECPHQEGKSIHELRAQLCDLS
PATR.RPA4   ESVPVSPSEVNDAGDNDE------SHRNFIQDEVLRLIHECPHQEGKSIHELRAQLCDLS
POAB.RPA4   ESVPVSPSEVNDAGDNDE------SHRSFIRDEVLRLIHECPHQEGKSIHELQAQLCDLS
CAJA.RPA4   ESVPVSPSEVDDAGDNDE------SRRNFIRDEVLRLIHECPRQEGRSIHELQAQLCDLS
MAMU.RPA4   ESVPVFPSEVDDAGDNDE------SHRSFIRDEVLRLIHECPQQEGKSIYELQAQLCDLS
EQCA.RPA4   QNAPVTPLEMDGVQESGE------DCPDYILKEVLRLIRECPRKEGKSLQQLQTELCSLS
              .*:    :. . : .       .      .:**.**: **: ** .: :*: :*  :*
Hosa.RPA2   VSSIKQAVDFLSNEGHIYSTVDDDHFKSTDAE
HOSA.RPA4   VKAIKEAIDYLTVEGHIYPTVDREHFKS-AD
PATR.RPA4   VKAIKEAIDYLTVEGHIYPTVDREHFKS-AD
POAB.RPA4   VKAIKEAIDYLTVEGHIYPTVDREHFKS-AD
CAJA.RPA4   IQAIKEVIDYLTLEGHIYPTVDREHFKS-AD
MAMU.RPA4   LKAIKEAIEYLTVEGHIYPTVDQEHFKS-AD
EQCA.RPA4   IKTIKQAIDYLTIEGHVYCTVDGEHFKS--AD
            :.:**:.:::*: ***:* *** :****  *:
```

CHAPTER 2

AN ALTERNATIVE FORM OF REPLICATION PROTEIN A PREVENTS VIRAL REPLICATION IN VITRO

Abstract

Replication Protein A, the eukaryotic single-stranded DNA-binding complex, is essential for multiple processes in cellular DNA metabolism. The ‘canonical’ RPA is composed of three subunits (RPA1, RPA2, and RPA3); however, there is a human homolog to the RPA2 subunit, called RPA4 that can substitute for RPA2 in complex formation. I demonstrate that the resulting ‘alternative’ RPA (aRPA) complex has solution and DNA binding properties indistinguishable from the ‘canonical’ RPA complex; however, aRPA is unable to support DNA replication and inhibits canonical RPA function. Two regions of RPA4, the putative L34 loop and the C-terminus, are responsible for inhibiting SV40 DNA replication. Given that aRPA inhibits canonical RPA function *in vitro* and is found in non-proliferative tissues, these studies indicate that RPA4 expression may prevent cellular proliferation via replication inhibition while playing a role in maintaining the viability of quiescent cells.

Introduction

These studies describe the purification and functional analysis of an alternative RPA complex containing RPA1, RPA3, and RPA4 (Figure 2-1A). I show that the aRPA complex is a stable heterotrimeric complex similar in size and stability to the canonical RPA complex (RPA1, RPA3, and RPA2). aRPA interacts with ssDNA in a manner indistinguishable from canonical RPA; however, it does not support DNA replication *in vitro*. Mixing experiments demonstrate that aRPA also inhibits canonical RPA from functioning in DNA replication. Hybrid protein studies paired with structural modeling have allowed for the identification of two regions of RPA4 responsible for this inhibitory activity. Data presented here are consistent with recent analyses of RPA4 function in human cells [110], and I conclude that RPA4 has anti-proliferative properties and has the potential to play a regulatory role in human cell proliferation through the control of DNA replication.

Materials and Methods

Materials

J buffers used for purification of RPA and aRPA contain 30 mM HEPES (diluted from 1 M stock at pH 7.8), 1 mM tris(2-carboxyethyl)phosphine, 0.25 mM EDTA, 0.5% (w/v) inositol, and 0.02% (v/v) Tween-20. J buffers were supplemented with different salt concentrations as indicated. Creatine phosphokinase from rabbit skeletal muscle and creatine phosphate disodium salt were purchased from Calbiochem. [γ-^{32}P] ATP (250 μCi), [α-^{32}P] dCTP (250 μCi) were purchased from Perkin Elmer.

Construction of aRPA and aRPA Hybrid Expression Plasmids

To purify RPA4 in a complex with RPA1 and RPA3, a PCR fragment containing RPA4 cDNA was amplified using primers 5'-CACCTGACGTCAAAAACCCCTC AAGACCCGTTTAGAGGCCCCAAGGGGTTATGCTATTATCAATCAGCAGACTT AAAATGCTC-3' and 5'-TTGATGGATCCTAGAAAT AATTTTGTTTAACTTTAAGAAGGAGATATACATATGAGTAAGAGTGGGTTTG GGAGC-3'. This fragment was then cloned into the *Bam*HI-*Aat*II sites of pET16b-hSSB[115], replacing the RPA2 cDNA. Subsequently, a *Bsr*GI-*Sca*I fragment containing the 3' end of RPA3 and the entire RPA4 coding region was cloned into p11d-tRPA[116] to generate the plasmid p11d-aRPA. Plasmids for expressing RPA4 alone or with RPA3 were generated by inserting the *Bam*HI-*Aat*II fragment into pET-11d or pET16b-RPA32/his14 (a derivative of pET16b-hSSB in which RPA1 has been deleted), respectively. A 10XHis tag was added to the N-terminus of RPA4 and cloned into pET11d using the same method with the primer 5’- TTGATGGATCCTAGAAA TAATTTTGTTTAACTTTAAGAAGGAGATATACATATGGGCCATCATCATCATC ATCATCATCATCATCACAGCAGCGGCCATATCGAAGGTCGTCATATGAGTAA GAGTGGGTTTGGGAGC-3’. All plasmids were confirmed by restriction digest and DNA sequencing.

Hybrid constructs were amplified from their corresponding pEGFP plasmids [110] using either primers 5’-TCTCGAGGTGGATTAATGAGT AAGAGT-3’ or 5’-CTCGAGGTGGATTAATGT GGAACAGT-3’ and 5’-AGATCCGGTGGAT CCCGGGCCCGC-3’. The fragment was digested with *AseI* and *KpnI* and then cloned into the *NdeI* and *KpnI* sites of pRSF. All plasmids were confirmed by restriction analysis and DNA sequencing.

Protein Expression and Purification

RPA, aRPA, and aRPA hybrids were expressed in BL21 (DE3) cells and purified as described previously [116, 117]. RPA4/3 complex was purified as described [118]. When dual vectors were used, both ampicillin (120 µg/ml) and kanamycin (30 µg/mL) were used for colony selection and growth.

Trimer Formation

RPA1, RPA2, RPA3 and RPA4 were co-expressed in *E.coli* and RPA complexes were purified as described for RPA and aRPA. The resulting RPA complexes were analyzed using standard immune-blotting techniques with anti-RPA1 (2H10), anti-RPA2 (719A) and anti-RPA4 antibodies (sheepαRPA4/3-bleed2). Purified RPA and aRPA were mixed (100 ng total protein) from 100 ng RPA to 100 ng aRPA.

DNA Binding Assays

Gel mobility shift assays were carried out as described previously [117]. Briefly, indicated amounts of protein and radiolabeled oligonucleotide were incubated for 20 min at 25°C in filter binding buffer (30 mM HEPES (diluted from 1 M stock at pH 7.8), 100 mM NaC1, 5 mM MgC12, 0.5% inositol, and 1 mM DTT). Reaction mixtures were separated on a 1% agarose gel in 0.1X Tris acetate-EDTA running buffer. Bound and free DNA from gel mobility shift experiments were quantitated using a Packard Instant Imager. Apparent affinity constants were calculated by nonlinear least squares fitting of the data to the Langmuir binding equation using KaleidaGraph (Synergy Software) as described previously [119].

SV40 Replication and Elongation Assays

SV40 reactions were carried out in 25 µL. Standard reactions contained 30 mM HEPES (pH 7.5); 7 mM $MgCl_2$; 50 µM dCTP with 2.5 µCi (92.5 kBq) of [α-^{32}P] dCTP; 100 µM each of dATP, dGTP and dTTP; 200 µM each of CTP, GTP and UTP; 4 mM ATP; 40 mM creatine phosphate; 2.5 µg creatine kinase; 15 mM potassium phosphate; and 50 ng of pUC.HSO DNA template. RPA, usually 300 ng, was added as indicated. Each reaction also contained 100 µg of HeLa cell cytoplasmic extract, and 0.2 – 0.5 µg of SV40 T-antigen. SV40 T-antigen was purified by immunoaffinity chromatography from Sf9 cells infected with a baculovirus vector containing the T-antigen gene as described previously [120]. Complementation assays were carried out using a 35-65% ammonium sulfate fraction of HeLa cell extract [117]. Briefly, 1 mL of complete extract was precipitated by the gradual addition of ammonium sulfate to 35%. The supernatant was further precipitated with 65% ammonium sulfate. The resulting precipitant was dissolved in 1/5 the initial volume with 50 mM Tris-HCl (pH 7.8), 1 mM dithiothreitol, 0.1 mM EDTA, 10% glycerol and dialyzed to remove any residual ammonium sulfate. All reaction mixtures were assembled on ice and incubated at 37°C for 2 hours. The reactions were analyzed on gels as described previously [117] or quantitated by precipitation by tricholoroacetic acid: reactions were quenched by the addition of 0.1M sodium pyrophosphate to a final concentration 80 mM and precipitated with 500 µL of

10% trichloroacetic acid. The reaction mixtures were filtered through glass microfiber filters and radioactive DNA was quantitated by liquid scintillation.

SV40 T-antigen dependent elongation assays [54] were done as described in the SV40 replication assay with the following modifications. Reactions were assembled as above except the [α-^{32}P] dCTP was excluded from stage 1. After incubation at 37°C for 2 hours, [α-^{32}P] dCTP and RPA or RPA variants were added and a stage 2 incubation carried out for an additional hour at 37°C. Products were analyzed as described above.

Results

RPA4 Forms a Stable, Functional ssDNA-Binding Complex

Recombinant RPA4 was produced using methodology previously described to generate recombinant canonical RPA [116]. The cDNA encoding RPA4 was cloned into a bacterial expression vector either alone, with RPA3 or with RPA1 and RPA3, and expressed in *E. coli*. Overall, RPA4 had properties that were similar to those of recombinant RPA2 [116]. A His-tagged RPA4 gene expressed alone was predominantly insoluble. When RPA4 was expressed with RPA3, both proteins were predominantly soluble and could be purified as a stable RPA4/3 complex (Figure 2-1B). When all three genes (RPA1, RPA4, RPA3) were expressed simultaneously, all three polypeptides were substantially soluble and a complex, aRPA, could be purified to near homogeneity following the purification procedure used for canonical RPA [117]. The expression of RPA4 in *E. coli* and the yield of aRPA complex after purification were similar to that for RPA (~0.8 mg per liter of culture). The purified aRPA contained three intense bands of 70, 34, and 14 kDa (Figure 1B). Although RPA4 has nine fewer amino acids than RPA2, and a predicted pI (6.07) slightly more basic than RPA2 (5.75), the RPA4 subunit consistently migrated slower in SDS-PAGE gels.

The hydrodynamic properties of aRPA were examined by glycerol gradient sedimentation and size exclusion chromatography and found to be nearly indistinguishable from those of the canonical RPA complex: the sedimentation and Stokes' radius of aRPA were determined to be 5.0 S and 52.0 Å (*vs.* 5.0 S and 51.2 Å for canonical RPA; Figure 2-1C). The mass calculated for aRPA is in close agreement to that predicted from the amino acid sequence (Figure 2-1C) and indicates RPA4 is forming a heterotrimeric complex with RPA1 and RPA3. The frictional coefficient for aRPA and RPA are both consistent with an elongated shape [121], which suggests that when RPA4 is substituted for RPA2, the overall shape of the complexes in solution is similar.

To investigate if RPA4 could form a trimeric complex with RPA1 and RPA3 as efficiently as RPA2, a plasmid carrying RPA1 and RPA3 and another plasmid carrying RPA2 and RPA4 were co-expressed in *E. coli* cells. The resulting RPA complexes were purified using the standard method for RPA and aRPA purification. This should not bias one complex over the other since the purification is mostly dependent on RPA1 and when RPA and aRPA are purified separately, the yields are similar. The purified protein and *E.coli* lysate was analyzed by immuno-blotting for RPA1, RPA2 and RPA4. To determine the amount of RPA2 and RPA4, a titration of purified RPA and aRPA was done. This showed the specificity of the antibodies used and allowed for an estimation of protein amount. As shown in Figure 2-2A, the amount of RPA2 and RPA4 detected in *E.coli* lysates when RPA1, RPA3, RPA2 and RPA4 were co-expressed was ~15% and ~70%, respectively. Following purification, the resulting RPA complexes were ~30% RPA and ~70% aRPA (Figure 2-2B). These data suggest that RPA4 is able to compete with RPA2 for trimer formation when both RPA2 and RPA4 are co-expressed.

The predicted sequence of RPA4 is 63% identical/similar to RPA2 [110]. This similarity allows homology modeling to be used to predict the structure of the putative domains of RPA4. The known structure of the DNA binding domain of RPA2 (DBD D;

2PI2.pdb) is shown in Figure 2-3A. The shallow, putative DNA binding cleft between the L12 and L45 loops is indicated [38]. Two other prominent features of the structure are the flexible L34 loop (at the top of structure) and the C-terminal alpha helix, which has been shown to be part of the subunit interface of RPA2 (right side of structure) [35, 38]. The known structure for DBD D of RPA2 was used to model DBD G of RPA4 using Geno3D (http://geno3d-pbil.ibcp.fr) (Figure 2-3A). The predicted structure of DBD G is very similar to that of DBD D, suggesting that the two domains may assume similar structures (Figure 2-3A). However, comparison of the predicted surface charge of the DBDs of RPA2 and RPA4 indicates that the surface of RPA2 is much more acidic than that of RPA4 (lower row, Figure 2-3A, see also below).

In canonical RPA, two domains in RPA1 (DBD A and B) are both necessary and sufficient for high affinity DNA binding and RPA2 contributes little to the overall affinity of the complex for ssDNA [18, 31, 122]. Therefore, aRPA, which contains RPA1, RPA4 and RPA3, was expected to bind ssDNA with high affinity. To examine aRPA-DNA interactions, gel mobility shift assays were used. This assay relies on the protein-DNA complex having reduced mobility relative to free ssDNA during electrophoresis. This method can also be used with different lengths of ssDNA, which allows for binding constants to be determined and an estimation of occluded binding site and cooperativity. I analyzed the binding affinity of purified aRPA to $(dT)_{30}$ by gel mobility shift assays. The binding of canonical RPA and aRPA are very similar: nearly equivalent concentrations of protein were needed to form a complex, and only one protein-DNA species was observed (Figure 2-4A). Quantitation of the titrations demonstrated that both RPA complexes have high affinity for ssDNA; K_d equals 7.5×10^{-9} M for RPA and 20×10^{-9} M for aRPA (Figure 2-4B). Binding was also examined with longer oligonucleotides, $(dT)_{50}$ and $(dT)_{70}$. Only one protein-DNA species was observed with $(dT)_{50}$, whereas two distinct protein-DNA bands were observed with dT_{70} for both aRPA and RPA (Figure 2-4A) suggesting that for high concentrations of both proteins, two molecules bind to dT_{70}. Together these data indicated that the occluded binding site of aRPA is 25-35 nucleotides, which is comparable to the binding site size of RPA [119]. RPA binds ssDNA with low cooperativity and has a cooperativity parameter (ω) of ~15. This level of cooperativity is significantly lower than that of T4 gene protein 32 (ω= ~2000) [123] and *E.coli* SSB (ω=~400 for $SSB_{(65)}$ binding mode [124]and $\omega=10^5$ for $SSB_{(35)}$ binding mode [21]). As shown in Figure 2-4A, there is a gradual transition between single- and double-liganded species, for both RPA and aRPA, which is consistent with previous reports for RPA [119]. These analyses indicated that aRPA binds with cooperativity similar to RPA. I conclude that aRPA has ssDNA-binding properties indistinguishable from canonical RPA: it binds ssDNA with high affinity and low cooperativity.

aRPA Function in SV40 Replication

RPA was originally identified as a protein essential for SV40 DNA replication [8]; therefore, I examined whether aRPA could support SV40 DNA replication. Cell extracts derived from human tissue culture cells contain all of the cellular proteins required for SV40 replication, except the viral protein large T antigen [125]. RPA is required for SV40 replication and is present in the cell extracts [8]; however, the extracts can be depleted of RPA using ammonium sulfate fractionation, making the DNA synthesis dependent on both Tag and RPA [117]. RPA-depleted, ammonium sulfate-fractionated extract (AS-Ex) is unable to support DNA synthesis in the presence of Tag unless the reaction is also supplemented with RPA (Figure 2-5A, bars 1-3). A complete reaction with canonical RPA gives robust DNA synthesis (Figure 2-5A, bar 3). In contrast, supplementation with aRPA results in only background levels of DNA synthesis (Figure 2-5A, bar 4). Background synthesis was also observed when purified RPA4/3 complex was added in place of RPA (Figure 2-5C, bar 6). Replication of the SV40 origin containing DNA occurs by two mechanisms in these reactions: circle-to-circle and rolling circle. These mechanisms produce different products, circles and long linear DNA, respectively (Figure 2-5B; [54]). Analysis of the products by gel electrophoresis, showed that aRPA did not support the formation of either type of product (Figure 2-5B, left panel). I conclude that even though aRPA binds ssDNA with high affinity, it is unable to support SV40 DNA replication.

Interestingly, addition of aRPA to unfractionated extracts also showed only background levels of synthesis (Figure 2-5C, bar 4). This is surprising, because canonical RPA is present in these unfractionated extracts and normally supports replication. Reactions containing both purified aRPA and purified RPA were analyzed. Additional canonical RPA (double the normal amount) in the reaction results in a modest increase in DNA synthesis (Figure 2-5A, bar 10). When aRPA was added in the presence of equal amounts of RPA, no DNA synthesis was observed (Figure 2-5A, bar 11). This demonstrates that aRPA has a dominant negative effect on the function of canonical RPA in SV40 DNA replication. To rule out the possibility that this effect is caused by the dissociation of the aRPA complex, which would result in an insoluble RPA1 protein and a soluble RPA4/3 subcomplex, purified RPA4/3 was added SV40 DNA replication reactions. As shown in Figure 2-5C (bar 5 and 6), RPA4/3 did not support DNA replication and did not inhibit DNA replication in the presence of canonical RPA. This is consistent with the aRPA complex being the active protein form in these assays.

RPA2 and RPA4 are both composed of three distinct functional domains: the phosphorylation domain, a DBD, and a winged-helix domain (Figure 2-1A). In order to determine what region(s) of RPA4 is responsible for the properties of aRPA in DNA replication, three hybrid proteins were generated in which the phosphorylation domain, the DBD, or the C-terminus of RPA2 was replaced with the corresponding domain of RPA4, named RPA2(422), RPA2(242) and RPA2(224), respectively (Figure 2-3B). These domain hybrid proteins were expressed with RPA1 and RPA3, and the resulting complexes were purified. All three complexes purified with a yield similar to RPA and bound $(dT)_{30}$ with an affinity equivalent to wild-type RPA. When the trimeric complexes, RPA•2(422), RPA•2(242), RPA•2(224), were examined for the ability to support DNA synthesis, only the RPA•2(422) hybrid complex was able to support wild-type levels of DNA synthesis (Figure 2-5A, bars 5-7). RPA•2(242) and RPA•2(224) both supported levels of synthesis that were slightly above background and aRPA levels. I conclude that the phosphorylation domain of RPA4 is not responsible for the phenotype observed with aRPA. These data also indicate that both the DBD and winged-helix domains of RPA2 are necessary for RPA function in SV40 DNA replication, and that both of these domains of RPA4 are contributing to the aRPA phenotype.

Mixing experiments were also carried out with the RPA2-RPA4 hybrids. RPA•2(422) did not inhibit the function of RPA and showed levels of synthesis comparable to that of RPA alone. Both RPA•2(242) and RPA•2(224) showed levels of DNA synthesis that were significantly reduced from that of RPA (t-test; $p<0.005$ and $p<0.001$, respectively) but greater than that of aRPA (Figure 4A, bars 12-14). RPA•2(224) consistently showed more inhibition than RPA•2(242), suggesting the two domains may have different effects on SV40 DNA replication. I conclude both the DBD and winged-helix domain of aRPA are contributing to the inhibitory effect of RPA4.

Mechanism of aRPA Inhibition of SV40 Replication

RPA is required for both initiation and elongation phases of DNA replication. To examine which phase of replication is being affected by aRPA, two-stage elongation assays were carried out. Time course experiments have shown that in the SV40 replication reaction, initiation predominantly occurs during early times (stage I), and at later times (stage II), only elongation synthesis on rolling-circle intermediates is occurring [54]. During rolling-circle replication, a single replication fork moves around the circular plasmid and normal termination processes do not occur. This results in products much longer than the template DNA. Previous analysis showed that the products of rolling circle are double-stranded DNA so both leading and lagging strand DNA synthesis are occurring at the one fork as would be observed during elongation [54]. It is therefore possible to examine aRPA function in elongation in a two-stage reaction. Stage I contains all the components necessary for initiation and elongation of SV40 origin-containing DNA except for the radioactive dCTP tracer. This stage is incubated for two hours at 37° C, during which normal initiation and elongation occur, but the DNA synthesized is not labeled. In stage II [α-^{32}P] dCTP and various forms of RPA are added, the incubation is continued for one hour, and the elongation DNA synthesis is quantitated. This assay measures DNA synthesis occurring during the elongation phase, which includes leading and lagging strand synthesis, and is independent of the initiation processes [54] .

Substantial elongation synthesis was observed in the stage II elongation phase (Figure 2-6A, bar 2). This synthesis was dependent on the presence of RPA from the start of the reaction and could be stimulated by additional RPA at the beginning of stage II (Figure 2-6A, bars 1-3). aRPA strongly inhibits elongation synthesis, demonstrating that aRPA inhibits the normal function of canonical RPA at the pre-existing replication fork (Figure 2-6A, bar 4). This strong inhibition was not observed with the hybrid subunits (Figure 2-6A, bars 5-7). RPA•2(422) causes a slight increase in elongation synthesis similar to the addition of canonical RPA (t-test; $p<0.0005$), and consistent with its ability to promote replication. RPA•2(224) had no effect on elongation synthesis (t-test; $p<0.11$) while RPA•2(242) showed slightly reduced levels of DNA synthesis (t-test; $p<0.001$). Together these experiments indicate that the putative phosphorylation domain of RPA4 has no role in inhibiting elongation synthesis, whereas DBD G of RPA4 inhibits elongation synthesis. Interestingly, the putative winged-helix of RPA4 appears to have a separation of function phenotype. Although this region results in inhibition of the complete SV40 DNA synthesis, it does not affect elongation synthesis. This suggests that the putative winged-helix containing C-terminus of RPA4 is defective for replication initiation only.

Structural Basis of RPA4 Inhibition

The DNA binding domains of RPA2 and RPA4 are predicted to have similar structures but very different electrostatic surface potentials (Figure 2-3A). Since the solution structure of the C-terminal region of RPA2 is known [126], I used homology modeling to predict the structure of the C-terminus of RPA4. Figure 2-3C shows that the predicted structure for the winged-helix of RPA4 is very similar to the known structure of the RPA2 winged-helix. The predicted surface potential is predominantly acidic for both winged-helix domains; however, the N-terminus of the predicted winged-helix of RPA4 is much more acidic than the equivalent region of RPA2 (Figure 2-3C). The inhibition studies discussed above suggest that the putative winged-helix domain of RPA4 is inhibiting initiation; RPA•2(224) inhibits the complete reaction, but has no effect on elongation synthesis. This is consistent with a previous analysis that described an important role for the winged-helix domain of RPA2 in initiation of SV40 replication [126]. In contrast, RPA•2(242) inhibits both the complete SV40 replication reaction and the elongation reaction. This suggests that DBD G of RPA4 (Figure 2-3A) is affecting an RPA function (or functions) normally required for both phases of replication.

Initiation of SV40 replication requires binding of the origin of replication by SV40 Tag and specific interactions between RPA and T antigen to promote unwinding of the origin sequence and loading of DNA polymerase alpha/primase complex [49, 127, 128]. Protein interaction assays were carried out to determine whether aRPA interacts with T antigen. aRPA interacts with SV40 T antigen to the same extent as RPA (Figure 2-6B). It has been shown that T antigen interacts with both the core DNA binding domain of RPA1 and the C-terminus (winged-helix) of RPA2 (key residues E252, Y256, S257, D261, T267, D268) [126, 129]. This region of the winged-helix of RPA2 is partially conserved in RPA4, with 3 of the 6 key residues differing between RPA2 and RPA4 (E252, Y256, P257*, R261*, A267*, D268 - asterisks indicate non-conserved residues). The finding that aRPA interacts strongly with T antigen (Figure 2-6B) suggests that either the interaction is primarily mediated through RPA1, or that the partial conservation of the C-terminus of the winged-helix in RPA4 is sufficient for interaction with Tag.

The inability of aRPA to support SV40 DNA replication indicates that either aRPA is forming a nonfunctional initiation complex with Tag, or aRPA is inhibiting another part of the initiation reaction. T antigen has origin dependent helicase activity which can be stimulated non-specifically by RPA or other single-stranded DNA-binding proteins [3, 8]. I found that aRPA stimulated T antigen-dependent unwinding at levels comparable to canonical RPA (Figure 2-6C). This indicates that aRPA does not inhibit T antigen helicase and that the defects in replication are more likely to be in subsequent steps of initiation such as primer synthesis by the DNA polymerase alpha/primase complex.

Construction of a Dominant Negative Form of RPA2

DBD G has a more basic surface charge than DBD D and is capable of inhibiting the function of the canonical RPA complex. This suggests that electrostatic interactions may be responsible for the altered function of DBD G. A comparison of the sequences of RPA2 and RPA4 identified one region that was very poorly conserved between RPA2 and RPA4, amino acids 108 to 123 in RPA2, referred to as the L34 loop (Figure 2-3A). These residues are acidic in DBD D (5/17 acidic and 0/17 basic residues) and basic in DBD G (1/16 acidic and 3/16 basic residues). To test whether this region is responsible for the difference in activity between RPA4 and RPA2, the acidic region of RPA2 and the basic region of RPA4 were exchanged for one another. This resulted in two mutated subunits: an RPA2 subunit that has the basic L34 loop of DBD G (RPA2Basic) and an

RPA4 subunit with the acidic L34 loop of DBD D (RPA4Acidic). These structures were again modeled against the crystal structure of DBD D (2PI2.pdb;[38]) and the electrostatic surface potential was displayed for each (Figure 2-3A). The electrostatic surface potential shows that RPA2Basic has a predicted surface potential similar to RPA4 and RPA4Acidic has a predicted surface potential similar to RPA2.

The RPA2Basic and RPA4Acidic complexes were expressed in *E. coli* and purified. Both complexes bound $(dT)_{30}$ with an affinity equivalent to wild-type RPA. Each was then tested for the ability to support SV40 DNA replication as described above. Neither trimeric complex, RPA•2Basic nor RPA•4Acidic, were able to support DNA synthesis in the SV40 system (Figure 2-5A, bars 8-9). Mixing experiments containing equal amounts of RPA and RPA•2Basic had background levels of DNA synthesis (Figure 2-5A, bars 8 and15) indicating that RPA•2Basic is strongly inhibitory of RPA activity in DNA replication. This is similar to that observed for aRPA. In contrast, mixing RPA and RPA•4Acidic resulted in intermediate levels of synthesis that were similar to those obtained with RPA•2(224) (Figure 2-5A, bars 9, 12, and16). This suggests that removing the basic L34 loop from DBD G reduces the inhibitory activity of this domain. In elongation assays, RPA•2Basic inhibited DNA synthesis almost as well as aRPA, while RPA•4Acidic had no inhibitory effect on elongation synthesis (Figure 2-6A). These findings indicate that the L34 loop of RPA4 is both necessary and sufficient for the inhibitory activity of DBD G. In HeLa cells studies, RPA•2Basic is defective in chromosomal DNA replication and has a dominant negative effect [110]. Therefore, replication inhibition (both viral and cellular) appears to be a general property of this short amino acid stretch of RPA4.

Discussion

I have shown that aRPA and RPA have similar biochemical properties but not similar functions. Both complexes have similar solution structures and DNA binding activity, but aRPA is unable to support *in vitro* SV40 DNA replication. Analysis of the mechanism of aRPA action indicates that aRPA inhibits the function of canonical RPA in the initiation and elongation phases of DNA replication (Figure 2-7). Recent findings suggest that RPA4 also does not support chromosomal replication in the absence of RPA2 suggesting that these properties identified *in vitro* also hold true for cellular replication [110]. Our findings suggest a model by which RPA4 levels could regulate DNA replication in the cell. At low concentrations of RPA4, aRPA complex formation is also low and efficient DNA replication will occur utilizing canonical RPA. When RPA4 is expressed at higher levels, aRPA forms and exists at a level that can inhibit the replication activity of canonical RPA. RPA4 is expressed in some human tissues [109] (see also Chapter 3), suggesting that cell viability is maintained in the presence of RPA4. Thus, I would predict that in cells that need to perform genome maintenance, but not genome duplication (*i.e.*, quiescent cells), aRPA might be able to substitute for canonical RPA. Alternatively, it has been recently shown that there is another single-stranded binding protein (hSSB1) in human cells that may have a role in DNA repair [130]. This protein could help maintain viability in RPA4-expressing cells. It will be important to determine if aRPA and/or hSSB1 can support at least some basal processes normally performed by RPA, such as DNA repair.

Multiple protein-protein interactions are important for RPA function in SV40 DNA replication. These include interactions with SV40 Tag, DNA polymerase α and topoisomerase I during initiation [18, 131] and interactions with RFC, DNA polymerase α and polymerase δ in elongation [132]. Since aRPA has ssDNA-binding properties similar to RPA, it is most likely that altered protein interactions are responsible for the inability of aRPA to function in replication. aRPA interacts with SV40 Tag and can stimulate Tag DNA unwinding at the same level as RPA suggesting that the inhibitory properties of aRPA result from aRPA either forming nonfunctional complexes with the replication machinery or being unable to participate in a subset of essential protein interactions.

Two regions of RPA4 have been identified to be involved in its activity: the basic L34 loop of DBD G and the winged-helix domain (Figure 2-7). Analysis of RPA4Acidic and RPA2Basic indicated that the L34 loop in RPA4 both necessary and sufficient for inhibition of SV40 DNA replication. The RPA4Acidic complex, which contains RPA4 with the L34 loop from RPA2, has properties similar to RPA•2(224) in both DNA replication and elongation. In contrast, the RPA2Basic complex, which contains RPA2 with the L34 loop of RPA4, strongly inhibits all replication reactions, identical to the full aRPA complex. Recent analysis of RPA4 function in human cells indicates that the L34 loop also inhibits cellular chromosomal replication[110] suggesting that this is a general property of this loop. The importance of the L34 loop in RPA function has not been previously identified. Modeling of the electrostatic surface potential of DBD G (Figure 2-3A) indicates that the basic loop from RPA4 has a large influence on the surface potential of this domain. It seems likely this change in surface potential is causing the inhibitory activity of this domain.

The second domain of RPA4, the C-terminus containing a putative winged-helix, also affects SV40 DNA replication. RPA•2(224) strongly inhibited a complete replication reaction but had minimal effects on elongation suggesting that the putative winged-helix domain is only playing a critical role in the initiation of SV40 replication. Structure-function analysis of RPA2 previously mapped the T antigen interaction domain to the C-terminus of the winged-helix domain and showed that this interaction was important for initiation of SV40 replication [126]. Our analysis of hybrid RPA2 complexes demonstrates that this interaction is either only necessary for initiation or can also occur with RPA4. In contrast, the DNA binding domain of RPA4 is inhibitory in both complete and elongation assays. Furthermore, previous studies have shown that DNA binding domain is the only domain of RPA2 essential for life in yeast [23, 118].

Additional analysis is necessary to understand the complete function of the winged-helix containing domains of RPA2 and RPA4.

It has recently been demonstrated that RPA4 expression in human cells does not allow the cell to replicate its genome nor proceed through the cell cycle [110]. In addition, the original analysis of RPA4 by Keshav *et al*. showed that RPA4 expression occurs in predominantly quiescent cells and not in cell lines, which are by definition proliferative [109]. Our detailed biochemical characterization of purified alternative RPA complex (containing RPA1, RPA3, and RPA4) provides definitive evidence that not only does aRPA prevent DNA replication, it does so in the presence of canonical RPA. The fact that RPA4 is expressed in at least some tissues suggests that it may have an active role in preventing cell proliferation and promoting quiescence. Canonical RPA is crucial for maintenance of the genome. aRPA has similar solution properties and DNA-binding activity, so it seems likely that aRPA can function in at least some cell maintenance processes normally carried out by RPA. These findings suggest that RPA4 has potential functions as a therapeutic agent and/or target not only in preventing cell proliferation (*i.e.*, cancer) but also as a potential antiviral agent (*i.e.*, through prevention of viral duplication)

Figure 2-1: Properties of aRPA complex.

(A) Schematic diagram of the structural and functional domains of the three subunits of RPA and (proposed for) RPA4: DNA binding domains (DBD A-G), the phosphorylation domain (PD), winged-helix domain (WH) and linker regions (lines). The sequence similarity between RPA2 and RPA4 is indicated for each domain of the subunit. (B) Gel analysis of 2 μg of RPA4/3, RPA or aRPA separated on 8-14% SDS-PAGE gels and visualized coomassie blue staining. Position of each RPA subunit is indicated. (C) Hydrodynamic properties of aRPA and RPA complexes. Sedimentation Coefficient and Stokes' Radius were determined as described previously by sedimentation on a 15-35% glycerol gradient and chromatography on a Superose 6 10/300 GL column (GE Healthcare), respectively [119]. Mass and frictional coefficients were calculated using the method of Siegal and Monty [133]. Predicted mass was based upon the amino acid sequence derived from the DNA sequence. Hydrodynamic properties were determined by Dr. Stuart Haring.

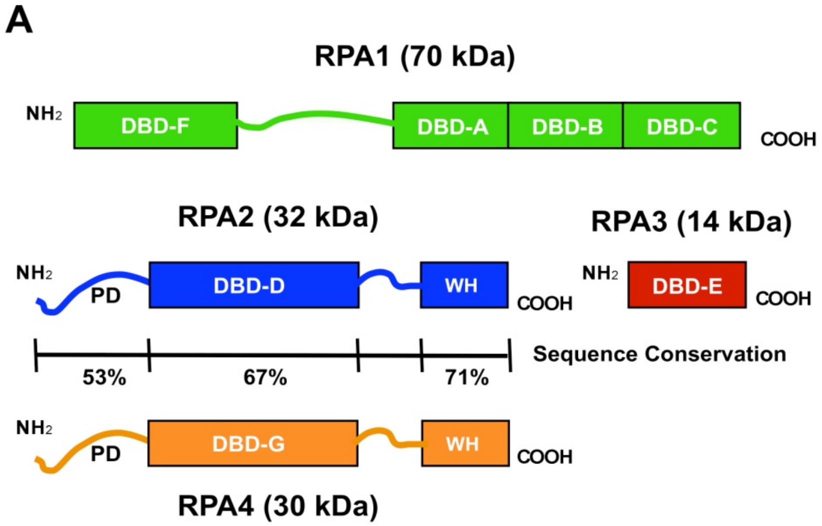
A
RPA1 (70 kDa)
NH2
DBD-F
DBD-A
DBD-B
DBD-C
COOH
RPA2 (32 kDa)
NH2
PD
DBD-D
WH
COOH
RPA3 (14 kDa)
NH2
DBD-E
COOH
53%
67%
71%
Sequence Conservation
NH2
PD
DBD-G
WH
COOH
RPA4 (30 kDa)

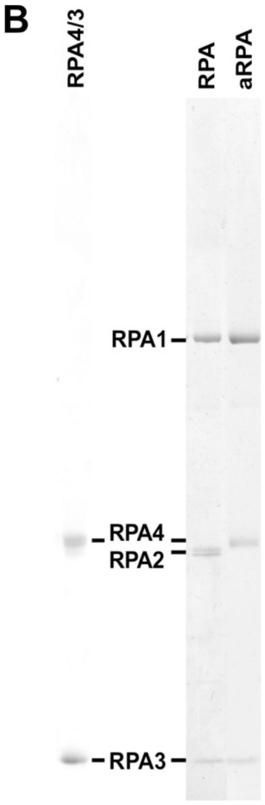
B
RPA4/3
RPA
aRPA
RPA1
RPA4
RPA2
RPA3

C

	Sedimentation coefficient (S)	Stokes' radius (Å)	Predicted mass (kDa)	Experimental mass (kDa)	Frictional coefficient (*f/f0*)
RPA (RPA2)	5.0	51.2 ±0.4	110.9	114.3 ±7.8	1.60 ±0.04
aRPA (RPA4)	5.0	52.0 ±0.2	110.6	116.1 ±8.0	1.62 ±0.04

Figure 2-2: Trimer Formation.

RPA1, RPA2, RPA3 and RPA4 were co-expressed in *E.coli* and RPA complexes were purified. As a loading control, decreasing amounts of RPA and increasing amounts of aRPA were mixed to keep the total protein at 100 ng. (A) *E.coli* lysate from RPA1, RPA2, RPA3 and RPA4 co-expression (B) 100 ng of purified RPA1234. Samples separated on 8-14% SDS-PAGE gels and analyzed by immuno-blotting with anti-RPA1, anti-RPA2 and anti-RPA4 antibodies. Boxes (red: RPA2 and blue: RPA4) indicate the amount of the middle subunit that was detected in the lysate and RPA1234.

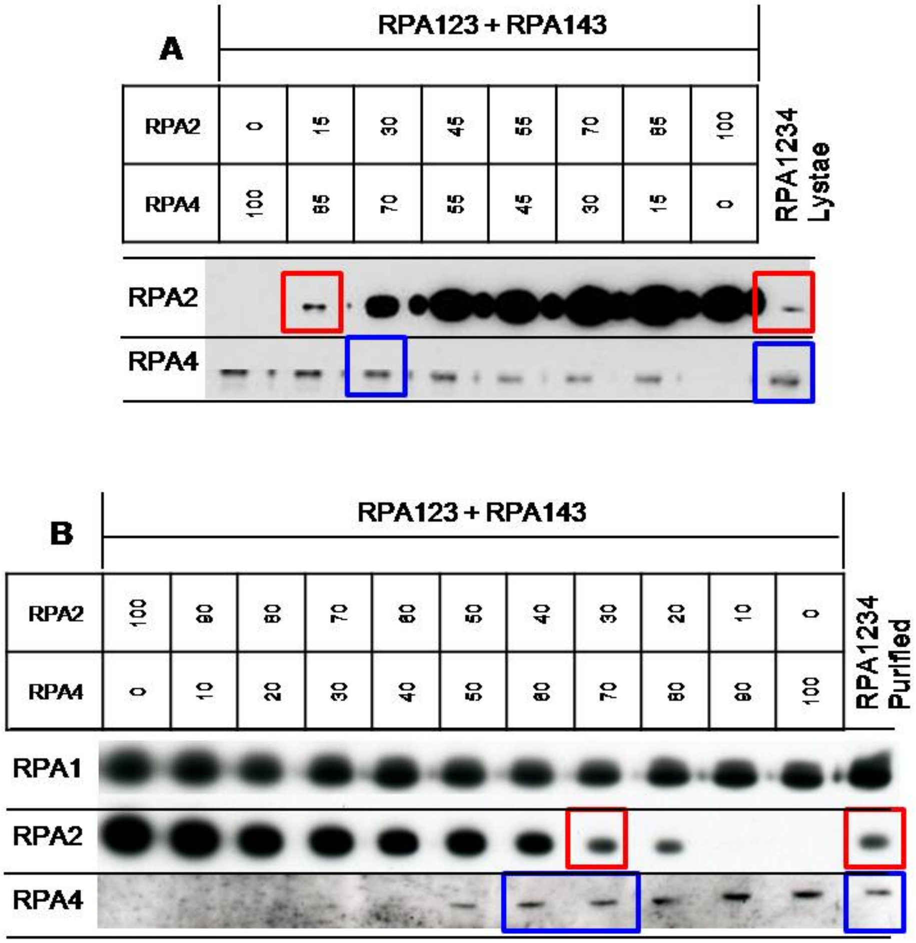
A
RPA123 + RPA143
RPA2 0 15 30 45 55 70 85 100
RPA4 100 85 70 55 45 30 15 0
RPA1234 Lystae
RPA2
RPA4
B
RPA123 + RPA143
RPA2 100 90 80 70 60 50 40 30 20 10 0
RPA4 0 10 20 30 40 50 60 70 80 90 100
RPA1234 Purified
RPA1
RPA2
RPA4

Figure 2-3: Structural Models of RPA2 and RPA4.

(A) Structural models of RPA2 DBD D (2PI2.pdb) and proposed RPA4 DBD G. The proposed structure of DBD G was generated using Geno3D by modeling against DBD D. Top: The ribbon representation was generated by Swiss-PdbViewer; helices are red, β-sheet regions are blue, and coil regions are green. Putative DNA binding cleft and important loops on DBD D are indicated. Below: The electrostatic surface potential of the above models are shown with regions of basic (blue), acidic (red), and neutral (white) surface potential. (B) Schematic of RPA2-RPA4 hybrid proteins generated. RPA2 (blue) and RPA4 (orange) domains are indicated for each hybrid. (C) Structure of winged-helix domain. Structure of RPA2 winged-helix domain (1Z1D.pdb) and the proposed structure of the winged-helix domain of RPA4 (generated using Geno3D) are shown. Top: The ribbon representation was generated by Swiss-PdbViewer. Side chain structures of residues in RPA2 winged-helix demonstrated to interact with T antigen (interface)[126]. Below: The electrostatic surface potential of the above model are shown. All colors as in (A).

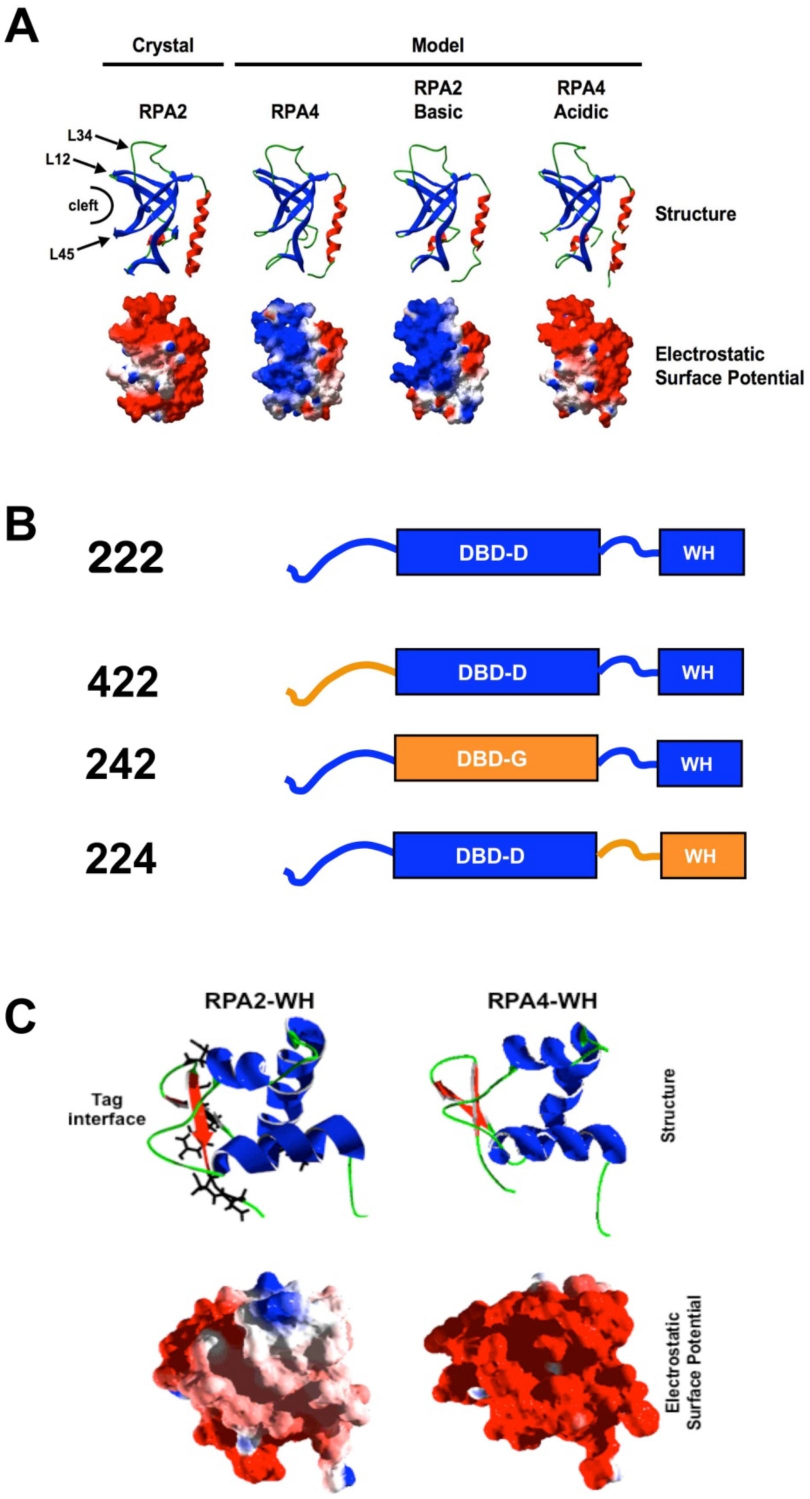
A
Crystal
Model
RPA2
RPA4
RPA2 Basic
RPA4 Acidic
L34
L12
cleft
L45
Structure
Electrostatic Surface Potential
B
222
422
242
224
DBD-D
DBD-G
WH
C
RPA2-WH
RPA4-WH
Tag interface
Structure
Electrostatic Surface Potential

Figure 2-4: DNA binding properties of RPA complexes.

(A) DNA binding properties of RPA complexes. Gel mobility shift assays were carried out as described previously [117]. Autoradiograms of representative gel mobility shift assays of aRPA and RPA using radiolabeled dT_{30}, dT_{50} and dT_{70} are shown. Radiolabeled dT_{30} (0.2 fmol), dT_{50} (2 fmol) or dT_{70} (2 fmol) was incubated with the indicated various amounts of protein (dT_{30}: 0, 0.0067, 0.02, 0.067, 0.2 nM; dT_{50} and dT_{70}: 0, 0.067, 0.2, 0.67, 2.0 nM). The position of free DNA and shifted protein-DNA complex are indicated. (B) Representative binding isotherms for aRPA and RPA binding dT_{30} determined as described in Methods. Binding data for RPA (closed circles), aRPA (closed squares) and best-fit curves are shown.

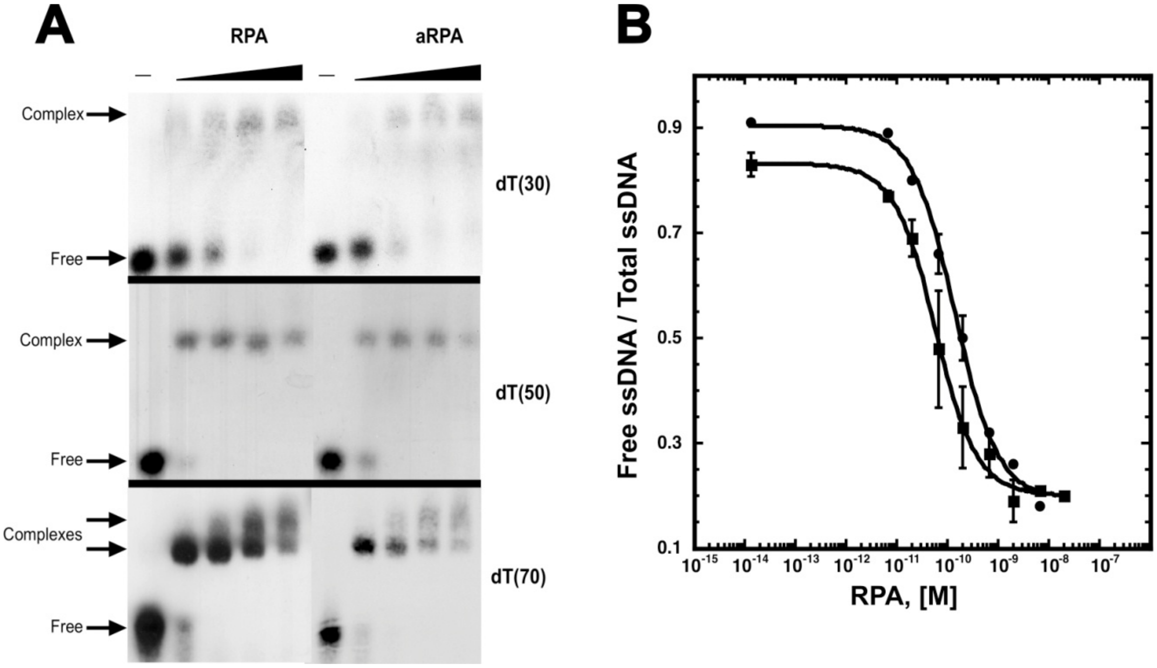
A
RPA
aRPA
–
–
Complex
Free
dT(30)
Complex
Free
dT(50)
Complexes
Free
dT(70)
B
Free ssDNA / Total ssDNA
0.9
0.7
0.5
0.3
0.1
10^{-15}
10^{-14}
10^{-13}
10^{-12}
10^{-11}
10^{-10}
10^{-9}
10^{-8}
10^{-7}
RPA, [M]

Figure 2-5: SV40 DNA replication with various forms of RPA.

SV40 DNA replication with various forms of RPA. A plus in the table indicates an addition of the indicated component: 300 ng RPA forms, 0.2-0.5 µg SV40 large T antigen (Tag), 100 µg HeLa cytosolic extract (ammonium sulfate precipitated; AS-Ex). 2+ indicates 600 ng RPA. The amount of DNA synthesis after 2 hours of incubation at 37° was quantitated by scintillation counting or analyzed by agarose gel electrophoresis. (A) Summary of quantitative analysis of replication. Five independent experiments with duplicate points at each condition were completed. The data from each experiment were normalized to the minus Tag and RPA control (bar 1) for that experiment, averaged and plotted. Maximal DNA synthesis for individual experiments ranged from 23 to 60 pmoles. Error bars represent standard deviation for the combined data. (B) Autoradiograph of the products of a representative reactions (containing the indicated components) after separation on a 1% agarose gel. The mobility of various DNA forms is indicated. (C) SV40 DNA replication with unfractionated HeLa cytosolic extracts and RPA4/3.

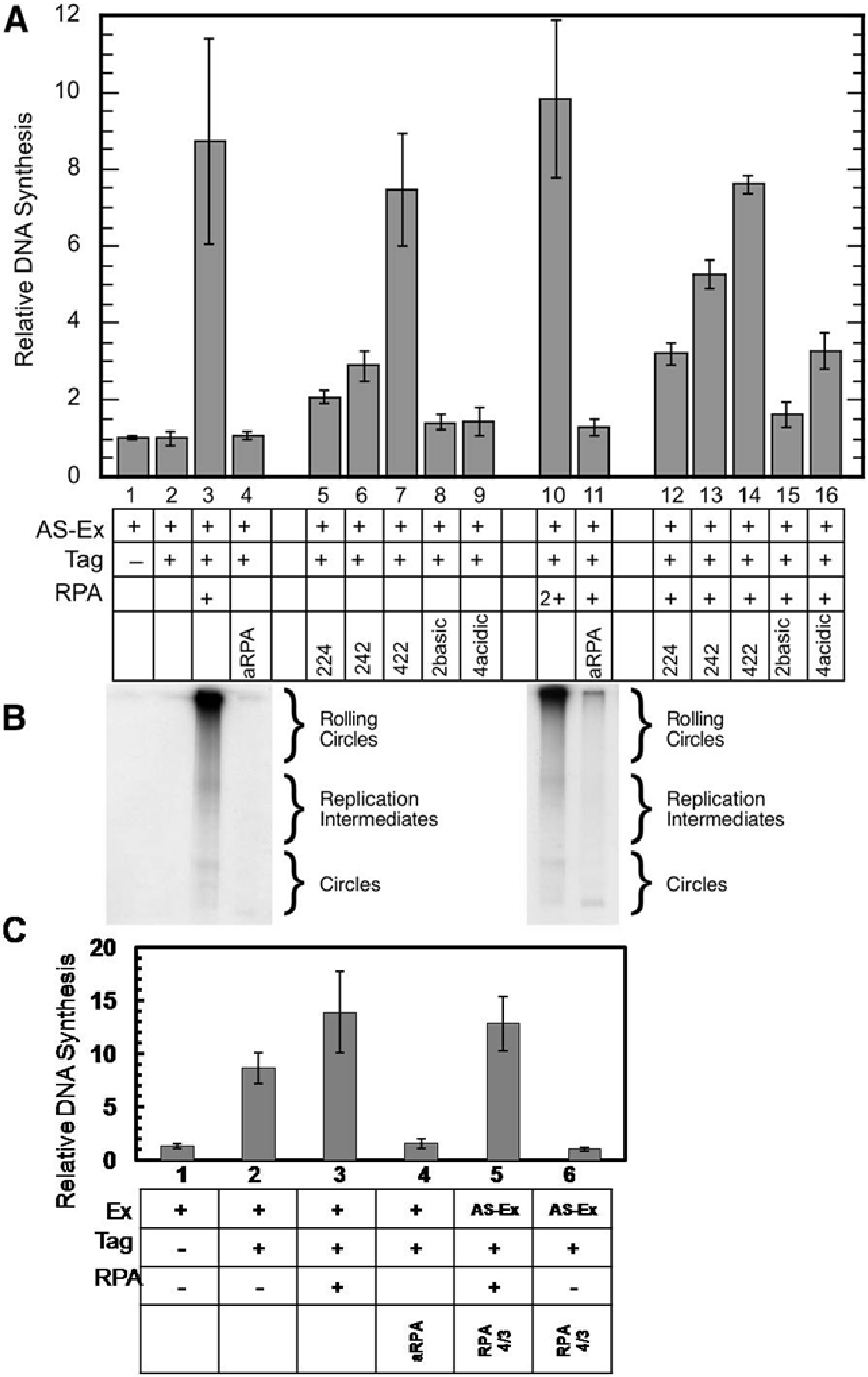
A
Relative DNA Synthesis
0
2
4
6
8
10
12
1 2 3 4 5 6 7 8 9 10 11 12 13 14 15 16
AS-Ex + + + + + + + + + + + + + + + +
Tag – + + + + + + + + + + + + + + +
RPA + 2+ + + + + + +
aRPA 224 242 422 2basic 4acidic aRPA 224 242 422 2basic 4acidic
B
Rolling Circles
Replication Intermediates
Circles
Rolling Circles
Replication Intermediates
Circles
C
Relative DNA Synthesis
0
5
10
15
20
1 2 3 4 5 6
Ex + + + + AS-Ex AS-Ex
Tag - + + + + +
RPA - - + + -
aRPA RPA 4/3 RPA 4/3

Figure 2-6: Function in elongation and Tag interactions.

(A) SV40 Elongation assay. Two stage SV40 elongation assays were carried out as described in Methods. A plus in the table indicates the addition of 300 ng RPA in stage I or 300 ng of the indicated form of RPA in stage II. 100 μg HeLa cytosolic extract (ammonium sulfate precipitated; AS-Ex) and 0.2-0.5 μg SV40 large T antigen (Tag) were added to all reactions. Three independent experiments with all reactions done in duplicate were completed. The data from each experiment were normalized to the minus Tag and RPA control (bar 1) for that experiment, averaged and plotted. Maximal DNA synthesis for individual experiments ranged from 128-135 pmoles. Error bars represent standard deviation for the combined data. (B) Interactions of aRPA or RPA with Tag monitored by ELISA [117]. Lines drawn indicate the average of two independent experiments: aRPA (blue triangle), RPA (orange square). Microtiter plate wells were coated with 1 μg of indicated protein for 1 hr, blocked and washed. Indicated quantities of SV40 large T antigen (Tag) were then incubated in each well for 1hr. After washing, wells were incubated sequentially with Pab419 SV40 Tag antibody [134] and peroxidase conjugated secondary antibody each for 1 hr. After the final incubation, the wells were washed and developed using 200 μL of 0.8 mg/ml o-phenylenediamine in a 0.50 M phosphate-citrate buffer and absorbance at 450 nm determined. All steps carried out at room temperature. (C) DNA unwinding assay. Reactions contained Tag (0.9 μg), ATP (4 mM), DNA (pUC.HSO, 100 ng), Topo I (10 ng), RPA (250 ng) and aRPA (250 ng) where indicated. Reactions were separated in 1.3% agarose gels and DNA was visualized with ethidium bromide.

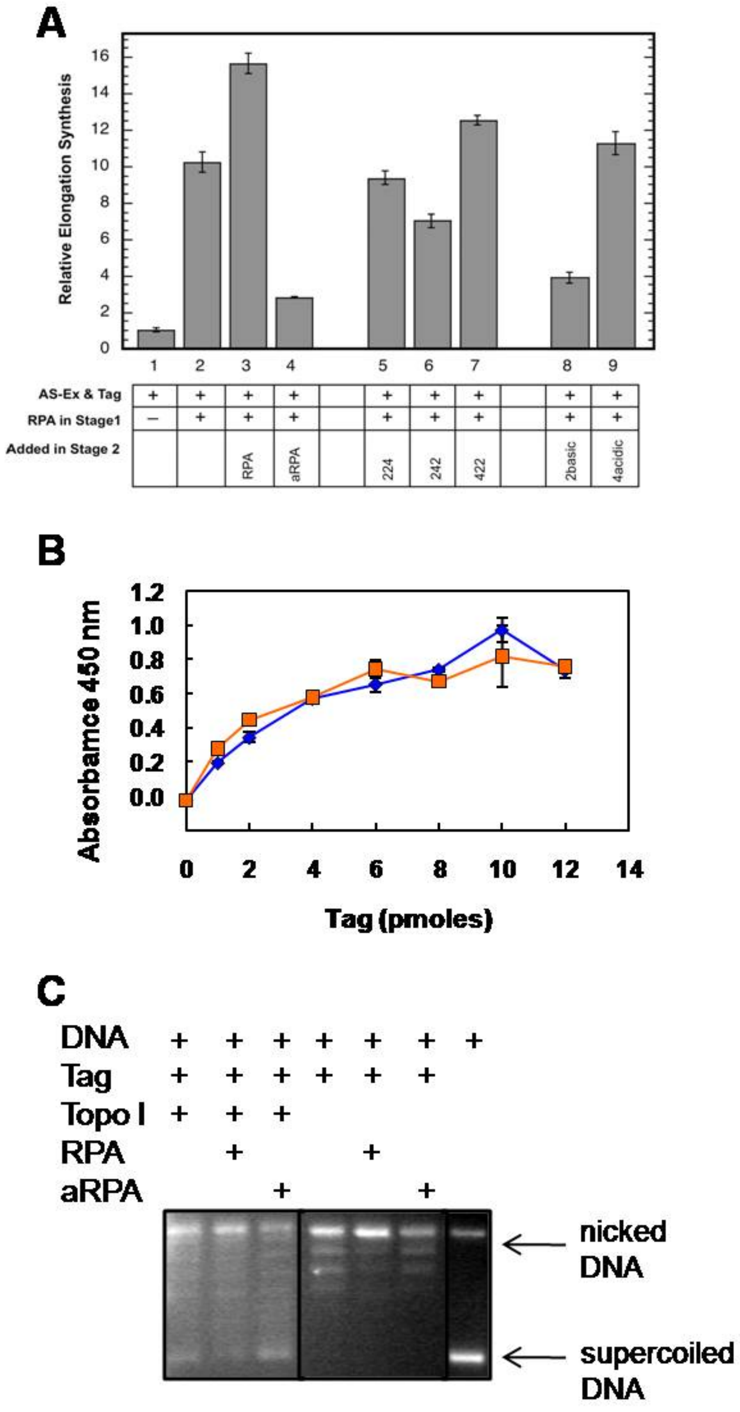
A
Relative Elongation Synthesis
0
2
4
6
8
10
12
14
16
1 2 3 4 5 6 7 8 9
AS-Ex & Tag + + + + + + + + +
RPA in Stage1 – + + + + + + + +
Added in Stage 2
RPA
aRPA
224
242
422
2basic
4acidic
B
Absorbamce 450 nm
0.0
0.2
0.4
0.6
0.8
1.0
1.2
0 2 4 6 8 10 12 14
Tag (pmoles)
C
DNA + + + + + + +
Tag + + + + + +
Topo I + + +
RPA + +
aRPA + +
nicked DNA
supercoiled DNA

Figure 2-7: Schematic showing observed properties for RPA2, RPA4 and RPA2 hybrids.

Schematic showing observed properties for RPA2, RPA4 and RPA2 hybrids.

Form	PD DBD WH	Trimer Formation	ssDNA Binding	SV40 Replication	Inhibition of Repliction Stage I	Stage II
RPA2	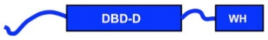	yes	yes	yes	supports	supports
RPA4	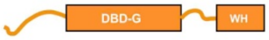	yes	yes	no	inhibits	inhibits
2basic	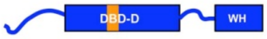	yes	yes	no	inhibits	inhibits
4acidic	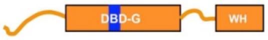	yes	yes	no	partial	no effect
422	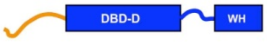	yes	yes	yes	no effect	no effect
242	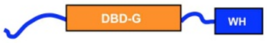	yes	yes	intermediate	partial	partial
224	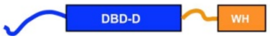	yes	yes	no	partial	no effect

CHAPTER 3

AN ALTERNATIVE FORM OF RPA EXPRESSED IN NORMAL HUMAN TISSUES SUPPORTS DNA REPAIR

Abstract

Replication Protein A (RPA) is a heterotrimeric protein complex required for a large number of DNA metabolic processes, including DNA replication and repair. An alternative form of RPA (aRPA) has been described in which the RPA2 subunit of canonical RPA is replaced by a homologous subunit, RPA4. The normal function of aRPA is not known; however, previous studies have shown that it does not support DNA replication *in vitro* or S-phase progression *in vivo*. In this work, I show that the *RPA4* gene is expressed in normal human tissues and that its expression is decreased in cancerous tissues. To determine if aRPA plays a role in cellular physiology, aRPA was investigated in DNA repair. aRPA interacted with both Rad52 and Rad51 and stimulated Rad51 strand exchange. aRPA can also support the dual incision/excision reaction of nucleotide excision repair. aRPA is less efficient in nucleotide excision repair than canonical RPA, showing reduced interactions with the repair factor XPA and no stimulation of XPF-ERCC1 endonuclease activity. In contrast, aRPA exhibits higher affinity for damaged DNA than canonical RPA, which may explain its ability to substitute for RPA in the excision step of nucleotide excision repair. These findings provide the first direct evidence for the function of aRPA in human DNA metabolism and support a model for aRPA functioning in chromosome maintenance functions in non-proliferating cells.

Introduction

Nucleotide excision repair is the main mechanism in humans for the removal of helix-distorting lesions from DNA induced by agents such as UV light from the sun [70-72]. This multi-component excision repair reaction requires six repair factors that recognize the lesion-containing DNA and make dual incisions bracketing the base adduct to remove (excise) the damaged base(s) in 24-32 nucleotide-long oligonucleotides. One of the six core excision repair factors is RPA [73]. RPA is thought to participate in multiple steps in excision repair [70, 71, 76]. It appears to play an important role in damage recognition because of its higher affinity for damaged DNA than undamaged DNA [76, 77]. RPA and XPA act cooperatively in DNA damage recognition [78, 81, 83], and the presence of RPA in the various “preincision complexes” [83, 84] that can be detected on damaged DNA prior to lesion removal provides additional evidence for a role of RPA in promoting or stabilizing the proper assembly of the excision nuclease. In addition, RPA participates in the dual incision by stimulating the XPF-ERCC1 endonuclease [42, 86, 87]. Lastly, RPA has been implicated in the coordination of DNA synthesis after removal of DNA lesions [88]. Because RPA appears to have multiple roles in excision repair, the ability of aRPA to replace the canonical RPA in carrying out the excision reaction by the six-factor ensemble was examined.

A pathway that allows cells to repair double-stranded DNA breaks is homology directed repair [60]. This form of repair uses homologous recombination and is dependent on proteins in the *RAD52* epistasis group, including Rad51 and Rad52, and RPA [60]. Rad51 is central to this process, forming filaments on single-strand DNA and mediating strand exchange [60, 61]. The other *RAD52* epistasis group proteins (and other mediators) modulate filament formation and regulate recombination [60, 66]. RPA interacts with both Rad51 and Rad52 [63-65], and these interactions are thought to mediate the formation of the Rad51 filament needed for efficient recombination [135-137].

I show that *RPA4* is expressed in all normal human tissues examined but at different levels in different tissues. *RPA4* expression is reduced in cancerous tissues and is very low in human cell lines. In addition, aRPA can support the dual incision/excision reaction, albeit less efficiently and by a different mechanism than RPA. aRPA can also support the initial steps of recombination such as Rad51 dependent DNA strand exchange. These results provide the first evidence for a physiological function of aRPA in human DNA metabolism.

Materials and Methods

Protein Purification

Recombinant RPA and aRPA were expressed in BL21 (DE3) cells and purified as previously described [116, 117, 138]. The purification of the core nucleotide excision repair factors, XPA, XPC, XPF-ERCC1, XPG, and TFIIH was reported earlier [139]. Recombinant DNA, Rad51 and Rad52 were purified as described previously [65, 140].

Quantitative PCR

RNA from cell lines was isolated using Qiagen RNeasy Mini Kit according to manufacturer's protocol. Normal human RNA was purchased from Ambion as the FirstChoice Human Total RNA Survey Panel (Table 3-1) and tumor RNA was purchased from Ambion as FirstChoice Human Tumor RNA. cDNA was generated using *Taq*Man Reverse Transcription Reagents according to the manufacture's protocol using oligo $d(T)_{16}$ and 2 μg total RNA in a 20 μL RT reaction.

Quantitative PCR was carried out using *Taq*Man Universal PCR Master Mix according to the manufacture's recommendations using the following primers and probes: *GAPDH* – primers: 5'-GCACCACCAACTGCTTAGCA-3', 5'-GTCTTCTGGGTGGCACTGATG-3'; probe: 5'-TET-TCGTGGAAGGACTCATGACCACAGTCC-Black Hole Quencher-3' *RPA2* – primers: TTGTTTGAAGCTCAGAGGGAGAT-3', 5'-GGTAGCATCCTTCCAATTCCAT3'; probe: 5'-6-FAM-CCCACCCTGGATTGCATCCC-Black Hole Quencher-3' *RPA4* – primers: 5'-CTCATCAGGAAGGGAAGAGCAT-3', 5'-GCCCTCAACGGTCAGATAATCA-3'; probe: 5'-JOE NHS Ester-

AGCTCCGGGCTCAGCTCTGC-Black Hole Quencher-3’. Data was analyzed using SDS2.3 software by Applied Biosystems. All data was compared using the comparative C_T method [141]. All probe pairs amplify their target with equal efficiency (Figure 3-1D).

Enzyme-Linked Immunosorbent Assay (ELISA)

All incubations were carried out at 25°C as described previously [117]. Wells in microtiter plates were coated with 1 μg of RPA or aRPA for interactions with XPA and 1 μg of Rad51 or Rad52 in 50 μL of water and incubated for 1 hour. Plates were washed with phosphate buffered saline (PBS) with 0.2% Tween 20 three times to remove unbound protein. Plates were blocked with 300 μL of 5% milk in PBS for 10 min and washed. The indicated amount of XPA, RPA, aRPA, or BSA was added to each well, incubated for 1 hour, and washed. Primary antibodies in PBS with 5% milk for XPA (1:100), RPA/aRPA (1:300) were added to the plates, incubated for 30 min, and washed. Goat-α-mouse IgG-HRP (1:1000) in 50 μL of PBS with 5% milk was added to the plates, incubated for 30 min, and washed. Plates were developed using 200 μL of 0.8 mg/mL o-phenylenediamine in 0.005 M phosphate citrate buffer with 0.03% sodium perborate. OD_{450} was then quantified after 10 – 60 min using a microtiter plate reader. Background was determined by using BSA as the secondary protein and all data shown have these values subtracted. In all assays, the background values were similar and close to zero.

Excision Repair Assay

The assay measures the release of base lesions in the form of 24-32 nucleotide-long oligomers [142]. An internally ^{32}P-labeled 140-bp DNA substrate containing a single centrally located (6-4) UV photoproduct was prepared as described [139] by ligating and annealing four oligonucleotides one of which was radiolabeled and contained a T-T (6-4) photoproduct. The oligomer containing the (6-4) photoproduct was from the Synthetic Organic Chemistry Core at the University of Texas Medical Branch, Galveston, TX. Sequences of the oligomers: 18-1: 5’-CTAGCGGGATCCGGTGCA, 18-2: 5’-AATTCGTAGATCTGCGTC-3’, 64-A: 5’-GACGCAGATCTACGAATTTCCTTAATTCCTTGCACCGGATCCCGCTAG-3’, 6-4PP: 5’-AGGAAT-TAAGGA-3’, Unmodified – 5’- AGGAATTAAGGA-3’. Excision assays involved incubation of 5 fmol of substrate in a 10 μL reaction containing the essential excision repair factors (XPA, XPC, XPF-ERCC1, XPG and TFIIH) and either RPA or aRPA, using conditions described previously [139]. Excision products were separated on DNA sequencing gels and detected with a Phosphorimager. The excision repair activity was quantified using ImageQuant 5.2 software (Molecular Dynamics).

Immunoblotting

Conventional immunoblotting techniques were used to detect the indicated proteins using antibodies that recognize RPA1 (Santa Cruz sc-28304), RPA2 (Calbiochem NA18), RPA4 (Abnova H00029935-B01), and maltose-binding protein (MBP) (Santa Cruz sc-809).

DNA Strand Exchange Assay

DNA strand exchange reaction (20 μL) was performed as described previously [140, 143]. Briefly, 15 μM φX174 viral (+)-strand (nucleotide) DNA was incubated with 3.75 μM Rad51 in buffer containing 25 mM TrisOAc pH 7.5, 2 mM ATP, 1 mM $MgCl_2$, 2 mM $CaCl_2$, at 37 °C. After 5 min, RPA or aRPA (1 μM) was added and incubation continued for 5 min. The reaction was started by addition of *XhoI*-linearized ^{32}P-labeled φX174 dsDNA (15 μM). After 2 hr at 37 °C, the samples were treated with Proteinase K (Roche) for 15 min at 37 °C. The reaction products were separated by electrophoresis on a 1% agarose gel (1 X TAE) at 40V overnight. The gels were dried and analyzed on a Molecular Dynamics Storm 840 PhosphorImager using ImageQuant Software.

Results

RPA4 mRNA is Found in Normal Human Tissues

The initial characterization of RPA4 by Keshav et al. examined three human tissues for the presence of RPA4 protein [109]. They showed that RPA4 protein was detectable in placental and colon tissue but not in kidney. If RPA4 is playing a general physiological role in cellular DNA metabolism, it would be expected to be expressed in a variety of tissues. To determine the normal distribution of RPA4, mRNA expression in a panel of human tissues was determined by quantitative PCR.

Since it was not known which tissues normally express *RPA4*, I carried out initial studies on HeLa cells transiently expressing a plasmid containing *RPA4* under control of a CMV promoter. These cells express RPA4 protein at high levels [110]. PCR amplification of cDNA from untransfected and transfected HeLa cells was compared. Messenger RNA levels for *RPA2* and *RPA4* were then compared using *GAPDH* as a reference. HeLa cells transfected with the *RPA4* plasmid express *RPA4* at levels greater than endogenous *RPA2* (Figure 3-1A, right two columns). In contrast, mock transfected HeLa cells do not have an appreciable amount of *RPA4* mRNA (Figure 3-1A). The endogenous level of *RPA4* mRNA is close to the level of detection of this assay and may not be statistically significant. I also examined other stable human cell lines (for example HEK-293 and HepG2) and did not find significant expression of *RPA4* in any of the lines tested (Figure 3-1C).

RNA from 20 different normal adult tissues was analyzed for *RPA2* and *RPA4* expression. In agreement with the protein studies by Keshav and coworkers [109], *RPA4* mRNA was detected at levels above *RPA2* mRNA in placental tissue (Figure 3-1A). *RPA4* mRNA was also detected at levels similar to or above *RPA2* mRNA in a number of tissues including bladder, colon, esophagus, lung and prostate. In other tissues, *RPA4* was expressed at levels less than 20% of the total middle subunit mRNA (*RPA2* mRNA +

RPA4 mRNA) include brain, kidney, ovary and spleen (Figure 3-1A). The remaining tissues expressed *RPA4* at intermediate levels. These results are consistent with an initial analysis of RPA4 protein levels in placenta and colon tissues (Figure 3-1E) and the analysis performed by Keshav and coworkers [109]. Similar variations were observed for *RPA2* mRNA (Figure 3-1A). For example, heart, liver and skeletal muscle all have low amounts of *RPA2* mRNA compared to ovary, spleen, testes and thyroid, which have the most *RPA2* mRNA in the tissues sampled. I conclude that all normal adult tissues examined transcribe *RPA4* at significant levels and, although there is tissue specific variation, in many tissues *RPA4* mRNA levels are comparable to the *RPA2* mRNA.

To determine whether *RPA4* was also expressed in cancerous tissues, RNA from several types of tumors was examined. *RPA4* mRNA was expressed at reduced levels in tumors from cervix, colon, kidney and liver when compared to non-matched normal adult tissue (Figure 3-1B). In three out of the four tissues compared, the levels of *RPA2* mRNA increased. This is in agreement with the literature that has found increased expression of RPA in metastatic cancers [6, 7]. These data, together with the finding that *RPA4* is not expressed at significant levels in stable cultured cell lines suggests that *RPA4* is down regulated in transformed cells. This supports the hypothesis that RPA4 plays a role in normal adult tissues but not in tissues with a large fraction of proliferating cells, such as tumors. However, further studies are needed to determine the cell-type expression profile of *RPA4,* as there are cells with different proliferative capacity within a given tissue. For example, in colon tissue, cell proliferation is limited to the lower one-third of the crypts [144]. Based on our hypothesis, *RPA4* expression would not occur in this region.

aRPA Supports Rad51 Dependent Strand Exchange

I next examined the ability of aRPA to interact with Rad51 and Rad52 which are required for homologous recombination. aRPA interacted with Rad52 at a level similar to RPA even though Rad52–RPA interactions are mediated through both RPA1 and RPA2 ([65]; Figure 3-2A). In contrast to Rad52, aRPA exhibited a decreased interaction with Rad51 when compared to RPA (Figure 3-2A). Rad51 also interacts with both RPA1 and RPA2 [63, 145]. To explore domains involved in the altered interactions I also examined interactions with a mutant form of RPA1 composed solely of two copies of a fragment of the core DNA binding domain that does not form a complex with RPA2 and RPA3, AA-His (containing residues 177-303 of RPA1; [43]). This fragment interacts with Rad51 to the same level as aRPA (Figure 3-2B). I conclude that in aRPA, the interaction between RPA2 and Rad51 was lost but that Rad51–RPA1 interaction was retained.

To investigate whether the altered interactions with Rad51 affected function, Rad51 dependent DNA strand exchange assays were performed by collaborators, Aura Carreira and Dr. Steve Kowalczykowski (University of California, Davis). It has been shown that RPA can stimulate DNA strand exchange by Rad51 *in vitro* [146]; shown schematically in Figure 3-2C). When compared to RPA, aRPA can stimulate the Rad51 DNA strand exchange as well as RPA. Both RPA and aRPA extensively stimulate formation of nicked circular dsDNA and the slower migrating joint molecules of which none are detected in the absence of RPA or aRPA (Figure 3-2D) [147]. These data suggest that aRPA can support the central steps of recombination.

aRPA Substitutes for RPA in Nucleotide Excision Repair

I established a collaboration with Dr. Aziz Sancar's laboratory to determine whether the RPA4-containing aRPA protein supports nucleotide excision repair. I am including this data, generated by Dr. Michael Kemp of Dr. Aziz Sancar's (University of North Carolina) laboratory, because it is key support for my conclusions. aRPA or RPA was incubated in reactions containing the other 5 excision repair factors (XPA, XPC-HR23B, TFIIH, XPF-ERCC1, and XPG) and an internally ^{32}P-labeled 140-bp DNA substrate containing a site-specific (6-4) UV photoproduct (Figure 3-3A) [147]. The excision assay involves damage recognition and dual incisions of the damaged strand at 20±5 nt 5' and 6±3 nt 3' to the damage, resulting in the release of damage-containing oligomers 24- to 32-nt in size that can be visualized on a denaturing polyacrylamide gel [139, 142]. As seen in Figure 3-3B (lanes 1-4) and in agreement with previous reports [73-75], the excision exhibits absolute requirement for RPA. Significantly, aRPA can be substituted for RPA in the excision reaction (Figure 3-3B, lane 7) [147]. However, at equimolar concentrations, aRPA is less effective than canonical RPA (Figure 3-3B, lanes 3-4 and 5-6) and about a 3- to 4-fold higher concentration of aRPA is required to achieve similar levels of excision as the reaction reconstituted with RPA. Further increase in aRPA concentration did not increase the excision efficiency and actually had a modest inhibitory effect (lanes 8 and 9) [147]. These results indicated that even though aRPA can substitute for RPA in the excision reaction it does so with lower efficiency.

Next, they carried out a kinetic experiment to determine whether aRPA affected the rate or the extent of the excision reaction. They used the concentrations that were determined to be optimal for RPA and aRPA in the excision assays in Figure 3-3B for the kinetic assays. The results shown in Figure 3-3C, D show that under these conditions the rate of excision by aRPA reconstituted excision nuclease is approximately two times slower than the rate with the canonical RPA [147]. Taking into account that the optimal aRPA concentration for the excision assay is about 3-fold higher than that of RPA it can be stated that aRPA exhibits 5- to 8-fold lower activity in reconstituting excision nuclease. It should be noted that the lower activity of aRPA compared to RPA was seen with two independent preparations of aRPA and RPA and thus must reflect the intrinsic properties of these proteins. However, even though there is a difference in activity, it is clear that aRPA can substitute for RPA in this important cellular process. This finding provides additional direct evidence for aRPA functioning in cellular DNA metabolism.

aRPA Does Not Stably Bind XPA

Next I determined whether aRPA bound to the excision repair factor XPA. It is known that XPA, along with RPA and XPC is involved in the initial steps of damage recognition of DNA lesions inducing distortion to the DNA duplex [72, 148] and that both RPA1 and RPA2 interact with XPA [79, 80] enabling cooperative binding of RPA and XPA to damaged DNA [77, 78, 83]. ELISAs were done to examine the direct interaction between purified aRPA and XPA. As shown in Figure 3-4A, RPA shows a strong interaction with XPA as previously reported [78, 79, 81]. However, aRPA has a reduced interaction with XPA when compared to RPA.

To investigate the stability of the aRPA-XPA interaction, Dr. Kemp immobilized MBP-tagged XPA on amylose resin and then incubated it with either RPA or aRPA. The resin was separated from the solvent by centrifugation and the resin-bound proteins were detected by SDS-PAGE and western blotting using antibodies recognizing RPA1, RPA2, and RPA4. Although RPA2 and RPA4 show significant sequence homology the antibodies against these proteins do not cross-react (Figure 3-4B). Consistent with the well-described interaction of RPA with XPA [78, 79, 81], RPA binds to the MBP-XPA resin, as indicated by the presence of both RPA1 and RPA2 subunits in the XPA pull-down (Figure 3-4C). In contrast, neither RPA1 nor RPA4 were pulled down with the MBP-XPA resin when aRPA was used in the binding experiment (Figure 3-4C lanes 3 and 6) [147]. These results indicate that the RPA2 subunit of RPA plays a critical role in stabilizing the interaction of the heterotrimeric complex with XPA, consistent with earlier observations [77, 82]. These data indicate that aRPA can interact with XPA but that the complex is less stable *in vitro* than the RPA-XPA complex. This difference may contribute to the reduced efficiency of aRPA in excision nuclease reconstitution (Figure 3-3). However, the finding that aRPA can support excision in the reconstituted reaction indicates that RPA-XPA interaction, although important for efficient excision nuclease activity, is not essential for the assembly of the holoenzyme dual incision complex on DNA.

Other Functions of aRPA in Nucleotide Excision Repair

The data summarized in this section was generated by Dr. Kemp of the Sancar laboratory and is included as support of my findings. RPA plays multiple roles in nucleotide excision repair, including stimulation of XPF-ERCC1 nuclease activity, binding to XPA to aid in cooperative recognition of DNA damage and finally directly recognizing damaged DNA. To gain an insight into the lower activity of aRPA in the overall excision reaction they tested aRPA for each of these partial excision reactions.

The role of XPF-ERCC1 in excision repair is to make the 5’ incision of the dual incision reaction. It has previously been found that RPA stimulates the structure-specific endonuclease activity of XPF-ERCC1. To determine whether aRPA functions like RPA in the stimulation of XPF-ERCC1, either RPA or aRPA were examined in XPF-ERCC1 stimulation assays. As expected, RPA stimulated the junction cutting activity of XPF-ERCC1. No stimulation was observed with aRPA and at high concentrations of the protein the intrinsic junction cutting activity of XPF-ERCC1 was inhibited by aRPA [147].

It has been shown that XPA and RPA bind to damaged DNA cooperatively [77, 78, 80, 83]. To examine if aRPA has a similar activity, XPA and RPA or aRPA were incubated with plasmid DNA containing AAAF-guanine adducts and immobilized on magnetic beads. Drs. Kemp and Sancar found that RPA stimulated the association of XPA with damaged DNA but aRPA did not. Control studies with DNA alone showed that RPA had a modest preference (~2-fold) for damaged over undamaged DNA under these experimental conditions, which is consistent with earlier measurements [76, 83], approximately 20-fold more aRPA associated with the AAAF-damaged DNA compared to undamaged DNA. This increased affinity of aRPA to alkylated DNA may account for its ability to support NER even though it appears to lack some of the other nucleotide excision repair related interactions.

Discussion

These results provide the first direct evidence for a physiological function for human aRPA. My collaborators and I show that aRPA is able to support the dual incision/excision steps of NER and support Rad51-dependent DNA strand exchange. These results are consistent with aRPA having a role in cellular DNA maintenance.

I also show that *RPA4* is expressed in normal adult human tissues and that, while expression varies between tissues, *RPA4* mRNA levels are in the same range as *RPA2* in many tissues. The relative mRNA levels in tissues range from *RPA2* being several times higher than *RPA4* to *RPA4* being several times higher than *RPA2*. Biochemical analysis of recombinant protein indicates that aRPA forms with similar efficiency to canonical RPA (Chapter 2). The stability of the RPA2 and RPA4 proteins are similar when expressed in tissue culture cells [110]. Thus, it is likely that the ratio of RPA and aRPA complexes in cells will be proportional to their respective messenger RNA levels.

RPA4 mRNA expression is decreased in tumors relative to normal adult tissue. *RPA4* expression is also very low in proliferating cell lines. These findings are consistent with the original analysis of RPA4 that suggested that it was primarily expressed in non-proliferating tissues [109]. *RPA4* also appears to be expressed higher in tissues that are exposed to harsh environments that would promote DNA damage. For example, *RPA4* is expressed at similar levels to *RPA2* in bladder, colon, esophagus, lung and small intestine. Even though these tissues are continually renewing themselves through proliferation, the increase in DNA damage from environmental exposur must be dealt with. It is possible that *RPA4* is differentially expressed within these tissues where expression is higher in cells exposed to the harsh environment and lower where the cells are dividing. However, further studies will be needed to address the cell type expression of *RPA4* within a given tissue. Together these results are consistent with aRPA functioning in DNA maintenance in predominantly non-proliferating cells.

aRPA's ability to substitute for RPA in a reconstituted nucleotide excision repair system is unambiguous as this repair system has absolute requirement for RPA for the excision reaction [70, 71]. However, aRPA exhibits lower activity compared to RPA in the excision assay. This may be explained by the reduced stability of the aRPA-XPA complex or its failure to stimulate the activity of the repair endonuclease XPF-ERCC1. Interestingly, aRPA appears to have higher affinity for alkylated DNA than canonical RPA and this property of aRPA may partially compensate for its apparent lack of interactions with XPA and XPF-ERCC1. However, how aRPA interacts with other types of DNA damage repaired by NER remains to be determined. These findings suggest that both RPA and aRPA can support NER in cells expressing RPA4.

These data indicate that although an interaction of the RPA2 subunit of RPA with XPA may aid in dual incision, the interaction is not essential for repair. This conclusion is consistent with a previous report that showed that XPA-deficient cells expressing an N-terminal truncated form of XPA that is unable to interact with RPA2 shows little or no defect in nucleotide excision repair as evidenced by essentially the same UV survival as cells expressing full-length XPA [80, 82]. Thus, an RPA1-XPA interaction, which would be expected to be shared in both the canonical and alternative forms of RPA, is likely sufficient for excision repair.

aRPA is also able to interact with two proteins essential for DNA recombination, Rad52 and Rad51. A decrease in the interaction with Rad51 similar to that with XPA was observed. However, aRPA is still able to support Rad51 dependent DNA strand exchange in spite of the reduced interaction indicating that the interaction between RPA1 and Rad51 is sufficient for this reaction. These results suggest aRPA may also be able to support recombination. The model that aRPA functions in non-proliferating cells predicts that the primary role of aRPA in recombination would be in recombination-mediated double-strand break-repair.

Protein interactions are essential for the function of canonical RPA. Several domains of RPA including the C-terminus of RPA2 have been found to interact with multiple protein partners [18]. Structural studies have indicated that the C-terminus of RPA2 makes direct contacts with similar motifs in the repair and recombination factors XPA, UNG2, and Rad52 [149]. SV40 large T antigen also interacts with this domain but through a different motif [126]. Strikingly, interactions between aRPA and these different protein partners vary considerably. An early study found that RPA2 but not RPA4 interacted with UNG2 in a yeast two-hybrid analysis [91]. I show here that aRPA has a reduced interaction with XPA but that the Rad52-aRPA interaction is the same as the Rad52-RPA interaction. In addition, aRPA has reduced interactions with Rad51 (Figure 3-3) but unchanged interactions with SV40 T antigen [138]. Rad51, Rad52, T antigen and XPA all interact with both RPA1 and RPA2 [18]. Thus, multiple domains contribute to interactions between aRPA and protein partners and it appears that there is redundancy in the interactions essential for function.

It is also important to note that RPA is an abundant protein in human cells. It has been estimated that the concentration of canonical RPA ($3x10^4 – 2x10^5$ molecules/cell, 10 μM in the nucleus) in a normal cell is high enough to make single-stranded DNA-binding stoichiometric under physiological conditions [1]. Thus, RPA and aRPA are probably not limiting under most conditions *in vivo*. Therefore, even if aRPA has reduced protein interactions or supports repair less efficiently, this may not significantly limit these processes in the cell.

aRPA does not support SV40 DNA replication *in vitro* [138] and it has further been demonstrated that the aRPA prevents the loading of pol α but can support DNA synthesis by pol δ (Chapter 4). Therefore, the excision gaps coated with aRPA should support repair synthesis, which requires the concerted action of RFC, PCNA and pol δ.

Similarly, it remains to be determined whether the excision gaps covered with aRPA are as effective as those containing RPA in activating the ATR-mediated DNA damage response signaling [100, 150]. Clearly, additional work will be necessary to better understand the differences in mechanisms by which RPA and aRPA contribute to many DNA maintenance reactions that govern genomic stability.

Table 3-1: Source of FirstChoice® Total Human RNA used for quantitative PCR.

Tissue	Gender	Age	Race	C.O.D./Other
Adipose				
1	F	68	Caucasian	breast cancer/mets to lung and lymph nodes
2	M	42	Caucasian	Alzheimer's disease
3	F	30	Caucasian	Breast reduction surgery
Bladder				
1	M	80	Caucasian	Cardiopulmonary arrest
2	M	79	Caucasian	Cardiac arrest
3	F	58	Caucasian	Cardiopulmonary arrest
Brain				
1	M	61	Unknown	Cardiopulmonary arrest
2	M	23	Caucasian	Cardiac arrest
3	M	81	Caucasian	Congestive heart failure
Cervix				
1	F	50	Caucasian	Total abdominal hysterectomy
2	F	40	African American	unknown
3	F	49	Caucasian	Surgery-bilateral salpingo-oophorectomy
4	F	45	Caucasian	Total abdominal hysterectomy
Colon				
1	M	23	Caucasian	Blunt force trauma
2	F	78	Caucasian	Congestive heart failure
3	F	75	Unknown	Congestive heart failure
Esophagus				
1	F	74	Caucasian	Chronic obstructive pulmonary disease
2	F	68	Caucasian	Myocardial infarction
3	M	74	Caucasian	Cardiac arrest
Heart				
1	F	70	Caucasian	Alzheimer's disease
2	M	77	Caucasian	Cerebral vascular accident
3	M	71	Caucasian	Congestive heart failure
Kidney				
1	F	60	Caucasian	Sub-arachnoid hemorrhage
2	F	63	African American	Intracranial bleed
3	F	62	Hispanic	Intracranial bleed
Liver				
1	M	69	Unknown	Intracranial hemorrhage
2	M	64	Caucasian	Intracranial hemorrhage
3	F	70	Caucasian	Chronic obstructive pulmonary disease
Lung				
1	F	94	Caucasian	Cardiac arrest
2	M	65	Caucasian	Myocardial infarction
3	M	46	Caucasian	Intracranial hemorrhage

Table 3-1: Continued.

Ovary				
1	F	45	Caucasian	N/A - sample obtained from hysterectomy
2	F	42	Caucasian	N/A - total abdominal hysterectomy
3	F	34	Caucasian	N/A - sample obtained from hysterectomy
4	F	61	Caucasian	N/A - sample obtained from hysterectomy
Placenta				
1	F	33	Caucasian	Child birth
2	F	N/A	Caucasian	Child birth
3	F	N/A	Caucasian	Child birth
Prostate				
1	M	79	Caucasian	Alzheimer's disease
2	M	79	Caucasian	Chronic obstructive pulmonary disease
3	M	72	Caucasian	unknown
Skeletal Muscle				
1	F	84	Caucasian	Respiratory arrest
2	F	55	Caucasian	Uterine cancer
3	F	79	Caucasian	Cardiac arrest
Small Intestine				
1	M	85	Caucasian	Intracranial hemorrhage
2	F	40	Caucasian	Hemorrhagic stroke
3	M	15	Caucasian	Anoxia
Spleen				
1	M	70	Caucasian	Anoxia
2	M	39	African American	Motor vehicle accident
3	M	50	Caucasian	Cerebral vascular accident
Testes				
1	M	75	Caucasian	Respiratory arrest
2	M	19	Caucasian	Anoxic encephalopathy
3	M	53	Caucasian	Colon cancer
Thymus				
1	M	78	Caucasian	Respiratory arrest
2	M	25	Caucasian	Gun shot wound
3	M	24	Caucasian	Trauma
Thyroid				
1	M	78	Caucasian	Aortic rupture
2	M	87	Caucasian	Lung cancer
3	F	69	Caucasian	Gall bladder cancer
Trachea				
1	M	20	African American	Suicide
2	F	78	Caucasian	Congestive heart failure
3	M	72	Caucasian	Chronic obstructive pulmonary disease

Figure 3-1: Quantitative PCR of *RPA4* and *RPA2* mRNA from different tissues.

Relative mRNA expression of *RPA2* (blue) and *RPA4* (orange) was determined by the comparative Ct method. Errors bars indicate the average of three technical and two experimental replicates. (A) cDNA was made from a panel of 20 normal human tissues **(**Ambion**)**, HeLa cells either mock transformed and HeLa cells transformed with GFP-*RPA4* fusion protein under the control of the CMV promoter [110]. (B) cDNA made from normal and tumor tissue samples (Ambion). (C) cDNA was made from established cell lines. (D) Efficiency of primer sets and probes used for quantitative PCR. (E) Immuno-blot of whole tissue lysates (ProSci Incorporated) from placenta, colon, liver and kidney. Recombinant aRPA was used a positive control.

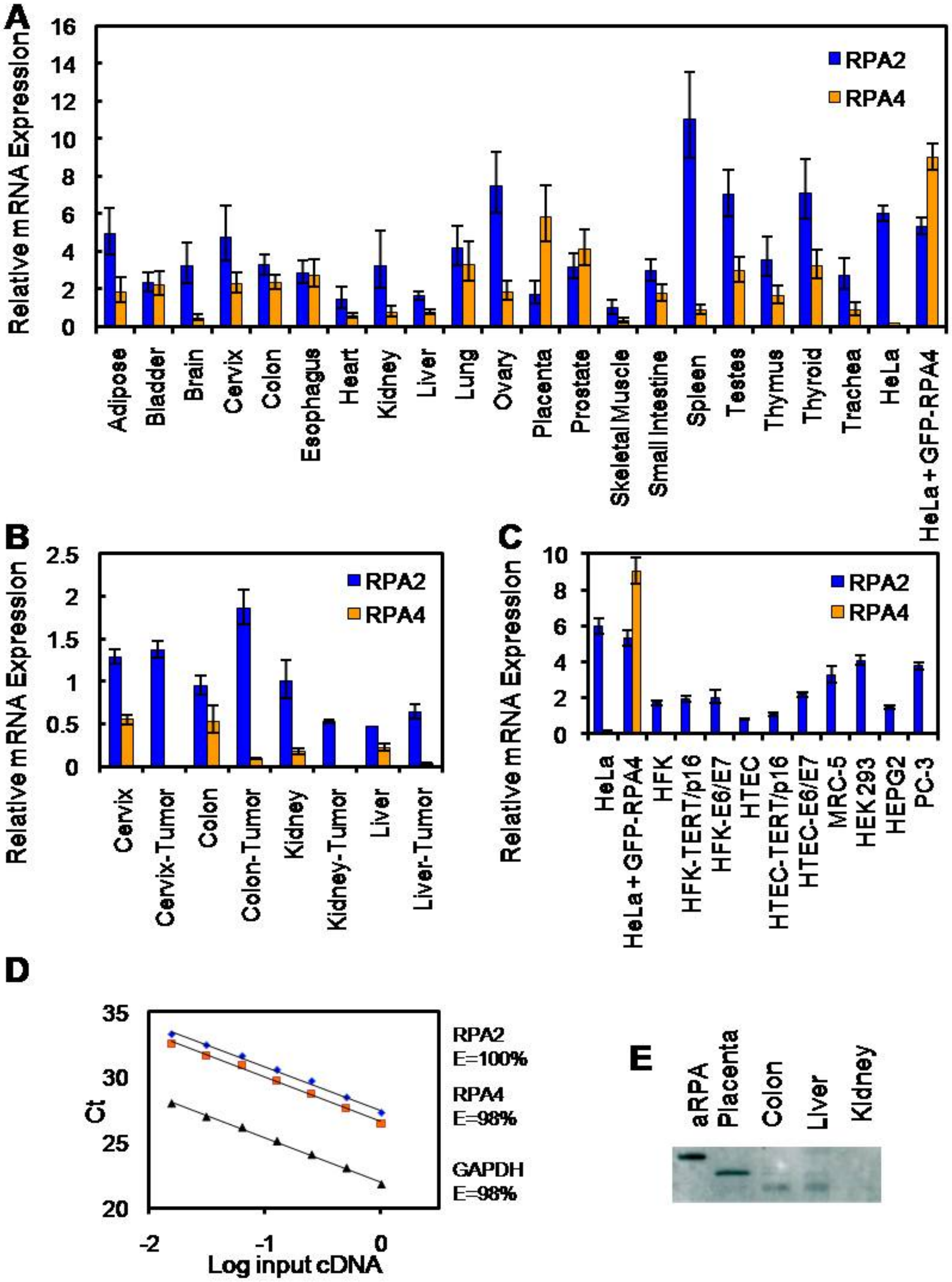
A
Relative mRNA Expression
16
14
12
10
8
6
4
2
0
RPA2
RPA4
Adipose
Bladder
Brain
Cervix
Colon
Esophagus
Heart
Kidney
Liver
Lung
Ovary
Placenta
Prostate
Skeletal Muscle
Small Intestine
Spleen
Testes
Thymus
Thyroid
Trachea
HeLa
HeLa+GFP-RPA4
B
Relative mRNA Expression
2.5
2
1.5
1
0.5
0
RPA2
RPA4
Cervix
Cervix-Tumor
Colon
Colon-Tumor
Kidney
Kidney-Tumor
Liver
Liver-Tumor
C
Relative mRNA Expression
10
8
6
4
2
0
RPA2
RPA4
HeLa
HeLa+GFP-RPA4
HFK
HFK-TERT/p16
HFK-E6/E7
HTEC
HTEC-TERT/p16
HTEC-E6/E7
MRC-5
HEK293
HEPG2
PC-3
D
Ct
35
30
25
20
-2
-1
0
Log input cDNA
RPA2
E=100%
RPA4
E=98%
GAPDH
E=98%
E
aRPA
Placenta
Colon
Liver
Kidney

Figure 3-2: aRPA interacts with Rad51 and Rad52 and stimulates strand exchange.

Enzyme linked immunosorbant assay in which interactions were measured between different forms of RPA and either Rad52 (A) or Rad51 (B). Forms of RPA used: RPA (blue diamonds), aRPA (orange squares) and AA-His (black triangles). Error bars indicate the average of two or more independent replicates. BSA was used to determine nonspecific background in each assay; BSA values which were generally less than 0.1 OD were subtracted. (C) Schematic of DNA strand exchange between circular ssDNA and homologous linear dsDNA to produce joint molecules (JM) and nicked circular DNA (NC). The asterisk shows the ^{32}P-label on each strand. D) DNA strand exchange assay where φX174 (+)-strand was incubated with Rad51 followed by RPA/aRPA and ^{32}P-labeled *XhoI* linearized φX174 dsDNA. Samples were deproteinized and reaction products were separated by electrophoresis through a 1.0% agarose gel. The positions of joint molecules, nicked circular DNA (NC DNA), dsDNA and displaced ssDNA are indicated. DNA strand exchange assays were carried out by Aura Carreira and Dr. Steve Kowalczykowski (University of California, Davis).

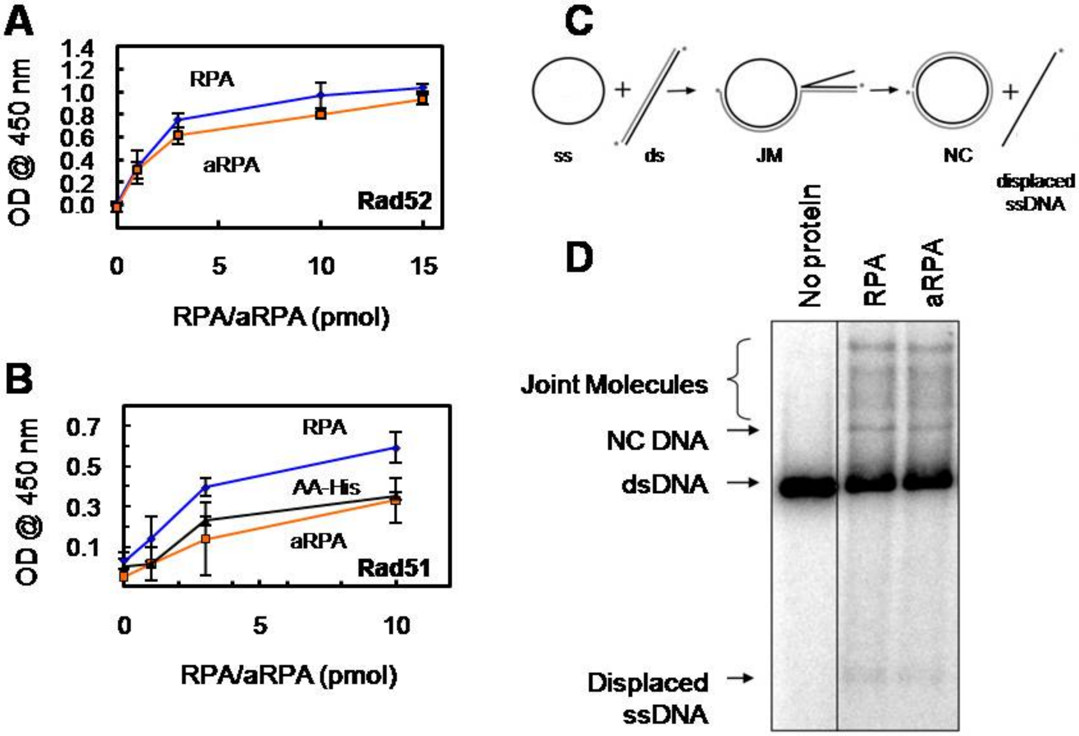
A
OD @ 450 nm
1.4
1.2
1.0
0.8
0.6
0.4
0.2
0.0
RPA
aRPA
Rad52
0
5
10
15
RPA/aRPA (pmol)
B
OD @ 450 nm
0.7
0.5
0.3
0.1
RPA
AA-His
aRPA
Rad51
0
5
10
RPA/aRPA (pmol)
C
ss
ds
JM
NC
displaced ssDNA
D
No protein
RPA
aRPA
Joint Molecules
NC DNA
dsDNA
Displaced ssDNA

Figure 3-3: aRPA supports nucleotide excision repair.

(A) Schematic of the nucleotide excision repair assay. An internally ^{32}P-labeled (circle) 140-bp duplex DNA substrate containing a single (6-4) photoproduct (triangle) is incubated with purified excision repair factors, which results in dual incisions and release of 24- to 32-nt-long damage-containing oligomers. (B) Damage-containing substrate was incubated with 60 nM XPA, 9 nM XPC, 4 nM XPF-ERCC1, 3 nM XPG and 12.5 nM THIIH supplemented with indicated amounts of RPA or aRPA where indicated. The location of the excision products is indicated to the right. The percent of substrate in each reaction undergoing excision is indicated. (C) Time course of reconstituted excision repair reactions containing optimal amounts of either aRPA (530 ng) or RPA (150 ng). (D) Quantification of excision repair assays. Results indicate the average and standard deviation from three independent experiments. Repair assays were carried out by Drs. Michael Kemp and Aziz Sancar (University of North Carolina).

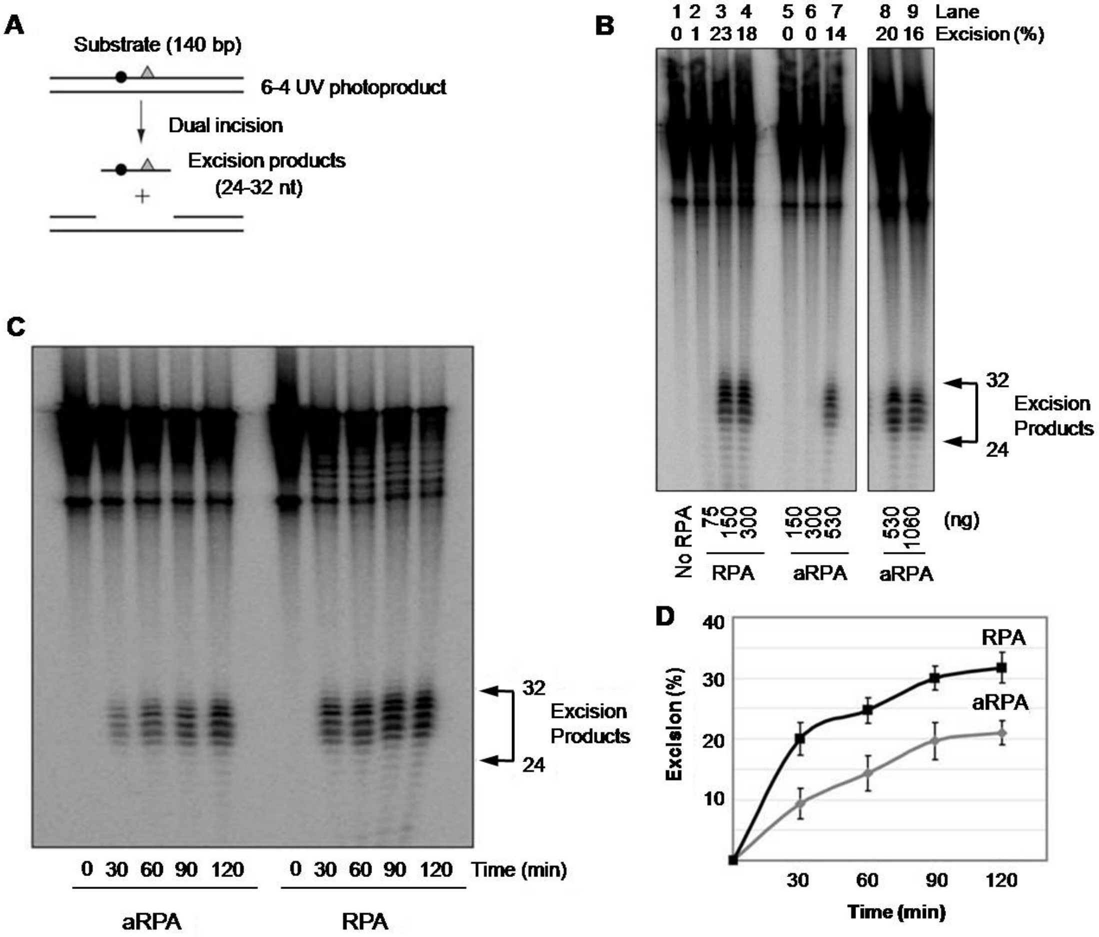
A
Substrate (140 bp)
6-4 UV photoproduct
Dual incision
Excision products
(24-32 nt)
+
B
1 2 3 4 5 6 7 8 9 Lane
0 1 23 18 0 0 14 20 16 Excision (%)
32
Excision
Products
24
No RPA
75 150 300
RPA
150 300 530
aRPA
530 1060
aRPA
(ng)
C
32
Excision
Products
24
0 30 60 90 120 0 30 60 90 120 Time (min)
aRPA
RPA
D
Excision (%)
40
30
20
10
RPA
aRPA
30 60 90 120
Time (min)

Figure 3-4: aRPA has altered interactions with XPA.

(A) Enzyme linked immunosorbant assay with RPA (blue diamonds) or aRPA (orange squares) and XPA. Errors bars indicate the average of two or more independent replicates. BSA was used to determine nonspecific background in each assay; BSA values which were generally less than 0.1 OD were subtracted. (B) Immunoblot analysis of RPA and aRPA showing that anti-RPA2 and anti-RPA4 antibodies specifically recognize the appropriate subunits in RPA and aRPA, respectively. (C) MBP-tagged XPA immobilized on amylose resin was incubated with RPA or aRPA overnight at 4ºC and then analyzed by SDS-PAGE and western blotting with a mixture of the indicated antibodies. The recovered MBP-XPA was stained with Coomassie Blue after SDS-PAGE. Input represents 10% (100 ng) of RPA and aRPA and 1 μg of MBP-XPA. Experiments shown in B and C were carried out by Drs. Michael Kemp and Aziz Sancar.

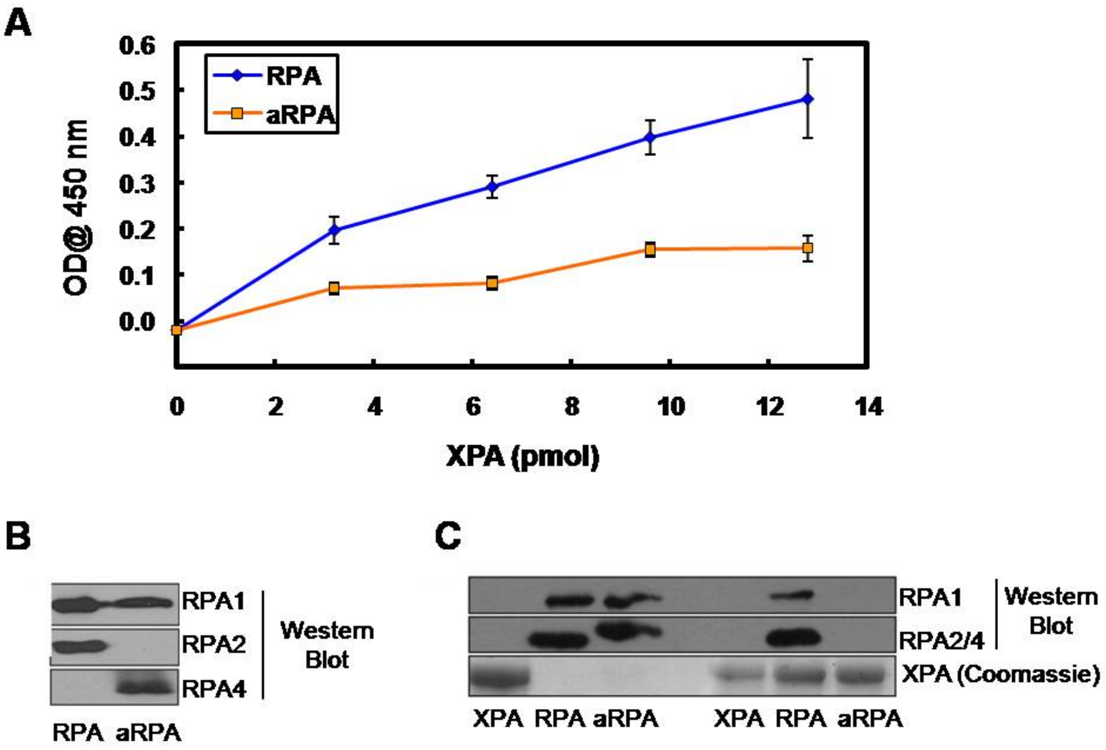
A
0.6
0.5
0.4
0.3
0.2
0.1
0.0
OD@ 450 nm
RPA
aRPA
0
2
4
6
8
10
12
14
XPA (pmol)
B
RPA1
RPA2
RPA4
Western Blot
RPA
aRPA
C
RPA1
RPA2/4
Western Blot
XPA (Coomassie)
XPA
RPA
aRPA
XPA
RPA
aRPA

CHAPTER 4

FUNCTIONS OF ALTERNATIVE REPLICATION PROTEIN A IN INITIATION AND ELONGATION

Abstract

Replication Protein A (RPA) is a single-stranded DNA-binding complex that is essential for DNA replication, repair and recombination in eukaryotic cells. In addition to this canonical complex, I have recently characterized an alternative Replication Protein A complex (aRPA) that is unique to primates and horse. aRPA is composed of three subunits: RPA1 and RPA3, also present in canonical RPA, and a primate-specific subunit RPA4, homologous to canonical RPA2. aRPA has biochemical properties similar to the canonical RPA complex but does not support DNA replication. I describe studies to identify what properties of aRPA prevent it from functioning in DNA replication. I show aRPA has reduced interaction with DNA polymerase α (pol α) and that aRPA is not able to efficiently stimulate DNA synthesis by pol α on aRPA coated DNA. Additionally, I show that aRPA is unable to support *de novo* priming by pol α. Because pol α activity is essential for both initiation and for Okazaki strand synthesis, I conclude that the inability of aRPA to support pol α loading causes aRPA to be defective in DNA replication. I also show that aRPA stimulates synthesis by DNA polymerase δ in the presence of PCNA and RFC. This indicates that aRPA can support extension of DNA strands by DNA polymerase δ. This finding along with the previous observation that aRPA supports early steps of nucleotide excision repair and recombination, indicates that aRPA can support DNA repair synthesis that requires polymerase δ, PCNA and RFC and supports a role for aRPA in DNA repair.

Introduction

The role of RPA in DNA replication has been characterized in detail using the SV40 system. SV40 initiation requires the concerted action of four proteins, SV40 large

T-antigen (Tag), polymerase α/primase (pol α), topoisomerase I (topo I) and RPA [45, 46, 151]. Tag is a 90 kDa polypeptide that performs multiple functions during SV40 replication. Tag binds specifically to SV40 origin DNA as double hexamer, serves as the sole replicative DNA helicase and orchestrates the assembly and operation of the viral replisome [45]. Pol α is a heterotetrameric complex of p180, p68, p58 and p48 subunits that synthesizes a short RNA-DNA primer on the leading strand and at the beginning of each Okazaki fragment on the lagging strand [49, 152]. Topo I is a 91 kDa polypeptide that relaxes both negatively and positively supercoiled DNA by transiently breaking a single strand, which allows for unwinding of positively supercoiled DNA or rewinding of negatively supercoiled DNA [153].

Once the SV40 DNA replication has been initiated, elongation DNA synthesis occurs utilizing two polymerases (DNA polymerase δ and ε) and their accessory factors. DNA polymerase δ (pol δ) is one of the replicative polymerases in eukaryotes and is the major polymerase used for lagging-strand synthesis[154]. During SV40 replication, pol δ can support synthesis of both leading and lagging strands [155]; however, during chromosomal DNA replication, pol δ extends the primers generated by pol α on the lagging strand while DNA polymerase ε (pol ε) continuously synthesizes DNA on the leading strand [52, 154, 156]. Both pol δ and pol ε utilize a ring-shaped sliding clamp (PCNA) that increases the processivity of these polymerases. PCNA is loaded onto the DNA by the pentameric complex RFC.

During initiation of SV40 DNA replication, Tag assembles at the origin of replication, bi-directionally unwinds the double-stranded DNA and recruits other proteins to establish a replication fork [157]. Topo I stimulates pol α by binding to Tag and releases torsional stress induced by unwinding of the parental strands [158, 159]. RPA is required to stabilize the emerging ssDNA and along with Tag, recruits pol α [48, 49]. Pol α synthesizes a short RNA primer of about 10-ribonucleotides in length, the complex then transitions to DNA synthesis, incorporating about 20 deoxynucleotides. This creates the initial RNA-DNA primers used to start DNA replication and each Okazaki fragment [160]. It has been shown that RPA acts as an auxiliary factor for pol α by stimulating synthesis and increasing processivity during initiation of DNA replication [51]. During initiation, RPA interacts with pol α to keep the polymerase at the primed site. To switch from initiation to elongation, RFC interacts with RPA disrupting the pol α – RPA interaction and causing the release of pol α [53]. RFC then loads PCNA and remains at the primed site by interacting with RPA. Pol δ can then access the primed site via contact with RPA. Pol δ competes with RFC for RPA, resulting in displacement of RFC from the 3' terminus, and replacement with pol δ [52]. RFC remains at the site by interacting with the PCNA ring.

The current model suggests multiple roles for RPA in DNA replication. These include binding to exposed ssDNA being created by the helicase, helping recruit polymerase α/primase, and coordinating the polymerase switch from polymerase α to polymerase δ/polymerase ε. Throughout the course of replication, RPA serves as a common interaction partner for many proteins and through a protein-mediated hand-off mechanism coordinates the ordered assembly of the proteins [18]. I have previously shown that aRPA does not support SV40 DNA replication at the initiation and elongation steps (Chapter 2). However, it is not known what activity prevents aRPA from functioning in DNA replication. The present study examines the role of aRPA during the initiation and elongation reactions of DNA replication using purified recombinant proteins. In particular, I wished to understand how aRPA affects the activities of pol α and pol δ. I also show that unlike RPA, aRPA has altered interactions with pol α and does not support efficient loading of or priming by pol α. The pattern of DNA synthesis by pol α in the presence of aRPA also suggests that aRPA cannot stabilize pol α on the DNA. In contrast, I find that aRPA does support pol δ synthesis in the presence of PCNA and RFC. These findings suggest that the defect of aRPA in replication is in promoting efficient priming by pol α but that aRPA can function in processive DNA synthesis by pol δ.

Experimental Procedures

Plasmids

pGBM-RFC1, pET-RFC4/2 and pCDFK-RFC5/3 were generous gifts from Dr. Yuji Masuda (Hiroshima University) [161]. pET-hPold1 and pCOLA-hPold234 were generous gifts from Dr. Yoshihiro Matsumoto (Fox Chase Cancer Center) [162]. p11d-tRPA and p11d-aRPA were described previously [138]. pT7-hPCNA was a generous gift from Dr. Bruce Stillman, Cold Spring Harbor Laboratory. This plasmid was used as a template for *in vitro* site directed mutagenesis to insert an N-terminal 6x Histidine tag. The primers used to generate pT7-His-hPCNA were 5’-CCGTTTACTTTAAGAAGGAGATATACATATGCATCACCATCATCACCACGGATCCGCTATGTTCGAGGCGCGCCTGGTCCAGGGCTCC-3’ and 5’-GGAGCCCTGGACCAGGCGCGCCTCGAACATAGCGGATCCGTGGTGATGATGGTGATGCATATGTATATCTCCTTCTTAAAGTAAACG-3’. The mutations were confirmed by DNA sequencing.

Protein Purification

Recombinant RPA and aRPA were expressed in BL21(DE3) cells and purified as previously described [116, 117, 138]. Recombinant human pol α was expressed and purified as described previously [131]. Recombinant human pol δ was expressed in BL21(DE3)(pLacRARE2) cells cotransformed with pET-hPold1 and pCOLA-hPold234 for 18h at 16°C after induction with 0.2 mM IPTG as described previously [161]. Cells were harvested by centrifugation and resuspended in Buffer R/L 500 mM NaCl (50 mM HEPES-NaOH (pH 7.5), 0.1 mM EDTA, 500 mM NaCl, 10 mM β-ME, 1 mM phenylmethylsulfonyl fluoride (PMSF), 2 μL/mL of bacterial protease inhibitor cocktail

(Sigma)) and frozen at -80°C. The cells were thawed on ice and lysed by 3 passes at 10,000-15,000 psi via EmulsiFlex. The lysate was cleared by centrifugation at 14,000 rpm in a Sorvall SS34 rotor for 30 min at 4°C. The recovered supernatant was supplemented with imidazole to a final concentration of 5 mM and loaded onto a Ni-NTA Agarose (Qiagen) column equilibrated with BufferR/D (50 mM HEPES-NaOH (pH 7.5), 10% glycerol (w/v), 10 mM β-ME) supplemented with 500 mM NaCl and 5 mM imidazole. The column was washed with 10 column volumes (CV) of equilibration buffer. pol δ was eluted with a 10 CV linear gradient from 5-100 mM imidazole. Peak fractions were pooled, diluted to 400 mM NaCl with Buffer R/D, and loaded onto a HiTrap Heparin HP column (GE Healthcare) equilibrated with Buffer R/D supplemented with 400 mM NaCl. Following a 10 CV wash, pol δ was eluted with a 10 CV linear gradient from 400-800 mM NaCl. Peak fractions were pooled and concentrated with Amicon Ultra-4 Centrifugal Filters (50K MWCO, Millipore). The protein was then applied to a Superose 6 HR 10/30 (GE Healthcare) column equilibrated with Buffer R/D supplemented with 500 mM NaCl. Purity of pol δ (~85%) was confirmed by SDS-PAGE visualized with Coomassie Blue staining.

Recombinant human RFC was expressed in BL21(DE3)(pLacRARE2) cells cotransformed with pGBM-RFC1, pET-RFC4/2 and pCDFK-RFC5/3 for 18h at 16°C after induction with 0.2 mM IPTG as described previously [161]. Cells were harvested and lysed similar to pol δ. The supernatant was adjusted to 400 mM NaCl with Buffer R/D, iced for 30 min and centrifuged for 30 min at 15,00 rpm at 4°C to remove precipitated material. The supernatant was loaded onto a HiTrap Heparin HP column equilibrated with Buffer R/D supplemented with 250 mM NaCl. Following a 10 CV wash, the protein was eluted with a 10 CV linear gradient from 250-800 mM NaCl. Peak fractions were pooled and diluted to 100 mM NaCl with Buffer R/D and applied to a 5 mL ATP agarose (Sigma) column equilibrated with Buffer R/D supplemented with 100 mM NaCl. RFC was eluted with a 10 CV linear gradient from 100-500 mM NaCL. Peak fractions were pooled and diluted to 125 mM NaCl with Buffer R/D. The fractions were applied to a Mono Q 10/100 GL (GE Healthcare) column equilibrated with Buffer R/D supplemented with 100 mM NaCl. RFC was eluted with a 10 CV linear gradient from 100-500 mM NaCl. Peak fractions were pooled and concentrated with Amicon Ultra-4 Centrifugal Filters (50K MWCO, Millipore). The protein was then applied to a Superose 6 HR 10/30 (GE Healthcare) column equilibrated with Buffer R/D supplemented with 300 mM NaCl. Purity of RFC (~85%) was confirmed by SDS-PAGE visualized with Coomassie Blue staining.

Recombinant human PCNA was expressed in BL21(DE3) cells transformed with pT7-His-hPCNA for 4 hr at 37°C. The cells were harvested and lysed similar to RPA and aRPA. The supernatant was loaded onto a Ni-NTA Agarose (Qiagen) column equilibrated with Buffer J (30 mM HEPES (pH 7.8), 0.25% (w/v) myo-inositol, 1 mM tris(2-carboxyethyl)phosphine and 0.02% Tween-20 (v/v) supplemented with 20 mM imidazole. Following a 3 column volume wash, PCNA was eluted with a 5 column volume linear gradient from 20-250 mM imidazole. The peak fractions were pooled and dialyzed for 16hr against Buffer J supplemented with 150 mM KCl to remove the imidazole. Purity of PCNA (>95%) was confirmed by SDS-PAGE visualized with Coomassie Blue staining.

Enzyme-Linked Immunosorbent Assay

ELISA was used to examine interactions between purified proteins as described previously [117]. Briefly, wells in microtiter plates were coated with 1 μg of RPA or aRPA for interactions with PCNA and pol α and 1 μg of RFC and pol δ in 50 μL of water and incubated for 1 hour. Plates were washed with phosphate buffered saline with 0.2% Tween 20 and blocked with 5% milk in phosphate buffered saline. The indicated amount of pol α, PCNA, RPA, aRPA or BSA was added to each well, incubated for 1 hour, and washed. Primary antibodies in phosphate buffered saline with 5% milk for pol α (1:100

of SJK237), RPA/aRPA (1:300 of 719A) and PCNA (1:50 of anti-human PCNA antibody was a generous gift from Dr. Thomas Kelly, Memorial Sloan-Kettering Cancer Center) were added to the plates, incubated for 30 min, and washed. Goat-α-mouse IgG-HRP (1:1000) was added and incubated for 30 min. Plates were developed using 200 μL of 0.8 mg/mL o-phenylenediamine in 0.005 M phosphate citrate buffer with 0.03% sodium perborate. OD_{450} was measured after 10-60 min using a microtiter plate reader. Background was determined by using BSA as the secondary protein and all data shown have these values subtracted. In all assays, the background values were similar and close to zero.

Pol α Extension Assay

Pol α activity was assayed with a singly primed d24:d66-mer oligodeoxynucleotide (d24: 5'-CTCGGACAATTTGGTGTGCTAGGT-3'; d66: 5'-AGGATGTATGTCTAGTAGGTACATAACTATTCAGTAGTATAGACCTAGCACACCAAATTGTCCGAG-3') as a template. The d24:d66-mer was prepared by labeling the 5'-end of the d24-mer primer with [γ-^{32}P]ATP and T4 polynucleotide kinase (NEB) according to the manufacturer's protocol. The d66-mer template oligonucleotide was then mixed with the complementary labeled d24-mer oliognucleotide in a 1:1 molar ratio in 20 mM Tris-HCl (pH 8.0) containing 20 mM KCl and 1 mM EDTA, heated for 5 min at 90 °C, and then incubated for 2 h at 65 °C and slowly cooled to room temperature. A final volume of 15 μL contained 50 mM Tris-HCl (pH 7.6), 0.25 mg/mL BSA, 1 mM dithiothreitol, 6 mM $MgCl_2$, 20 nM (3'-OH ends) of the 5' ^{32}P-labeled d24:d66-mer DNA template, 10 μM dNTPs, 1 nM pol α, 50 nM RPA or aRPA as indicated. Reactions were assembled on ice and initiated by the addition of dNTPs and incubated for indicated time at 37°C. When order of addition was varied, reactions were pre-incubated at 37°C for 10 minutes and then initiated by the addition of indicated proteins and dNTPs. Reactions were quenched by the addition of formamide loading buffer (80% deionized formamide, 10 mM EDTA (pH 8.0), 1 mg/mL xylene cyanol, 1 mg/mL bromophenol blue), heated at 95 °C for 5 min and products were separated in a 15% polyacrylamide sequencing gel containing 8 M urea. Products were visualized with a FLA-7000 phosphorimager (Fujifilm Global) and quantified using Multi Gauge software (Fujifilm Global).

Pol δ Extension on Singly Primed ssM13mp18 Assay

Pol δ activity was assayed on singly primed single-stranded M13mp18. The standard reaction (10 μL) contained 20 mM HEPES-NaOH (pH 7.5), 0.2 mg/mL BSA, 1 mM dithiothreitol, 1 mM ATP, 1 mM EDTA, 50 fmol (364 pmol for nucleotides) of singly primed ssM13mp18 (5' ^{32}P-labeled 36-mer primer, CAGGGTTTTCCCAGTCACGACGTTGTAAAACGACGG is complementary to 6330-6295 nt), 555 nM RPA or aRPA, 50 nM PCNA, 50 nM RFC and 20 nM pol δ. Reactions were initiated by the addition of dNTP's and $MgCl_2$ to a final concentration of 150 μM and 10 mM, respectively. After incubation at 37°C for indicated time, the reactions were quenched by the addition of formamide loading buffer (80% deionized formamide, 10 mM EDTA (pH 8.0), 1 mg/mL xylene cyanol, 1 mg/mL bromophenol blue), heated at 95 °C for 5 min and products were separated in a 15% polyacrylamide sequencing gel containing 8 M urea. Products were visualized with a FLA-7000 phosphorimager (Fujifilm Global) and quantified using Multi Gauge software (Fujifilm Global).

Results

Effect of aRPA on pol α

Initiation of SV40 DNA replication requires the concerted action of SV40 large Tag, topoisomerase I, pol α and RPA, which form an 'initiation complex' [46]. In Chapter 2, I showed that aRPA interacts with Tag at levels similar to RPA [138]. This suggests that the inability of aRPA to support DNA replication is a result of aRPA affecting one of the other proteins in initiation or at the replication fork. I initially examined the effect of aRPA on the function of pol α using a 66-mer oligonucleotide primed with a 24-mer oligonucleotide. It is worth noting that this DNA structure is not the substrate recognized by pol α during primer synthesis. However, it would be when pol α dissociates prior to completing the DNA portion of the RNA-DNA primer. Given that pol α can initiate primer synthesis *de novo* and in a sequence independent manner, I feel this is a suitable substrate to examine the effects of aRPA on pol α activity. Pol α and either RPA or aRPA were incubated with the primed template in the presence of deoxynucleotides (dNTPs) and products of the reaction were separated on a 15% denaturing polyacrylamide gel, which allowed for separation of single nucleotide incorporation events creating a laddering of products from +1 nt to +42 nt. By allowing some components to pre-bind to the DNA, I was able to examine the effect of aRPA on the polymerization of a pre-bound pol α (Figure 4-1A) or on the loading and subsequent polymerization of pol α (Figure 4-2A). When pol α was allowed to bind to the template before the addition of dNTPs, it efficiently synthesized DNA with full-length product being observed in less than one minute (Figure 4-1B, lanes 1-5). Intermediate length products, notably two major pause sites at +17 and +25 were observed. The major pause sites are both two purines in a row (AA and GG, respectively) and the degree of pausing is consistent with the low processivity of pol α [51, 163]. Similar experiments were carried out in which pol α was allowed to bind to the primer-template junction and then either RPA or aRPA was added with the initiating dNTPs. The amount of RPA or aRPA used was enough to saturate the ssDNA region of the substrate with two RPA molecules bound per DNA substrate. In these reactions, addition of either RPA or aRPA resulted in levels of synthesis similar to that observed with pol α alone (Figure 4-1B, C). Addition of RPA caused a decrease in the accumulation of products at the two major pause sites by an average of 56% over the time course (Figure 4-1D). In contrast, there was only a slight change in the level of pausing (16%) when aRPA was added. Together these finding suggest that aRPA does not affect the polymerization of pol α that is associated with the primer-template junction.

I next examined the ability of aRPA to facilitate the loading of pol α. This was done using the template described above, but the order of addition was changed: RPA or aRPA were allowed to pre-bind to exposed ssDNA on the template strand and reactions were initiated by the addition of pol α (Figure 4-2A). Pol α alone showed decreased total synthesis under these conditions, which is consistent with association of the polymerase being the rate-limiting step with these types of templates (Figure 4-2B). When RPA is pre-bound, total DNA synthesis by pol α is similar to conditions in which pol α is pre-bound to the template (compare Figure 4-1B with Figure 4-2B). This suggests RPA promotes loading of pol α on primer template junctions. In contrast, when aRPA was pre-bound to the ssDNA of the template, there was a 64% decrease in total DNA synthesis (compared to pre-binding RPA and a decrease of 42% compared to pol α alone; Figure 4-2C). This suggests, that unlike RPA, aRPA does not support efficient loading of pol α and actually inhibits its association with the primer-template junction.

I next examined the concentration dependence of RPA and aRPA on pol α synthesis. The concentrations of RPA and aRPA were varied from 0 to 100 nM with a fixed amount of DNA substrate (20 nM). RPA and aRPA had minimal effect on pol α when the polymerase was allowed to pre-bind the DNA substrate (Figure 4-3A, B). When either RPA or aRPA were allowed to pre-bind the DNA substrate, there was minimal change in DNA synthesis at low concentrations but DNA synthesis quickly decreased when aRPA concentrations went above 30 nM (Figure 4-3A). However, DNA synthesis with RPA increased up to 30 nM then remained constant for multiple incorporation events (Figure 4-3A). I also examined incorporation of the first nucleotide to determine whether the form of RPA affected the initial polymerization reaction. Single nucleotide incorporation was examined by carrying out the reactions in the presence of only the next nucleotide in the sequence (dCTP). RPA had a minimal effect up to 50 nM but inhibited synthesis at higher concentrations (Figure 4-3B). In contrast, aRPA decreased the amount single nucleotide incorporation at all concentrations examined (Figure 4-3B). The results suggest that over this concentration range, aRPA is inhibitory while RPA had minimal effect on synthesis by pol α.

Mechanism of pol α Inhibition by aRPA

I next determined whether there were altered interactions between aRPA and pol α. Enzyme linked immunosorbant assays were carried out with purified proteins. Compared to RPA the interaction between aRPA and pol α was decreased by ~75% (Figure 4-4A). Both RPA1 and RPA2 interact with the pol α complex so either the pol α interaction with RPA2 is most important for the interactions monitored in these assays or the presence of RPA4 in the aRPA complex causes altered interactions of pol α with RPA1. These findings suggest that aRPA has reduced interactions with pol α and that this prevents efficient loading when aRPA is bound to the DNA. However, they do not rule out aRPA allosterically modulating the activity of pol α. To test this possibility, a series of mixing experiments were done. Either RPA or aRPA was pre-bound to the DNA substrate while at the same time DNA pol α was pre-incubated with the other form of RPA. DNA synthesis was then initiated by mixing the two mixtures and primer extension monitored (Figure 4-5A). When RPA is pre-bound and the reaction initiated by the addition of aRPA-pol α, there is a slight decrease in DNA synthesis compared to pol α alone (Figure 4-5B). In contrast, when aRPA is pre-bound to ssDNA and the reaction initiated by the addition of RPA-pol α, there is a further decrease in DNA synthesis (Figure 4-5B). Together these findings suggest that the majority of the inhibition of pol α by aRPA is a result of reduced protein interactions between aRPA-pol α preventing either pol α association on aRPA coated primer-template junctions or pol α from displacing aRPA from the DNA template.

Previously, RPA2-4 hybrids were used to show that the L34 loop of DBD G and the winged helix of RPA4 contributed to the inhibition of DNA synthesis. To examine if these regions also contributed to an inhibition of pol α, these hybrid complexes were assayed in the d24:d66 primer extension assay (Figure 4-6A). The RPA-422 and RPA-242 complexes, where the putative phosphorylation or DBD G of RPA4 replaced the cognate domain of RPA2, respectively, both had levels of DNA synthesis similar to RPA (Figure 4-6B, C). In contrast, when the winged helix of *RPA4* replaced that of RPA2 (RPA-224), DNA synthesis was reduced (Figure 4-6B, C). This suggests that the winged helix domain of *RPA4* has the largest effect on modulating pol α synthesis. I also examined a hybrid form of RPA2 in which the L34 loop of RPA4 replaced that of RPA2 (RPA-2Basic). This form has been shown to be a dominant inhibitor of DNA replication both *in vitro* and *in vivo* [110, 164]. This form also reduced DNA synthesis by pol α (Figure 4-6B, C). This finding is consistent with the RPA-2Basic complex having properties similar to the full aRPA complex. This finding suggests that the L34 loop from RPA4 has a greater effect when it is in the context of the RPA2 subunit.

Effect of aRPA on the Synthesis of RNA-DNA Primers

To examine the effect these altered interactions have on initiation, a collaborator (Dr. Daniel Simmons, University of Delaware) examined the ability of aRPA to support pol α dependent priming using a SV40 based monopolymerase assay. RNA-DNA primers of approximately 36 nucleotides were synthesized and readily detected in the presence of RPA. However, no synthesis was detected in the presence of aRPA. This demonstrates that aRPA is unable to support efficient initiation of DNA replication by preventing priming by pol α.

Effect of aRPA on pol δ DNA synthesis

Thus far, I have shown that aRPA does not support the efficient loading of pol α onto the primer-template junction. This agrees with our earlier findings that aRPA does not support the initiation steps of SV40 DNA replication. However, I have also shown that aRPA also does not support the elongation phase of SV40 DNA replication [138]. One possibility is that like pol α inhibition, aRPA could also inhibit DNA synthesis by pol δ. Another possibility is that the inhibition of pol α, which is required for Okazaki fragment synthesis, is enough to uncouple leading and lagging strand synthesis thus halting DNA synthesis.

To discriminate between these two possibilities, pol δ, RFC and PCNA were purified and the effect of aRPA on pol δ DNA synthesis was examined on a singly-primed ssM13mp18 plasmid. As shown in Figure 4-7A lanes 2 and 3, DNA synthesis by pol δ by itself is limited to a few nucleotides incorporated, which is consistent with its low processivity in the absence of the accessory factors PCNA and RFC [165]. When RFC and PCNA were added to the reaction (Figure 4-7A, lanes 11 and 12), there was an increase in the length of products formed indicating that RFC actively loaded PCNA onto the single-strand plasmid and PCNA formed a complex with pol δ. The addition of RPA to the RFC, PCNA and pol δ reaction showed a dramatic increase in the length of products formed (Figure 4-7A, lanes 5 and 6). Interestingly, addition of aRPA to RFC, PCNA and pol δ resulted in products that are identical to those synthesized in the presence of RPA (Figure 4-7A, compare lanes 8 and 9 to 5 and 6 and quantitation of the products in Figure 4-7B). A time course of these reactions indicated that while there was a slight lag with aRPA, overall the rate of synthesis is similar with either RPA or aRPA (Figure 4-7C). I conclude that aRPA does support processive DNA synthesis by pol δ in the presence of RFC and PCNA.

I also examined whether there were altered interactions between aRPA and RFC, PCNA and pol δ. Both RFC and pol δ interact with RPA while PCNA does not directly interact with RPA [18, 132]. As shown in Figure 4C, the interaction between aRPA-RFC was the same as RPA-RFC. RPA and aRPA do not directly interact with PCNA (Figure 4-4B). By comparing the RPA-pol δ and the aRPA-pol δ interaction, aRPA also interacted strongly with pol δ but at a slightly reduced level (60%, Figure 4-4D). In the absence of the accessory proteins RFC and PCNA, RPA but not aRPA caused a modest stimulation of pol δ synthesis (Figure 4-7A, compare lane 3 to lanes 15 and 18). This suggests that the altered interactions between aRPA and pol δ might reduce the direct stimulation of pol δ by aRPA. However, even if there is a miscommunication between aRPA and pol δ, it is readily overcome by the accessory proteins (Figure 4-7A).

While optimizing pol δ DNA synthesis on the ssM13mp18 plasmid, I examined the salt dependence of the reaction. Pol δ is sensitive to ionic strength and most previous analyses with RFC and PCNA have been carried out under low ionic strength conditions [161, 166, 167]. I find that the addition of RPA or aRPA can overcome the salt inhibition of pol δ synthesis (Figure 4-8). Synthesis was monitored and both short (≤ 40 nt) and long (≥ 41 nt) products were quantitated. At all salt conditions examined, minimal long products were observed with pol δ or with pol δ, PCNA and RFC in the absence of either form of RPA (Figure 4-8A-open circles and diamonds). At low salt concentrations, short products were observed but the amount of synthesis decreased as salt concentration increased (Figure 4-8B). In contrast, when RPA or aRPA was added to RFC, PCNA and pol δ, high levels of synthesis and full-length (long) products were observed from low to near physiological ionic strength (0-125 mM NaCl; Figure 4-8A-closed symbols). There is inhibition of synthesis at 250 mM NaCl in the presence of RPA or aRPA; however, even at this high ionic strength, synthesis of short products was observed while there was virtually complete inhibition of pol δ in the absence of RPA. These data clearly show that aRPA can stimulate pol δ under a variety of conditions and that both RPA and aRPA stimulate pol δ activity under physiological ionic strength.

Discussion

RPA has a central role in DNA replication, playing an essential function in both initiation and elongation [8, 54]. In Chapter 2 I demonstrated that aRPA does not support

DNA synthesis during the initiation and elongation phases of SV40 DNA replication or S-phase progression in human cells [111, 138]. The studies presented here provide a molecular explanation for this difference in activity. Through collaboration with Dr. Daniel Simmons, we have shown that aRPA bound to ssDNA prevents the synthesis of RNA-DNA primers by pol α by preventing efficient loading of the polymerase onto the ssDNA. This effect is probably caused by altered interactions between pol α and aRPA. However, aRPA has minimal effects on the polymerization of pol α once it has started synthesizing DNA. These findings indicate that aRPA is unlikely to support the association of pol α on ssDNA leading to priming and the initiation of DNA replication. This mechanism is also supported by the finding that aRPA is unable to support primer synthesis in an SV40 initiation reaction. This defect would also be expected to prevent priming of Okazaki fragments needed for lagging strand synthesis. Walther et al. showed that inhibition of pol α during elongation phase of SV40 replication causes a complete halt to DNA synthesis consistent with coupled synthesis of leading and lagging strands [54]. This indicates that aRPA's inability to support pol α loading on the lagging strand would be expected to cause a defect in elongation.

I also show that aRPA supports pol δ DNA synthesis in the presence of RFC and PCNA to the same extent as canonical RPA and that both aRPA and RPA increase the processivity of the polymerase more than PCNA and RFC alone. This suggests that aRPA can support processive DNA synthesis on primed DNA templates. This activity would have little consequence during DNA replication in the absence of priming by pol α but would further support a role for aRPA in genome maintenance. It been shown that aRPA can function in multiple aspects of DNA repair from localization to sites of damage to supporting the dual incision/excision steps of nucleotide excision repair to supporting Rad51 dependent strand invasion [147]. My findings here suggest that aRPA can complete the nucleotide excision repair process by filling the gap left when the damaged DNA is removed. This gap filling reaction is carried out by PCNA, RFC and either pol δ or pol ε, in a continuous manner using the free 3'-OH left by the removal of the damaged DNA [168]. Similar gap filling reactions by a high fidelity polymerase, such as pol δ and DNA polymerase ε, are common to most other forms of DNA repair [150]. I suggest that aRPA, like canonical RPA, is capable of supporting gap synthesis in repair and thus help the cell maintain genome stability. Of the 14 identified human polymerases, RPA has been shown to interact with at least pol α, δ, ε, λ and κ [167, 169-171]. Interestingly, only pol α is able to initiate strand synthesis in DNA replication. All other DNA polymerases extend previously initiated DNA strands.

The number and role of RPA-like complexes in different processes in eukaryotic cells is diverse. Up until the last decade, it was thought that eukaryotic cells had primarily only one form of nuclear single-stranded binding protein, canonical RPA. However, it is now clear that there are a number of RPA-like proteins in cells. Several domains of the tumor suppressor, BRCA2 have structural and functional similarity to the DNA-binding domains of RPA [172, 173]. There are also a number of proteins with RPA homology that function in DNA metabolism as α accessory proteins [174] and the RPA-related complex, Cdc13, Stn1 and Ten1, that is involved in telomere maintenance [175-177]. Mammals also have non-RPA related single-stranded DNA binding proteins that function in DNA repair [130, 178]. Furthermore, a number of eukaryotes have multiple RPA complexes. *Cryptosporidium parvum* has two forms of RPA1 [108]. Plants such as *Oryza sativa* and *Arabidopsis thaliana* have multiple copies of RPA genes that form multiple different heterotrimeric RPA complexes [179]. These plant RPA complexes have non-redundant functions with respect to each other. For example, in rice the B type RPA plays a role in DNA damage repair while the C type RPA is required for DNA replication [104, 105]. RPA4 and RPA2 could be functioning similarly in human cells with aRPA and canonical RPA in humans are playing the same roles as B type and A type RPA in rice, respectively.

The findings presented in here, reveal the mechanism that prevents aRPA from functioning in DNA replication. They also show that aRPA can support DNA repair synthesis that depends on pol δ with its accessory proteins, RFC and PCNA. These and other recent findings on aRPA suggest that it functions in repair processes to maintain the genomic stability in non-dividing cells. The expression pattern of *RPA4* is also consistent with a function in reproduction-related behavior, similar to what has been observed with other primate orphan genes. However, additional studies will be needed to test this directly.

Figure 4-1: The effect of RPA and aRPA on pol α when polymerase is pre-mixed with the DNA substrate.

(A) Schematic illustrating experimental setup and order of addition of proteins. Asterisk indicates the location of the ^{32}-P label. (B) DNA pol α extension assays where pol α (1 nM) has been pre-incubated with the DNA substrate (20 nM 3'-OH ends). Following pre-incubation, either RPA (50 nM) or aRPA (50 nM) was added and the reaction initiated by the addition of dNTP's (10 μM). Reaction products were separated by electrophoresis on a denaturing polyacrylamide sequencing gel and visualized on a Fuji FLA-7000 phosphoimager. (C) Primer extension was quantified by dividing total products (+1 - +42 nt) by total DNA (products plus +0 nt). (D) The amount of products at +17 and +25 nt were quantified by dividing total DNA at +17 nt and +25 nt by total DNA.

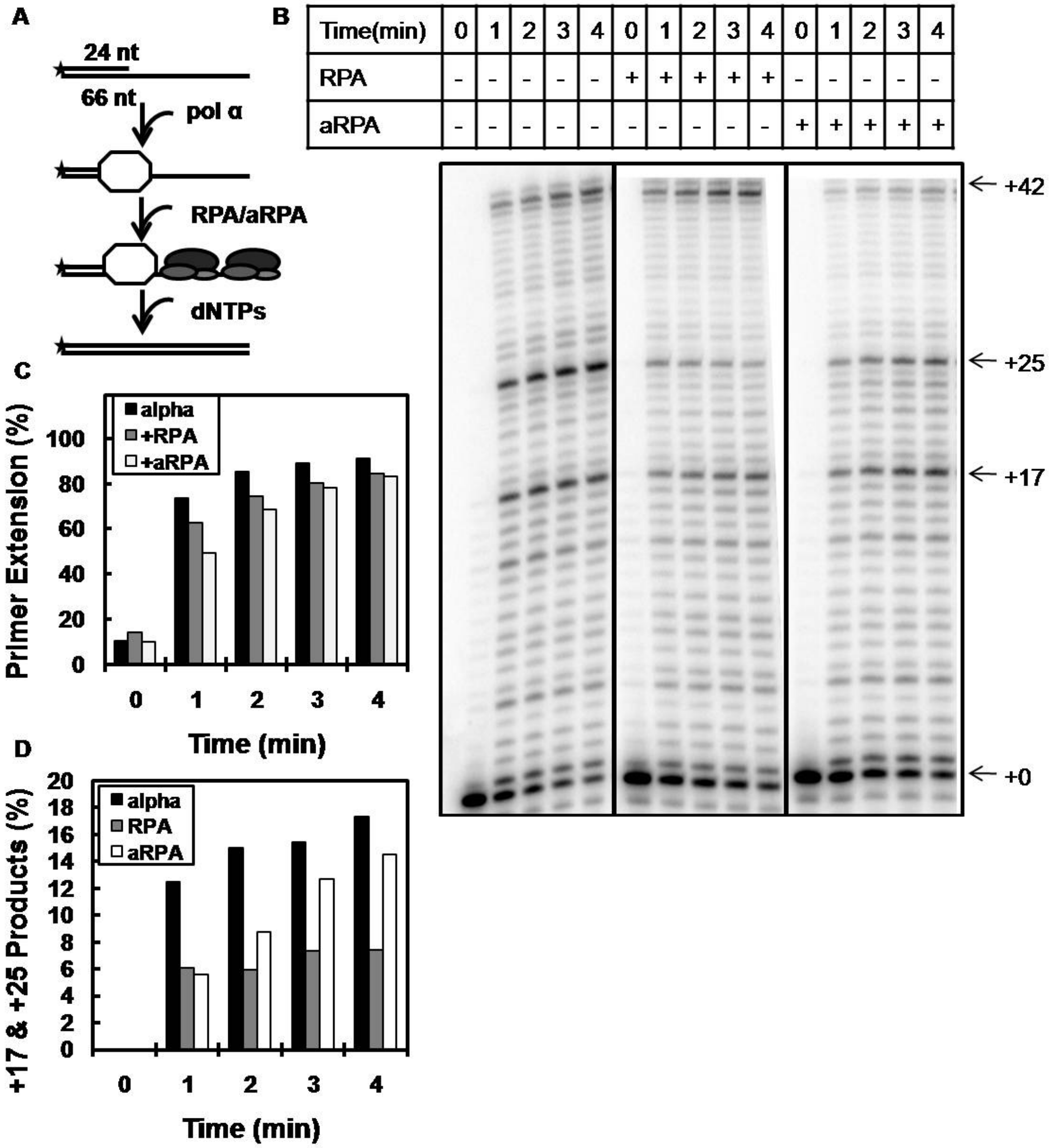
A
24 nt
66 nt
pol α
RPA/aRPA
dNTPs
B
Time(min) 0 1 2 3 4 0 1 2 3 4 0 1 2 3 4
RPA - - - - - + + + + + - - - - -
aRPA - - - - - - - - - - + + + + +
+42
+25
+17
+0
C
Primer Extension (%)
0 20 40 60 80 100
alpha
+RPA
+aRPA
0 1 2 3 4
Time (min)
D
+17 & +25 Products (%)
0 2 4 6 8 10 12 14 16 18 20
alpha
RPA
aRPA
0 1 2 3 4
Time (min)

Figure 4-2: The effect on pol α when either RPA or aRPA are pre-bound to the DNA substrate.

(A) Schematic illustrating experimental setup and order of addition of proteins. Asterisk indicates the location of the ^{32}-P label. (B) DNA pol α extension assays where either RPA (50 nM) or aRPA (50 nM) was pre-incubated with the DNA substrate (20 nM 3'-OH ends). Following pre-incubation, pol α (1 nM) was added and the reaction initiated by the addition of dNTP's (10 μM). Reaction products were separated and visualized as described in Figure 1. (C) Primer extension was quantified by dividing total products (+1 - +42 nt) by total DNA (products plus +0 nt).

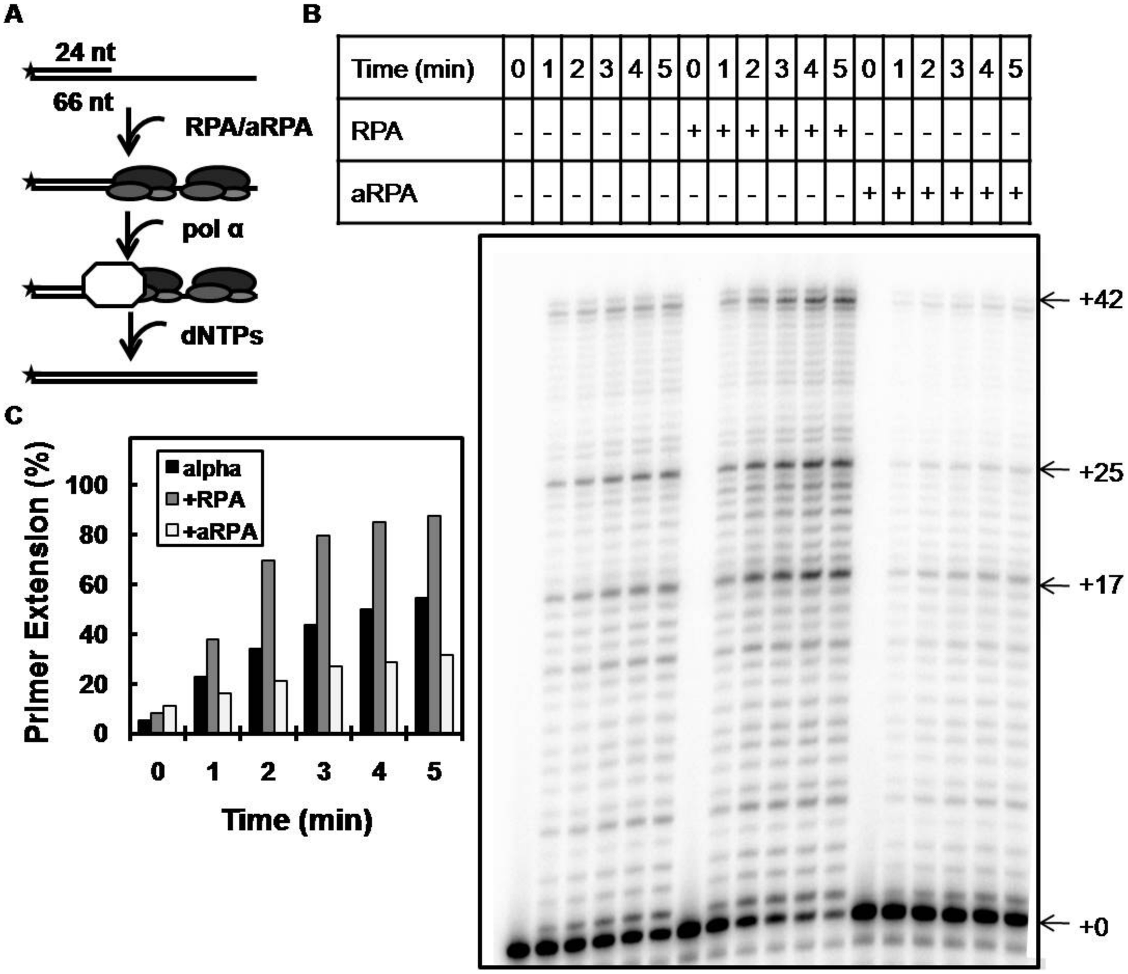
A
24 nt
66 nt
RPA/aRPA
pol α
dNTPs
B
Time (min) 0 1 2 3 4 5 0 1 2 3 4 5 0 1 2 3 4 5
RPA - - - - - - + + + + + + - - - - - -
aRPA - - - - - - - - - - - - + + + + + +
+42
+25
+17
+0
C
Primer Extension (%)
0
20
40
60
80
100
Time (min)
0 1 2 3 4 5
■ alpha
▨ +RPA
☐ +aRPA

Figure 4-3: Titration of RPA and aRPA in pol α extension assay.

Quantitation of DNA pol α extension assays where pol α was pre-incubated with the DNA substrate (20 nM 3'-OH ends). Following pre-incubation, RPA (closed circles) or aRPA (closed triangles) was added and the reaction initiated by the addition of (A) dNTP's (10 μM) or (B) dCTP (10 μM). RPA or aRPA were pre-incubated with the DNA substrate (20 nM 3'-OH ends). Following pre-incubation, pol α (1 nM) was added and the reaction initiated by the addition of (C) dNTP's (10 μM) or (D) dCTP (10 μM).

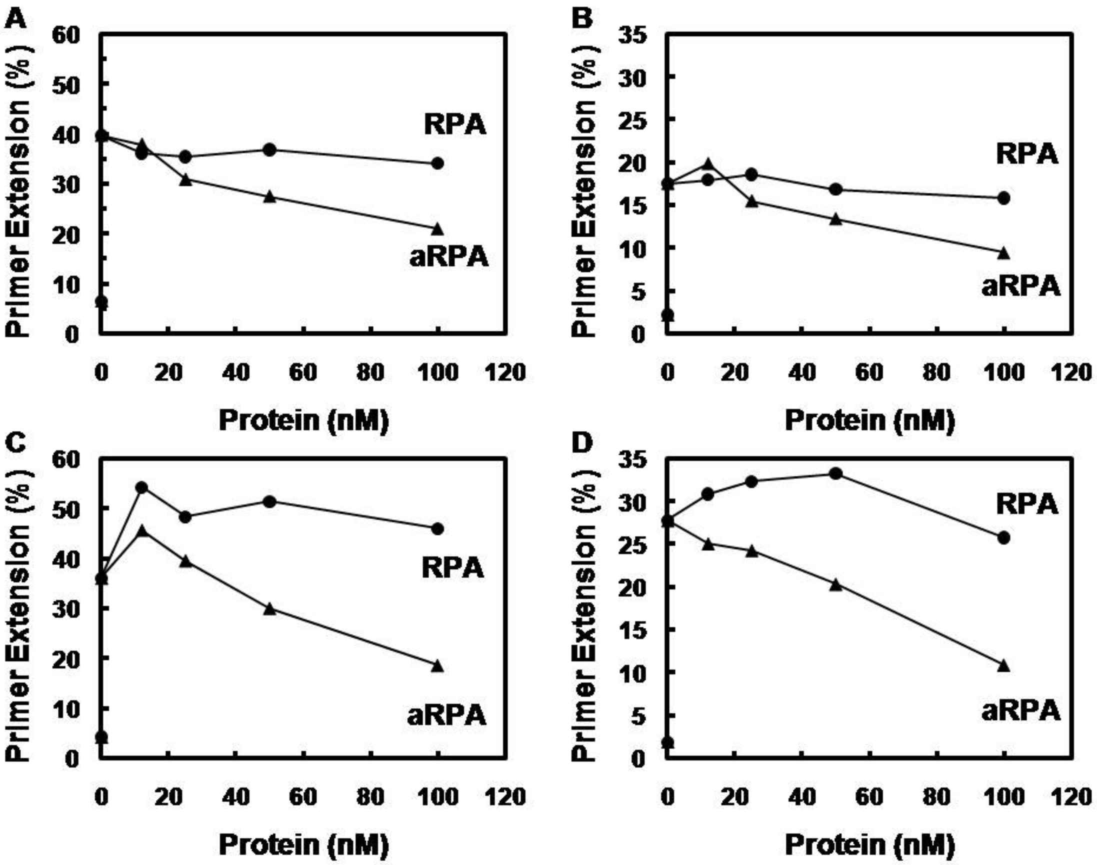
A
B
C
D
Primer Extension (%)
Protein (nM)
RPA
aRPA
0
10
20
30
40
50
60
5
15
25
35
80
100
120

Figure 4-4: Interactions with replication proteins.

Enzyme linked immunosorbant assay in which interactions were measured between different forms of RPA and either (A) pol α, (B) PCNA, (C) RFC or (D) pol δ. Forms of RPA used: RPA (blue circles) and aRPA (orange triangles). The data from each experiment was normalized to the highest absorbance in each experiment, averaged and plotted. Error bars indicate the average of two or more independent replicates. BSA was used to determine nonspecific background (< 0.1) in each assay and subtracted. (B) PCNA (closed squares) was also placed directly on the plate as a positive control.

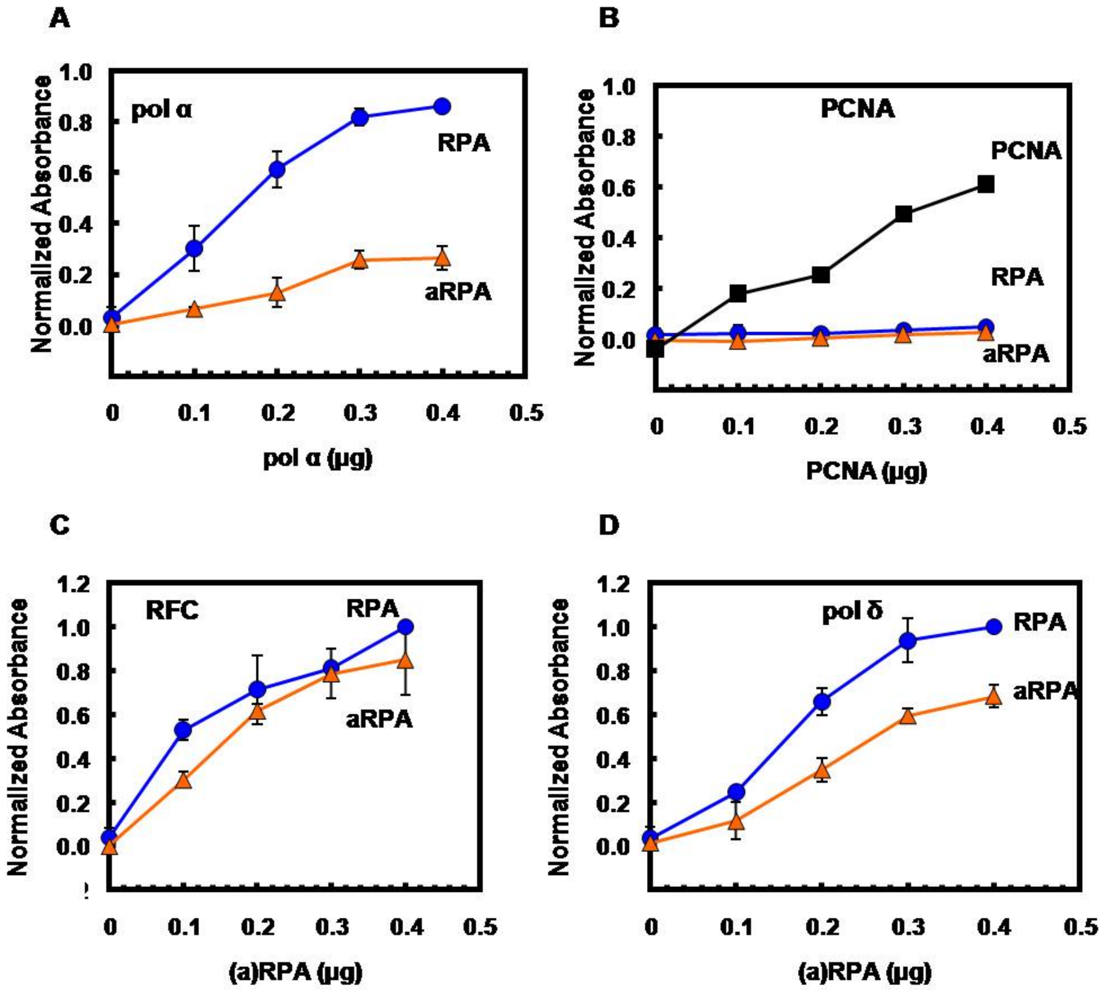
A
Normalized Absorbance
1.0
0.8
0.6
0.4
0.2
0.0
pol α
RPA
aRPA
0
0.1
0.2
0.3
0.4
0.5
pol α (µg)
B
Normalized Absorbance
PCNA
PCNA
RPA
aRPA
PCNA (µg)
C
Normalized Absorbance
1.2
RFC
RPA
aRPA
(a)RPA (µg)
D
Normalized Absorbance
pol δ
RPA
aRPA
(a)RPA (µg)

Figure 4-5: Mechanism of pol α inhibition.

(A) Schematic illustrating experimental setup, order of addition of proteins and pre-incubation of proteins and DNA substrate. (B) DNA pol α extension assays where either RPA (50 nM) or aRPA (50 nM) was pre-incubated with the DNA substrate (20 nM 3'-OH ends) and the other form of RPA was pre-incubated with pol α (1 nM). The pre-incubated samples were mixed and the reaction initiated by the addition of dNTP's (10 μM). Reaction products were separated by electrophoresis on a denaturing polyacrylamide sequencing gel and visualized by phosphoimaging. (C) Primer extension was quantified by dividing total products (+1 - +42 nt) by total DNA (products plus +0 nt).

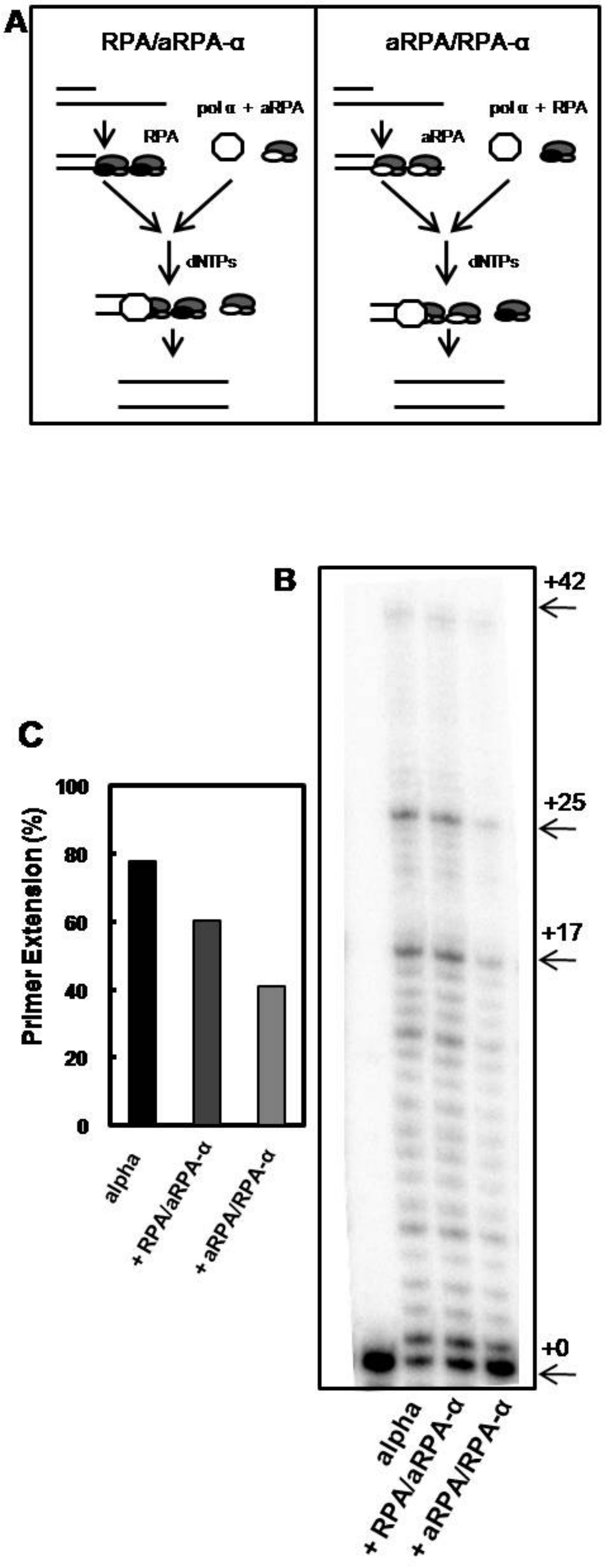
A
RPA/aRPA-α
pol α + aRPA
RPA
dNTPs
aRPA/RPA-α
pol α + RPA
aRPA
dNTPs
B
+42
+25
+17
+0
alpha
+ RPA/aRPA-α
+ aRPA/RPA-α
C
Primer Extension (%)
100
80
60
40
20
0
alpha
+ RPA/aRPA-α
+ aRPA/RPA-α

Figure 4-6: RPA2-RPA4 hybrids in pol α extension assays.

(A) Schematic of RPA2-RPA4 hybrid proteins. RPA2 (dark gray) and RPA4 (light gray) domains are indicated for each hybrid: phosphorylation or putative phosphorylation domain (P), DNA binding domain D and G (DBD-D and DBD-G) and winged-helix domain (WH). (B) DNA pol α extension assays with indicated form of RPA or RPA2-RPA4 hybrid (50 nM) was pre-incubated with the DNA substrate (20 nM 3'-OH ends). Following pre-incubation, pol α (1 nM) was added and the reaction initiated by the addition of dNTP's (10 μM). Reaction products were separated by electrophoresis on a denaturing polyacrylamide sequencing gel and visualized by phosphoimaging. (C) Primer extension was quantified by dividing total products (+1 - +42 nt) by total DNA (products plus +0 nt).

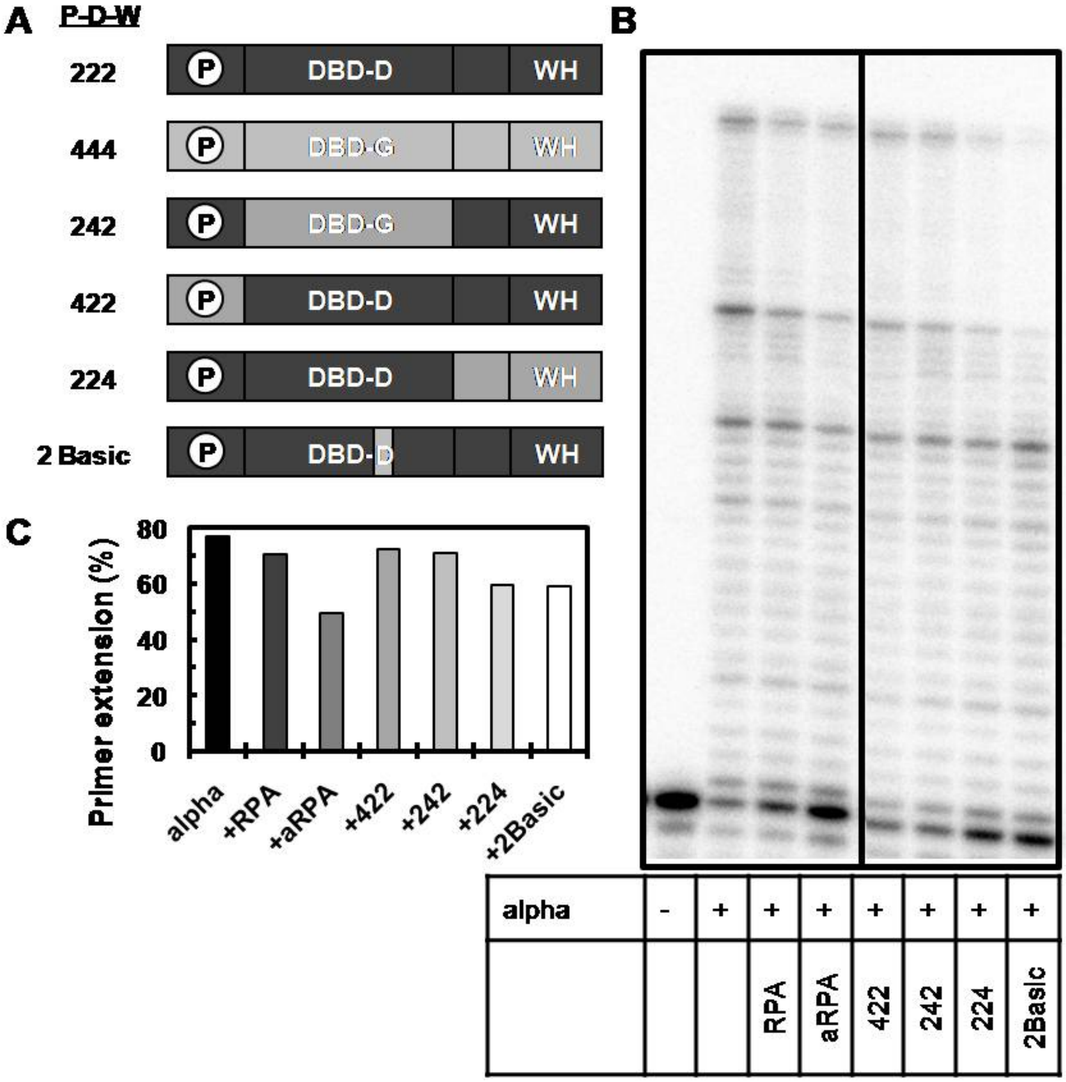
A
P-D-W
222
444
242
422
224
2 Basic
P
DBD-D
DBD-G
WH
B
C
Primer extension (%)
80
60
40
20
0
alpha
+RPA
+aRPA
+422
+242
+224
+2Basic
alpha
-
+
RPA
aRPA
422
242
224
2Basic

Figure 4-7: Pol δ synthesis on singly-primed single-stranded M13mp18 template.

(A) Pol δ activity was assayed on singly-primed single-stranded M13mp18 (50 fmol) in reaction initiated by the addition of dNTPs (150 μM). Addition of individual components is indicated by a plus sign: pol δ (20 nM), RPA (555 nM), aRPA (555 nM), PCNA (50 nM) and RFC (50 nM). The time of the reaction is indicated (0, 5, 15 min). Reaction products were separated by electrophoresis on a denaturing polyacrylamide sequencing gel and visualized by phosphoimaging. (B) Primer extension was quantified by dividing either short products (≤ 40 nt, dark gray) or long products (≥ 41 nt, light gray) by total DNA. (C) Expanded time course of complete reactions (pol δ (20 nM), PCNA (50 nM) and RFC (50 nM)) with the addition of either RPA (555 nM, dark gray) or aRPA (555 nM, light gray)

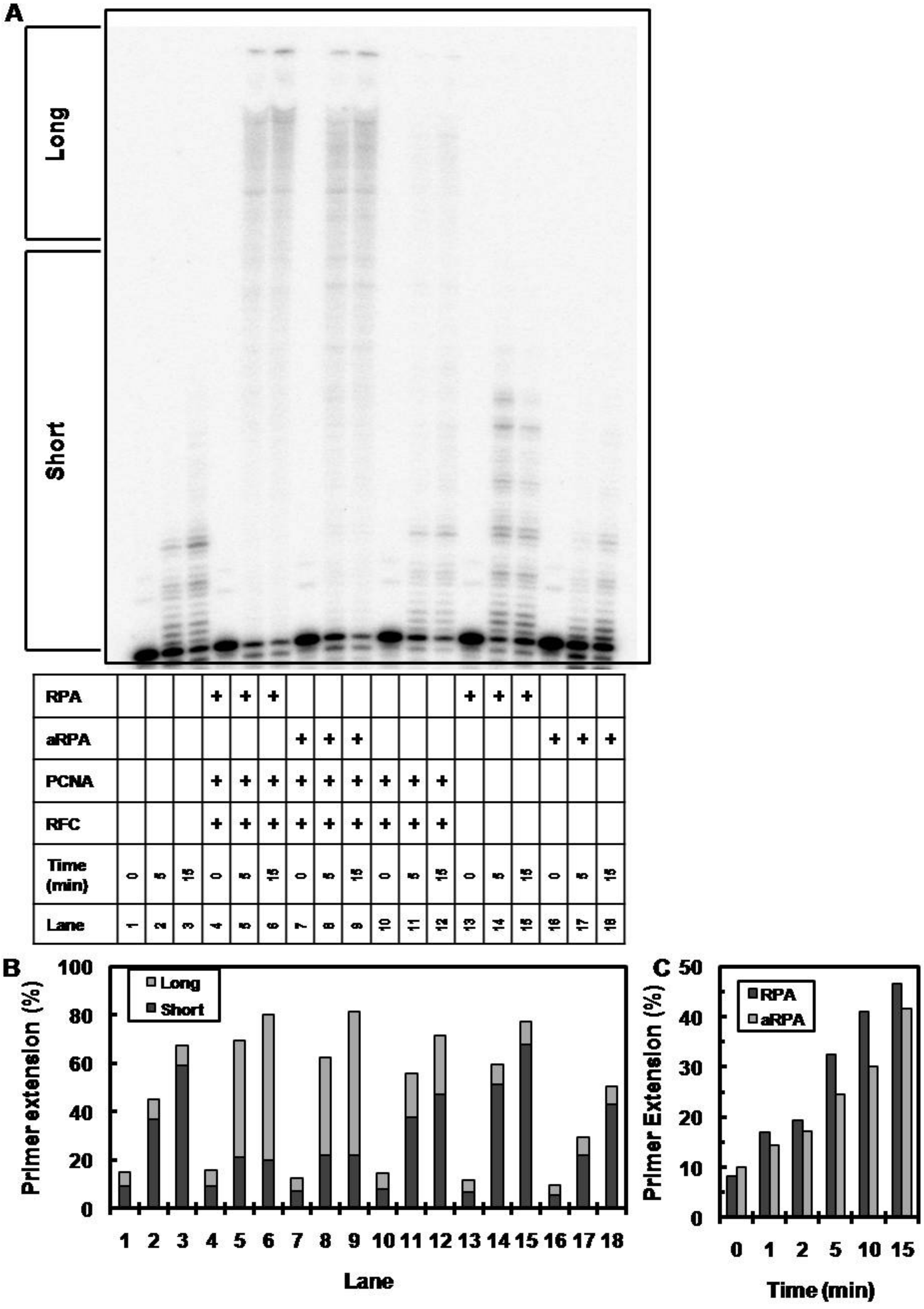

RPA				+	+	+							+	+	+			
aRPA							+	+	+							+	+	+
PCNA				+	+	+	+	+	+	+	+	+						
RFC				+	+	+	+	+	+	+	+	+						
Time (min)	0	5	15	0	5	15	0	5	15	0	5	15	0	5	15	0	5	15
Lane	1	2	3	4	5	6	7	8	9	10	11	12	13	14	15	16	17	18

Figure 4-8: Salt dependence of pol δ activity.

Pol δ activity was assayed on singly-primed single-stranded M13mp18 (50 fmol) in varying concentrations of NaCl initiated by the addition of dNTPs (150 μM). Reactions components: pol δ (20 nM)-open circles; pol δ (20 nM), RPA (555 nM), PCNA (50 nM) and RFC (50 nM)-closed circles; pol δ (20 nM), aRPA (555 nM), PCNA (50 nM) and RFC (50 nM)-closed triangles and pol δ (20 nM), PCNA (50 nM) and RFC (50 nM)-open diamonds. Primer extension was quantified by dividing either (A) long products (≥ 41 nt) or (B) short products (≤ 40 nt) by total DNA.

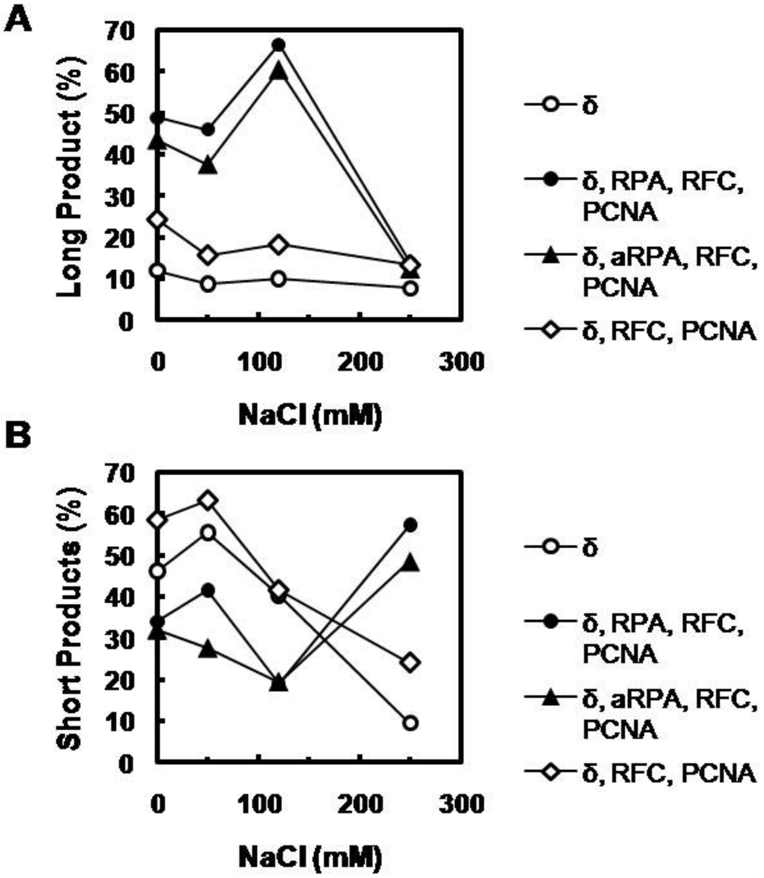
A
Long Product (%)
0
10
20
30
40
50
60
70
0
100
200
300
NaCl (mM)
δ
δ, RPA, RFC, PCNA
δ, aRPA, RFC, PCNA
δ, RFC, PCNA
B
Short Products (%)
0
10
20
30
40
50
60
70
0
100
200
300
NaCl (mM)
δ
δ, RPA, RFC, PCNA
δ, aRPA, RFC, PCNA
δ, RFC, PCNA

CHAPTER 5

SUMMARY AND PERSPECTIVE

Before I started my studies on RPA4 and the aRPA complex, little was known about the subunit or the complex. RPA4 was first reported in 1995 by Keshav and colleagues[109]. It was identified through a human interaction-trap/yeast two-hybrid screen as a factor that interacted with RPA1. They then went on to show only RPA4 or RPA2 could interact with RPA1 at the same time and the complex that contained RPA4 associated with ssDNA cellulose, like the complex that contained RPA2. Since the initial discovery, only a couple of papers mentioned RPA4, which was identified as a protein that did not interact with the tumor suppressor, Menin, and the uracil glycosylase, Ung2 [180-182]. The Wold laboratory became interested in RPA4 shortly after I joined the lab when they discovered that RPA4 did not restore the knockdown phenotype of RPA2 and did not support S-phase progress in HeLa cells. These findings raised many questions about what is the role of RPA4 and how this subunit altered the activities of the trimeric complex when RPA4 substituted for RPA2.

Summary

The goals of my studies were to characterize the biochemical properties of the RPA4 containing trimeric complex, termed alternative RPA (aRPA), and to determine if aRPA could support processes that required the canonical RPA complex. My findings showed that recombinant aRPA could be expressed and purified in a manner similar to RPA. The resulting purified aRPA complex was used to demonstrate that aRPA interacted with ssDNA with high affinity, had an occluded binding site of ~30 nt and low levels of cooperativity, which was similar to RPA. Even though it appeared that aRPA and RPA had the same ssDNA binding properties, it was then a surprising discovery that aRPA could not support SV40 DNA replication. In addition to not supporting SV40 DNA replication, aRPA inhibited the function of canonical RPA. By generating a series of RPA4-RPA2 hybrid proteins, I was able to identify a 16 amino acid region of the L34 loop of RPA4 that was sufficient to inhibit the replication function of RPA2 and the canonical RPA complex.

To determine what activity prevented aRPA from functioning in DNA replication, studies were done to examine the role of aRPA during initiation and elongation using purified recombinant proteins. In particular, I wished to understand how aRPA affected the activities of human DNA polymerase α and δ. These studies showed that unlike RPA, aRPA does not support efficient loading of pol α. The pattern of DNA synthesis by pol α in the presence of aRPA suggested that aRPA also could not stabilize pol α on the DNA. Additionally, aRPA did not support *de novo* RNA-DNA primer synthesis by pol α. In contrast, I found that aRPA does support pol δ DNA synthesis in the presence of PCNA and RFC.

Since aRPA did not support DNA replication *in vitro* or *in vivo*, I also investigated aRPA's ability to support DNA repair processes that require RPA. In contrast to aRPA's failure to support DNA replication, I was able to show in collaboration with Dr. Aziz Sancar and Dr. Stephen Kowalczykowski that aRPA could support the dual incision/excision steps nucleotide excision repair and support Rad51-dependent strand exchange used during the initial steps of homologous recombination. Even though aRPA could support these processes, it did so by a different mechanism than canonical RPA. For example, aRPA had reduced protein-protein interactions with essential proteins needed for nucleotide excision repair but was able to bind alkylated DNA with a higher affinity than RPA or XPA-RPA.

Perspective

The number and role of RPA-like complexes in different processes in eukaryotic cells is diverse. Up until the last decade, it was thought that eukaryotic cells had primarily one form of nuclear single-stranded binding protein, canonical RPA. However, it is now clear that there are a number of RPA like proteins in cells. Several domains of the tumor suppressor, BRCA2, have structural and functional similarity to the DNA-binding domains of RPA [172, 173]. Interestingly, a RPA1-BRCA2 hybrid protein, where the DBDs of BRCA2 are replaced with the entire RPA1 subunit, can restore the homology directed repair defect of BRCA2 knockdown in hamster cells when the hybrid protein is expressed either transiently or stably [172]. Other examples include the recently identified pol α accessory proteins that have homology to RPA and function in DNA metabolism [174] and the RPA-related CST complex that is involved in telomere maintenance [175-177]. Mammals also have non-RPA related single-stranded DNA binding proteins that function in DNA repair [130, 178]. Furthermore, a number of eukaryotes have multiple RPA complexes. *Cryptosporidium parvum* has two forms of RPA1 [108]. Plants such as *Oryza sativa* and *Arabidopsis thaliana* have multiple copies of RPA genes that form multiple different heterotrimeric RPA complexes [179]. These plant RPA complexes have non-redundant functions with respect to each other. For example, in rice the B type RPA plays a role in DNA damage repair while the C type RPA is required for DNA replication [104, 105]. RPA4 and RPA2 could be functioning similarly in human cells with aRPA and canonical RPA in humans playing the same roles as B type and C type RPA in rice, respectively. My current hypothesis is that aRPA is a non-proliferative RPA that functions to support the genomic integrity of the cell.

Replication

aRPA does not support SV40 DNA replication or chromosomal replication *in vivo*, which raises the question “is the function of aRPA to prevent and possibly impede replication, or is it a consequence of its other functions?” DNA replication and in particular, initiation of DNA replication, is a highly regulated process that requires many essential and non-essential proteins to spatially and temporally coordinate to preserve genomic integrity and stability of the cell. How the cell initiates DNA replication is still a highly active area of research, as many questions remain unanswered. The current model for eukaryotic DNA replication proposes that during the G1-phase of the cell cycle, origin bound origin recognition complex (ORC) recruits Cdc6 which in turn recruits Cdt1 and the MCM helicase to form the pre-replicative complex (pre-RC)[183]. The assembly of the pre-RC is regulated by protein phosphorylation and only occurs during the G1-phase of the cell cycle when levels of inhibitory CDK are low. In addition to phosphorylation as a regulatory mechanism, a protein-protein interaction mechanism exists that is dependent on geminin. Geminin binds to chromatin bound Cdt1 and prevents MCM loading without interfering with ORC or Cdc6 association [184]. Once the pre-RC is formed, S-phase CDK (S-CDK) and Cdc7-Dbf4 (DDK) are required to further promote initiation and function as kinases. S-CDK phosphorylates TOPBP1 and RecQL4, which then recruit Mcm10, Cdc45 and the pre-loading complex (including pol ε and GINS). Once activated, the helicase moves bi-directionally generating ssDNA to which RPA binds and recruits pol α to start primer synthesis.

It is clear that the initiation of DNA replication is a complex process and its regulation is not dependent on RPA, as it binds after the helicase complex has been activated. So how does aRPA fit into all of this? Perhaps aRPA could be functioning as a fail safe for a cell that is not ready to divide. If aRPA were to be the RPA complex that bound to the newly generated ssDNA during the initial unwinding of the origin, it would prevent pol α from associating with the ssDNA. This would prevent primer synthesis and stop replication. Current literature suggests that there is not much feedback between pol α and the helicase. It has been shown that pol α can be inhibited but the helicase still proceeds generating large regions of ssDNA [185-187]. Therefore, aRPA could stop replication even if the replisome had escaped all other regulatory mechanisms.

The above role for aRPA as a fail safe for a cell that is not ready to divide is dependent on there being enough aRPA to compete with the canonical RPA complex for exposed ssDNA. Based on mRNA expression of *RPA2* and *RPA4* in different tissues, there are usually lower amounts of *RPA4* than *RPA2* but their expression is of the same order of magnitude. It is interesting to point out that *RPA4* expression is decreased in human tumor tissues where *RPA2* is generally increased along with other proteins required for DNA replication (ex. MCM2-7, Cdc6, Cdt1 and geminin)[6, 188-190]. This would suggest that having the aRPA complex in cells that are dividing continually is detrimental to this process and does not promote efficient DNA replication. Additional evidence supports *RPA4* expression in non-proliferative tissues. Menezo *et al.* examined the expression of DNA repair genes in human oocytes [191]. Within the set of genes they examined were *RPA1, RPA2, RPA3* and *RPA4*. They found that expression of *RPA1* and *RPA3* was high but expression of *RPA2* was low. Interestingly, *RPA4* expression was medium suggesting more aRPA than RPA complex in oocytes.

Perhaps, aRPA does not have an active role in DNA replication. This would suggest a model similar to the one recently established in *Oryza sativa* and *Arabidopsis thaliana* where different RPA complexes function in discrete processes[107]. It is worth noting that of all the DNA polymerases identified to date, only pol α has a function restricted to DNA replication. Therefore, if aRPA were to function differently than RPA, a loss of function with a key protein that is restricted to one process would easily remove aRPA from functioning in that process. Conversely, it would be difficult to exclude RPA from processes outside of DNA replication, especially since *RPA4* appears to be a recent addition to the genome.

Further studies need to be done to determine if aRPA does actively participate in DNA replication. Current *in vivo* studies have only been done with transient expression of RPA4 either in the presence or absence (siRNA knockdown) of RPA2, which can only be achieved for a relatively short time. In order to determine the long-term effect of RPA4 expression, a cell line must be generated that stably expresses RPA4 or that allows RPA4 expression to be induced (eg. Tet-On/Tet-Off system). If RPA4 does have an active role in DNA replication, then one would expect a decrease in the proliferative capacity of the cells expressing RPA4, a halt in the cell cycle, senescence or apoptosis.

DNA Repair

There are multiple mechanisms to repair DNA when it is damaged either by endogenous or exogenous sources. Most of these processes involve generating ssDNA and are dependent on RPA. Through collaborations, we have shown that aRPA is able to substitute for RPA during NER and the initial steps of homologous recombination. However, the mechanism that aRPA uses during NER is different from RPA. This suggests that RPA4 has developed an alternative approach to responding to DNA damage. One key difference between aRPA and RPA was aRPA's higher affinity for alkylated DNA and low cooperativity with XPA. Even though further studies need to be done to characterize its affinity to other forms of damaged DNA, aRPA could be serving as an initial sensor for DNA damage. This would make the response time of the cell faster and allow it to deal with and resolve the damage quicker. This would suggest a model where aRPA is continually searching for damaged DNA and once it finds it, it recruits the repair machinery to that site. Interestingly, in HeLa cells that are expressing both endogenous RPA2 and exogenous RPA4 (transiently), RPA4 foci form in the absence of exogenous DNA damage suggesting additional DNA damage repair is taking place. Once the repair machinery is established, perhaps aRPA only binds the damaged strand and RPA binds the non-damaged strand. This would allow RPA to help coordinate the rest of the repair process efficiently and aRPA would be removed with the excised DNA damage. It remains to be determined if this observation is a result of increased detection or from RPA4 stalling active replication forks.

Recently, two new ssDNA binding protein complexes have been identified and shown to function in DNA repair. hSSB1/INTS3/hSSBIP1 and hSSB2/INTS3/hSSBIP1 have been to shown to have over-lapping function and function in homologous recombination-dependent repair of double strand breaks and ATM-dependent damage-response pathway[178]. Perhaps aRPA is another ssDNA binding protein that functions in repair pathways that do not involve a double strand break, such as NER, BER and MMR. This would then suggest that aRPA might play a role in the ATR-dependent damage-response pathway. Through initial collaborative studies with Dr. Aziz Sancar, *in vitro* kinase studies indicate that aRPA is able to activate the ATR response resulting in CHK1 phosphorylation, via TOPBP1 (Figure 5-1). Interestingly, in the same assay, hSSB1 is unable to elicit the same response suggesting specificity for either RPA or aRPA. However, further studies need to be done to establish significance *in vivo*.

Regulation by Phosphorylation

RPA is phosphorylated during the cell cycle and after cellular DNA damage on the N-terminus of RPA2 known as the phosphorylation domain [33]. This unstructured domain contains ~40 residues of which nine have been shown to be phosphorylated. During S- and G2-phase, RPA2 is phosphorylated at Ser-23 and Ser-29 by cyclin/Cdk. Following cellular DNA damage, RPA2 becomes hyper-phosphorylated by members of the phosphoinositide 3-like kinase family [192]. It has been proposed that the phosphorylation of RPA regulates its function. Specifically, hyper-phosphorylated RPA has reduced function in DNA replication but little effect on function in DNA repair [33]. RPA4 also has a putative N-terminal phosphorylation domain that is rich in serine (7) and threonine (2) residues; however, it is not known if RPA4 is phosphorylated. To explore the possibility of RPA4 phosphorylation, a phosphorylation prediction server (NetPhosK 1.0, http://www.cbs.dtu.dk/services/NetPhosK) was used for both RPA2 and RPA4. As shown in Figure 5-2, out of the nine known phosphorylation sites in RPA2, seven were predicted by NetPhosk plus an additional tyrosine residue. When phosphorylation sites were predicted for RPA4, only three potential sites of phosphorylation were identified, Ser-8, Thr-31 and Thr-36.

Of the two sites on RPA2 that are phosphorylated during the cell cycle, Ser-23 and Ser-29, only one of these sites is conserved in RPA4, Thr-31. This site is a partial consensus sequence for Cdk. The canonical consensus sequence is S/T-P-X-R/K and the site at Thr31 is T-P-X-X-K. Interestingly, the site at Ser-29 in RPA2 is S-P-X, which is also a partial consensus sequence. The other predicted sites on RPA4 were similar to Ser-8 of RPA2, which is thought to be a minor site of phosphorylated after DNA damage by DNA-PK and Ser-33, which is a major site of phosphorylation by ATR [193]. If the prediction is correct, then RPA4 is phosphorylated by the same kinases as RPA2 but to a lesser extent suggesting that RPA4 is regulated similarly to RPA2. The current model in the literature suggests that hyper-phosphorylation of RPA2 shifts the RPA pool from DNA replication to DNA repair processes [33]. However, since aRPA either impedes or does not support DNA replication it makes sense that RPA4 would not need to be phosphorylated as extensively as RPA2 in the canonical RPA complex.

Alternatively, phosphorylation of RPA4 could have an opposite effect as it does on RPA2. This model would predict that upon phosphorylation of RPA4, the aRPA complex is activated as a proliferative RPA, which could now function in DNA replication. As described above, the L34 loop of RPA4 can inactive RPA2 in DNA replication, which is presumably caused by the change in charge. If the overall charge of the RPA4 subunit and not the location of the L34 loop were most important factor, then phosphorylation would add negative charge to the subunit and might counteract the basic L34 loop. In this model, phosphorylated aRPA could potentially function in DNA replication. However, this model is less likely since RPA2 phosphorylation causes a decrease in interactions with pol α and Tag (Wold lab, unpublished data). This would suggest that a phosphorylated phosphorylation domain is altering the functions of RPA1 and might accentuate the inhibitory effects of RPA4. Future studies should examine the possibility of RPA4 phosphorylation and what role it plays with respect to aRPA function.

Therapeutic Potential

Both cancer and viral infection depend on DNA replication, either uncontrolled or of viral DNA by proteins supplied by the host. Therefore, one way to stop either of these processes is to inhibit DNA replication. In fact, there are currently anticancer drugs that do so but many of them are nucleoside analogs, which target the elongation phase of DNA replication[194]. A few drugs target proteins involved in DNA replication, topoisomerase I and topoisomerase II. However, these drugs cannot differentiate between a healthy cell that is going through S-phase and a cancer cell, which makes them dose limiting[194]. Therefore, a drug that stops DNA replication and does not kill healthy cells is desirable.

I have shown that aRPA does not support viral DNA replication in the SV40 system and inhibits the function of canonical RPA. Others in the Wold lab have shown that RPA4 does not support chromosomal replication in the absence of RPA2 and a L34 loop switch between RPA2 and RPA4 creates a dominant negative that inhibits RPA2 function[111]. These results raise the question: ‘Can RPA4 be useful as an antiviral or anticancer therapy?” Given that RPA4 and the aRPA complex inhibit DNA replication but support genomic maintenance functions, the possibility of RPA4 having therapeutic potential seems reasonable. One possibility would involve increasing the expression of RPA4 in cancerous or infected cells. Thus, RPA4 could possibly counteract the proliferative signals found in the cells. My findings that RPA4 expression is decreased in transformed tissues and not expressed in established cell lines supports the idea that RPA4 expression is not desirable when active DNA replication is occurring. However, no information is available regarding how RPA4 expression is regulated. Therefore, future studies could involve defining the regulation of the RPA4 promoter. Additionally, gene therapy methods could be explored as means to expressing RPA4.

Interestingly, a study was done by Basilion et al. that used variagenic targeting to target RPA1 in cancerous cells [195]. To summarize, they exploited cancerous cells that had lost one allele of RPA1 and targeted the intact allele with phosphorothioate oligonucleotides directed at polymorphisms within that allele. Thereby, they selectively killed the cancerous cells by depleting them of all RPA1 but not affecting normal cells with two intact RPA1 alleles. Another possibility could use a simpler approach to Basilion and colleagues that exploits the fact that there are two forms of RPA in the cell, proliferative (RPA) and non-proliferative (aRPA). Instead of targeting cancerous cell with a loss of heterozygosity, RPA2 could be targeted. This would deplete cells of the proliferative RPA complex and may cause an increase in RPA4 through feedback mechanisms that regulate total RPA abundance or could be used in combination with a gene therapy method.

In addition to increasing RPA4 expression, a small molecule could be designed to target RPA2 of the canonical RPA complex. I have shown that the basic L34 loop of RPA4 contains most of the properties of RPA4 and by replacing the L34 loop of RPA2 with that of RPA4 a dominant negative complex is generated. Therefore, by targeting the L34 loop of RPA2 with a small molecule that could mask or change the acidic charge to a basic charge, perhaps the anti-proliferative properties of RPA4 would be conferred to the complex but would still allow it to function in other processes. Andrews and Turchi developed a high-throughput screen for inhibitors of RPA but they looked for inhibitors that disrupted RPA’s ability to bind ssDNA [196]. This would prevent DNA replication but also prevent RPA from functioning in maintenance processes since ssDNA binding appears to be required for all processes of RPA. Therefore, targeting a DBD that is not required for high affinity ssDNA binding makes more sense.

RPA4 Evolution

The *RPA4* gene appeared relatively recently in evolution. *RPA4*-like sequences can be found in most mammals and specifically within the infraclass of eutheria, as a homologous region has not been identified in opossum or platypus. This region is a noncoding region in most eutheria members but is a coding region in primates and horse. This suggests that *RPA4* is an orphan gene that initially arose from a gene duplication event during the divergence of eutheria. Given that *RPA4* is intronless and contains a poly(A) tract suggests a retrotransposition followed by rapid divergence [111, 197]. It has been estimated that approximately 3% of human genes are restricted to primates [198]. However, very few have been well characterized experimentally. A well-characterized gene is dermcidin, which encodes a peptide that is secreted in sweat glands with antimicrobial activity and has been reported to be involved in neural survival and cancer [199]. Another example of an orphan gene with described function is the SPHAR, which is involved in the regulation of DNA synthesis [200]. Two more genes that function in DNA metabolism pathways are FAM9B and FAM9C, expressed solely in the testis, and now have been suggested to play a role in mediating recombination during meiosis [201].

It has been speculated that primate-specific genes are preferentially expressed in the reproductive system [202]. Recently, Tay *et al.* examined a subset of primate-specific genes for expression in reproductive tissues as well as neuronal tissues [202]. They report that primate-specific genes were preferentially expressed in reproductive organs and tissues at a 5% significance level. Of the 114 primate-specific genes examined, 48 were expressed solely in reproductive tissues, 19 solely expressed in neuronal tissues and 8 had both reproductive and neuronal expression [203].

RPA4 is also located on the X chromosome. A recent paper examining the origin and evolution of the therian X chromosome, described a high frequency (11-12 times more than expected) of gene retroposition in to and out of the X chromosome after it had differentiated into a sex chromosome [204]. By examining the expression of a subset of retrogenes on the X chromosome, it was determined that this subset was expressed before meiosis in spermatogonia and after meiosis in spermatids in testes. Additionally, retrogenes on the X chromosome were expressed in ovary tissue and oocytes and in one example almost exclusively in the placenta [204].

Given that *RPA4* is located on the X chromosome, appears to be an orphan gene and shown to be expressed in placenta, ovary, prostate and testis tissue and specifically in oocytes [147, 191], I would speculate that RPA4 functions in some aspect of reproduction. However, future studies would be needed to address this.

.

Figure 5-1: Effects of RPA/aRPA/hSSB1/*E. coli* SSB on TopBP1-dependent activation of ATR kinase activity in the presence of ssDNA.

Stimulation of TopBP1-dependent ATR kinase by single-stranded binding proteins. Kinase assays were performed with ATR-ATRIP (0.2 nM), Chk1-kd, TopBP1 (5 nM), RPA, aRPA, hSSB1 or *E. coli* SSB (4 -34 nM) and single-stranded plasmid DNA (0.07 nM). For binding of RPA, aRPA, hSSB1 or *E. coli* SSB to DNA, single-stranded plasmid DNA was pre-incubated with the protein for 10 min on ice. Kinase reactions were incubated at 30°C for 20 min, terminated by the addition of SDS-PAGE loading buffer, and the proteins were separated by SDS-PAGE. Chk1 phosphorylation was detected by immunoblotting using a phosphor-S345-Chk1 antibody. The highest level of phosphorylation in each experiment was set equal to 100, and the levels of phosphorylation in the other lanes were expressed relative to this value. Data generated by Dr. Aziz Sancar's laboratory.

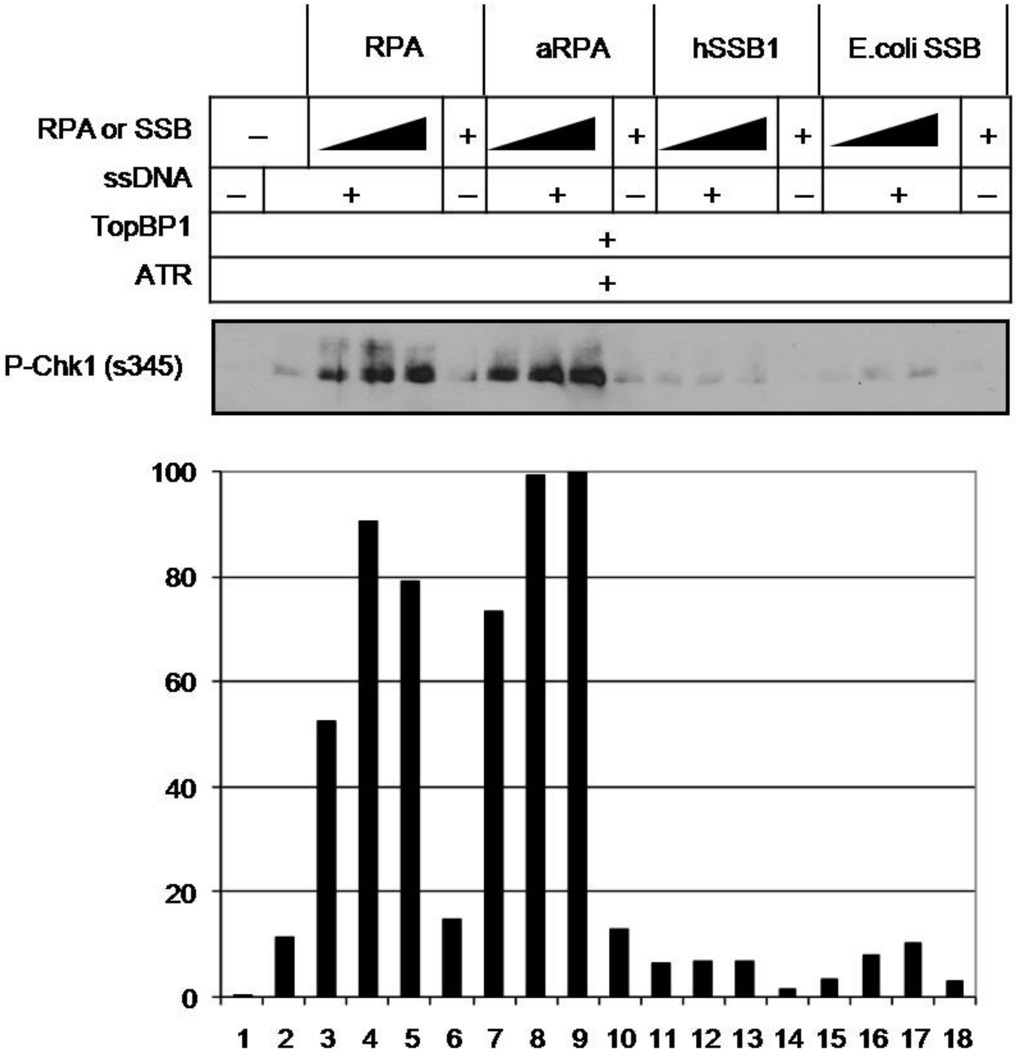
RPA
aRPA
hSSB1
E.coli SSB
RPA or SSB
ssDNA
TopBP1
ATR
–
+
P-Chk1 (s345)
100
80
60
40
20
0
1
2
3
4
5
6
7
8
9
10
11
12
13
14
15
16
17
18

Figure 5-2: Predicted sites of RPA2 and RPA4 phosphorylation.

RPA2 and RPA4 sequences were submitted to the NetPhosK 1.0 server (http://www.cbs.dtu.dk/services/NetPhosK). Residues that can be phosphorylated are in blue. Residues that are known or predicted to be phosphorylated are in red.

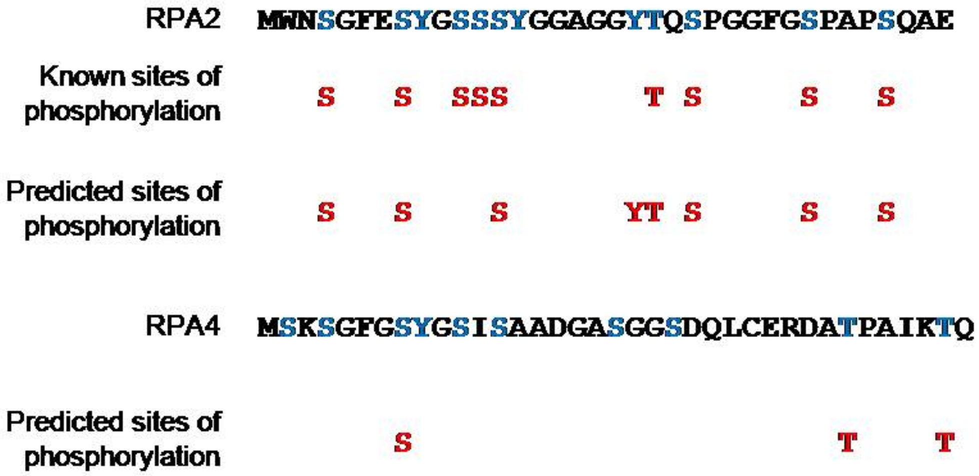
RPA2
MWNSGFESYGSSSYGGAGGYTQSPGGFGSPAPSQAE
Known sites of phosphorylation
S S SSS T S S S
Predicted sites of phosphorylation
S S S YT S S S
RPA4
MSKSGFGSYGSISAADGASGGSDQLCERDATPAIKTQ
Predicted sites of phosphorylation
S T T

APPENDIX A

DEFINING CONFORMATIONAL CHANGES OF RPA AFTER PHOSPHORYLATION OF THE N-TERMINUS OF RPA2

Introduction

RPA not only interacts with DNA but also interacts with other proteins involved with DNA metabolism [1]. There is also evidence that the N-terminal region of RPA2 interacts with other regions of RPA that is regulated by its phosphorylation state [205]. The N-terminal region (phosphorylation domain) of RPA2 contains at least six sites and at most nine sites of *in vivo* phosphorylation giving rise to at least four different phosphorylation states [206-209]. These sites are phosphorylated in a cell cycle dependent manner during S phase and G2 phase by cyclin-dependent kinases [210, 211]. Phosphorylation is also observed in response to DNA damage by members of the phosphatidylinositol 3-kinase-like serine/threonine protein kinase family, which include DNA-PK, ATM, and ATR [206, 212, 213]. Hyper-phosphorylated forms are generated by additional phosphorylation of the phosphorylation domain [214].

It has been proposed that the phosphorylation of RPA2 is used as a regulatory mechanism in the cell [205, 215]. After phosphorylation or hyper-phosphorylation occurs, a large negative charge is localized on the N-terminal region of RPA2. This negative charge has been hypothesized to change the conformation of RPA through subunit interactions and to alter interactions with DNA. Recent studies have suggested that upon phosphorylation, the phosphorylation domain interacts with DBDs of RPA1. One report using nuclear magnetic resonance spectroscopy (NMR) provides evidence that a phosphorylation mimetic peptide of the phosphorylation domain interacts with DBD F [205]. Another report suggests that the phosphorylation domain in its phosphorylated state interacts with DBD B, which was determined using a chemical modification protection assay [215]. Taken together these studies suggest that there may be multiple conformations of RPA in its phosphorylated state.

The studies presented here aim to show that phosphorylated RPA2 interacts with the individual DBDs in RPA1 and that these interactions cause RPA to adopt alternate conformations and regulate the function of the RPA in the cell. Specific inter- and intra-domain interactions of the RPA complex were examined by fluorescence resonance energy transfer (FRET) and domain interactions of RPA1 and RPA2/3 sub-complexes or a fragment of RPA1 containing DBD F, linker, DBD A, and DBD B and phosphorylation domain peptide were examined by NMR.

Materials and Methods

Materials

ReAsH (Resorufin Arsenical Helix binder) and FlAsH (Fluorescein Arsenical Helix binder) were purchased from Invitrogen.

Plasmids

Mutations were generated using standard site-directed mutagenesis and cloning procedures. Table A-1 lists mutations, primers used and nomenclature used.

ReAsH and FlAsH Protein Labeling

Proteins that contained the tetra-cysteine tag were labeled on ice for 30 minutes in reaction (25 μL) containing tagged RPA (2 μM), Filter Binding Buffer (30 mM HEPES pH 7.5, 5 mM $MgCl_2$, 100 mM NaCl, 0.5% inositol (w/v), 1 mM dithiothreitol), ethane dithiol (120 μM), 2,3-dimercaptopropanol (25 μM) and FlAsH and/or ReAsH (200 μM). Samples were electrophoresed on a 8-14% denaturing polyacrylamide gel and visualized by illumination at 302 nm.

Fluorescence Resonance Energy Transfer Assay

Standard samples (120 µL) contained tagged RPA (2 µM), Filter Binding Buffer (30 mM HEPES pH 7.5, 5 mM $MgCl_2$, 100 mM NaCl, 0.5% inositol (w/v), 1 mM dithiothreitol), ethane dithiol (120 µM), 2,3-dimercaptopropanol (25 µM) and FlAsH and/or ReAsH (200 µM). Samples and were excited at 490 nm and emission was monitored from 510 – 600 nm with an integration of 0.1 s using a FluroLog 3 spectrofluorometer.

Protein Expression and Purification

Proteins that were ^{15}N labeled were grown in media containing 1.8g K_2HPO_4, 1.4 g KH_2PO_4, 0.49 g $MgSO_4$, 0.011 g $CaCl_2$, 5 g Celtone-N, 4 g glucose and appropriate antibiotic per liter. A single colony was used to inoculate 250 mL of LB/L of ^{15}N media and grown overnight at 37°C with shaking. Cells were pelleted from the LB cultures and resuspended and added to the ^{15}N media. Cultures were induced with isopropyl-β-D-thiogalactoside (10 µM) at an OD of 0.8. For ^{15}N and ^{2}H labeled protein, the ^{15}N media was used but the components were dissolved in 1 L of D_2O. Proteins were purified using standard RPA purification procedures. Purified proteins were concentrated and buffer exchanged by centrifugation using Amicon Ultra – 15 centrifugal filter devices. Buffer exchange was achieved by diluting the sample four times with the correct buffer following centrifugation. Samples (560 µL) of RPA2/3 sub-complexes contained 20 mM potassium phosphate (pH 7.5), 0.002% sodium azide, 10% D_2O and 200 – 300 µM protein. Samples of RPA-FAB contained 30 mM piperazine-N,N'-bis(2-ethanesulfonic acid), 50 mM KCl, 0.002% sodium azide, 10% D_2O, 2 mM tris(2-carboxyethyl)phosphine and up to 350 µM RPA-FAB.

Nuclear Magneict Resonance Spectroscopy

Spectra were acquired on either a Unity Inova 600 MHz Oxford AS600 or an Avance II 800 MHz US2 instrument. Standard protocols were used to acquire

Heteronuclear Single Quantum Correlation and Transverse Relaxation Optimized Spectroscopy spectra. Data was analyzed using NMRViewJ.

Results

It has been suggested that upon phosphorylation of the N-terminus of RPA2, referred to as the phosphorylation domain, there is a conformational change of the RPA complex, which alters the physiological role of RPA[205]. To define the conformation changes after phosphorylation, fluorescence resonance energy transfer (FRET) was monitored between labeled domains of RPA. A Cys-Cys-Pro-Gly-Cys-Cys FlAsH/ReAsH recognition sequence (PG sequence) was inserted at the beginning of the phosphorylation domain (both the phosphorylation mimetic, RPA2-Asp8, and wild type form) and in the L12 loop of each of the DBDs of RPA1. Additionally, a Cys-Cys-Lys-Ala-Cys-Cys (KA sequence) recognition sequence were inserted into the DBDs of RPA1. Chen et al. reported selective labeling of FlAsH to the KA sequence and ReAsH to the PG sequence[216]. However, their results were not able to be reproduced. Therefore, FRET studies were carried out using only the PG sequence.

The expression of the proteins was examined by labeling cell lysates following the induction of DBD F/PD, DBD F/Asp, DBD A/PD, DBD A/Asp, DBD B/PD, DBD B/Asp, DBD C/PD, and DBD C/Asp (see Table 1 for nomenclature). Figure A-1 shows a SDS polyacrylamide gel illuminated with 302 nm light of lysates labeled with FlAsH prior to electrophoresis. Visible bands corresponded to RPA1 and to RPA2; however other bands were also visible. The other major band labeled by FlAsH was SlyD, which ran at 23 kDa. SlyD is an *E.coli* chaperone protein that has a cysteine rich region that is able to bind to FlAsH and ReAsH.

Cell lysates were hetero-labeled with FlAsH and ReAsH and analyzed for FRET. Figure A-2 shows the normalized data from the experiments. Figure A-2A shows no FRET was observed with either DBD F/Asp or DBD F/PD. However, Figure A-2B and

A-2C show that there was a FRET signal from DBD A/Asp and DBD B/Asp but not with DBD A/PD and DBD B/PD. The most intense FRET signal was from DBD B/Asp. These data suggest that the phosphorylation mimetic phosphorylation domain is closer to DBD B than DBD A. This argues that there is a conformational change with the phosphorylation mimetic that brings the phosphorylation domain in the proximity of the core DNA binding region of RPA (DBD A and DBD B). Figure A-2D shows that there were differences between DBD C/PD and DBD C/Asp. There was a slight FRET signal with DBD C/PD, which suggest that the phosphorylation domain is closer to DBD C with the wild-type phosphorylation domain and farther away with the phosphorylation mimetic. However, the difference between DBD C/Asp and DBD C/PD may be in the range of experimental error.

FRET was also examined using partially purified proteins to remove SlyD (Figure A-3). Following partial purification, the proteins were concentrated and buffer exchanged into conditions appropriate for the FRET experiments. The proteins were verified by labeling with FlAsH prior to SDS-PAGE and illumination at 302 nm. The gel shows that DBD F/Asp, DBD F/PD, DBD B/Asp, DBD B/PD samples contained only bands that correspond to RPA1 and RPA2 (Figure 7). DBD A /PD, DBD A/Asp, DBD C/PD, and DBD C/Asp did not label efficiently and further analysis showed that the protein was unstable after concentrating, buffer exchanging, and a freeze/thaw cycle.

The partially purified proteins: DBD F/Asp, DBD F/PD, DBD B/Asp, and DBD B/PD were further used to examine intra-molecular interactions observed in the cell lysates. Figure A-4 summarizes the findings from these experiments. The results for DBD B/Asp and DBD B/PD support the finding in cell lysates. Figure A-4B shows that when DBD B/Asp was heterolabeled with FlAsH and ReAsH, there was a significant increase in the spectrum corresponding to a FRET signal. This increase was not observed with DBD B/PD. DBD F/PD also did not show a FRET signal (Figure A-4A). In contrast to the cell lysate result for DBD F/Asp, there was an observable FRET signal (Figure A-4A).

In order to determine FRET distances between the donor and acceptor, a baseline in the absence of the acceptor must be established. This is challenging in this system because the donor and acceptor cannot be separated due to insolubility issues. The two possible ways to circumvent this issue are: (1) disrupt the complex and subunit interactions with SDS, (2) use a protease to digest the protein complex into small protein fragments. The first option formed a precipitate due to the potassium salts used in the buffers. The second option was addressed by using the protease, Subtilisin. The results showed that FlAsH and ReAsH labeled RPA could be proteolyzed into domain-sized fragments. Unexpectedly, after Subtilisin digestion the FRET signal did not change significantly (Figure A-5). This suggests that the protein fragments are still interacting even when the protein complex is no longer intact. It was anticipated that the interaction would be weak and interactions, predominately intra-molecular, would be aided by an intact RPA complex. However, the results suggest that this may not be the case.

To address the possibility that the interactions are inter-molecular, the proteins were labeled individually and then mixed. The mixing experiment showed that again DBD F/Asp and DBD B/Asp still showed a FRET signal (Figure A-6B and D) where DBD F/PD and DBD B/PD did not (Figure A-6A and C). These results suggest that the interaction between the phosphorylation mimetic phosphorylation domain and the DBDs of RPA1 is at least partially due to inter-molecular interactions but does not exclude intra-molecular interactions.

To identify amino acid specific interactions, NMR spectroscopic techniques were used. To determine if there are interactions between the RPA2/3 sub-complex and the individual RPA1 domains, the RPA2/3 sub-complex was labeled with ^{15}N while the DBDs of RPA1 were not labeled (Figure A-7). This allowed for changes in the Heteronuclear Single Quantum Correlation (HSQC) spectrum to be considered as changes in the sub-complex because of the addition of the DBD. To determine the residues that are interacting in RPA1, a C-terminal deletion of RPA1 was ^{15}N labeled and a phosphorylation domain peptide was used. The C-terminal deletion of RPA1 (FAB) was used because full length RPA1was insoluble and too large for NMR studies.

To assess the feasibility of peak assignment of the RPA2/3 sub-complex, initial HSQC experiments have been performed on both RPA2/3 and RPA2/3Asp (Figure A-8 and Figure A-9). Ideally, there should be one peak for every amino acid in the protein but this was not the case. However, there was a significant percent of peaks in the HSQC spectrum. The HSQC for RPA2/3 and RPA2/3Asp showed 313 and 283 resolvable peaks, respectively. Additionally, by overlaying the HSQC spectra of the two sub-complexes, differences in the proteins were observed (Figure A-10). Since the flexible regions of proteins had better resolution than rigid or buried regions, the phosphorylation domain should show a significant difference between the two sub-complexes (Figure A-11). Upon the addition of DBD F, there were peaks shifts seen in RPA2/3Asp that were not seen in RPA2/3. This suggests that DBD F and RPA2/3Asp are interacting where RPA2/3 and DBD F are not.

Initial experiments have been carried out with ^{15}N labeled FAB. These studies show that transverse relaxation optimized spectroscopy (TROSY) experiments have better resolution than standard HSQC experiments. Figure A-12 shows well dispersed peaks for FAB, which is an indication of a well-folded protein. There were 434 detectable peaks in the spectrum including side chain peaks. FAB has 442 amino acids with 39 asparagine and glutamine residues, which contribute to additional peaks. However, the 60 amino acid linker is flexible and the residues in this region usually are not detected. A 35 residue peptide corresponding to the phosphorylation mimetic phosphorylation domain was added to validate the experimental design. Upon addition of the Asp peptide, there were shifts in peaks seen in the FAB spectrum (Figure 13), indicating an interaction between FAB and the peptide.

These studies focused on using a fragment of RPA1 (FAB). Due to the large size of the fragment (50 kDa), the protein needed to be ^{2}H labeled as well as ^{15}N labeled. A ^{2}H, ^{15}N labeled FAB protein was purified; however, this protein exhibited decreased stability at high concentrations. Additionally, when the phosphorylation domain peptide was titrated into a sample of double labeled FAB, the amount of precipitated protein increased with each addition causing a continual decrease in the signal. The peptide additions only lead to minor changes in the HSQC spectrum, which indicates that the FAB – phosphorylation domain peptide complex was not soluble.

Discussion

The current results suggest that upon phosphorylation of RPA2, there is a conformational change. The data from DBD C/PD and DBD C/Asp lysate experiment implies that the phosphorylation domain is closer to DBD C when unphosphorylated and upon phosphorylation, moves away from DBD C. After phosphorylation, the phosphorylation domain then interacts with DBD F, DBD A, and DBD B of RPA1. The phosphorylation domain could be interacting with DBD B > DBD A > DBD F resulting in a population of interactions or the phosphorylation domain could be interacting with all of the DBDs at the same time with the N-terminus at DBD B. This interaction could be with the DBDs of the same molecule or of a different RPA molecule. The current data is unable to rule out the intra-molecular interaction. This interaction could be used to regulate protein – protein interactions that occur with RPA1 or could be used to remove RPA from ssDNA. It could also be used to regulate further phosphorylation of other RPA molecules. Anantha et al. suggest that RPA phosphorylation is regulated not only in *cis* but also in *trans* [217]. These results support a in *trans* mode of regulation where the phosphorylation of one RPA molecule stimulates the phosphorylation of a different RPA molecule.

Table A-1: Nomenclature of RPA proteins with FlAsH/ReAsH recognition sequence.

Lab Name	Plasmid #	Primers	Location of Mutation
DBD F/PD	565 572	639/680 cloned from #485	RPA1 G36 - N37 RPA2 N-terminus
DBD F/Asp	565 570	639/680 cloned from #485	RPA1 G36 - N37 RPA2 N-terminus
DBD A/PD	590 572	756/757 cloned from #485	RPA1 S215 - R216 RPA2 N-terminus
DBD A/Asp	590 570	756/757 cloned from #485	RPA1 S215 - R216 RPA2 N-terminus
DBD B/PD	591 572	758/789 cloned from #485	RPA1 S336 - N337 RPA2 N-terminus
DBD B/Asp	591 570	758/759 cloned from #485	RPA1 S336 - N337 RPA2 N-terminus
DBD C/PD	641 572	834/835 cloned from #485	RPA1 E534 - S535 RPA2 N-terminus
DBD C/Asp	641 570	834/835 cloned from #485	RPA1 E534 - S535 RPA2 N-terminus

Figure A-1: Detection of FlAsH labeled RPA1 and RPA2 subunits.

E. coli lysates expressing indicated proteins were labeled with FlAsH prior to electrophoresis on an 8-14% polyacrylamide gel. Labeled subunits were visualized by illumination at 302 nm.

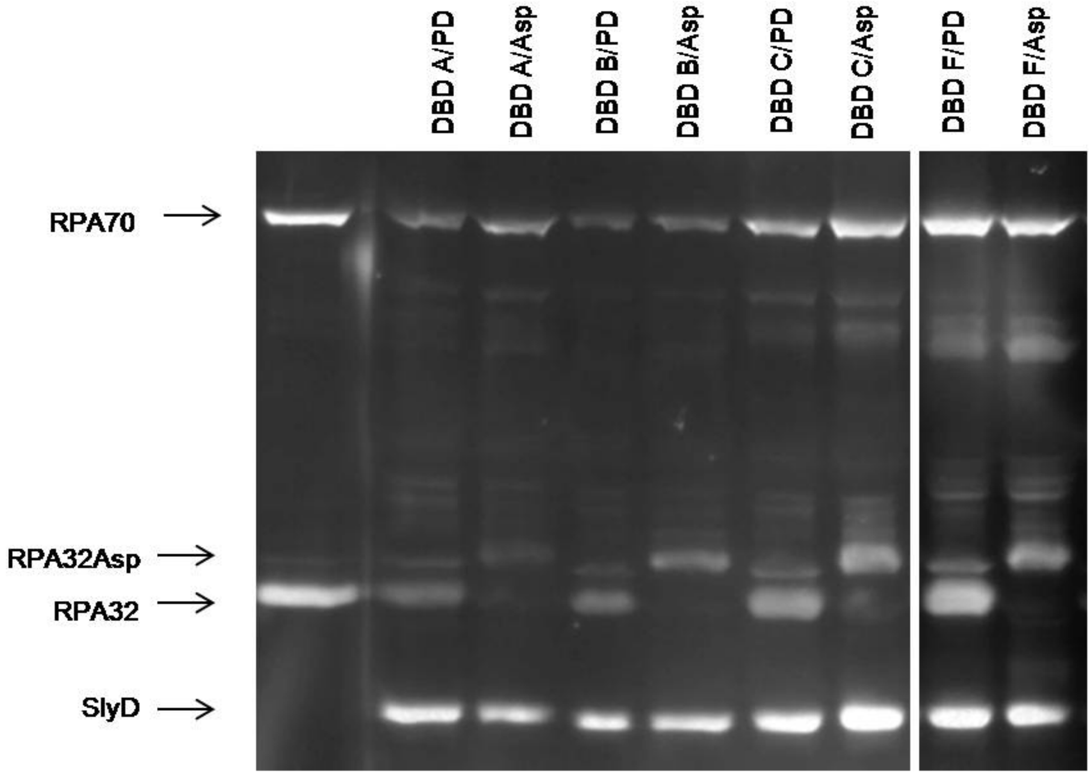
DBD A/PD
DBD A/Asp
DBD B/PD
DBD B/Asp
DBD C/PD
DBD C/Asp
DBD F/PD
DBD F/Asp
RPA70
RPA32Asp
RPA32
SlyD

Figure A-2: FRET analysis of heterolabeled RPA mutants in cell lysates.

Indicated proteins were expressed in *E. coli* cells and lysates were labeled with both FlAsH and ReAsH. Labeled lysates were monitored for FRET by excitation at 490 nm and emission monitored from 510 to 600 nm. Emission spectra were normalized where the highest signal was set to 1. (A) DBD F/PD (blue line) and DBD F/Asp (red line). (B) DBD A/PD (blue line) and DBD A/Asp (red line). (C) DBD B/PD (blue line) and DBD B/Asp (red line). (D) DBD C/PD (blue line) and DBD C/Asp.

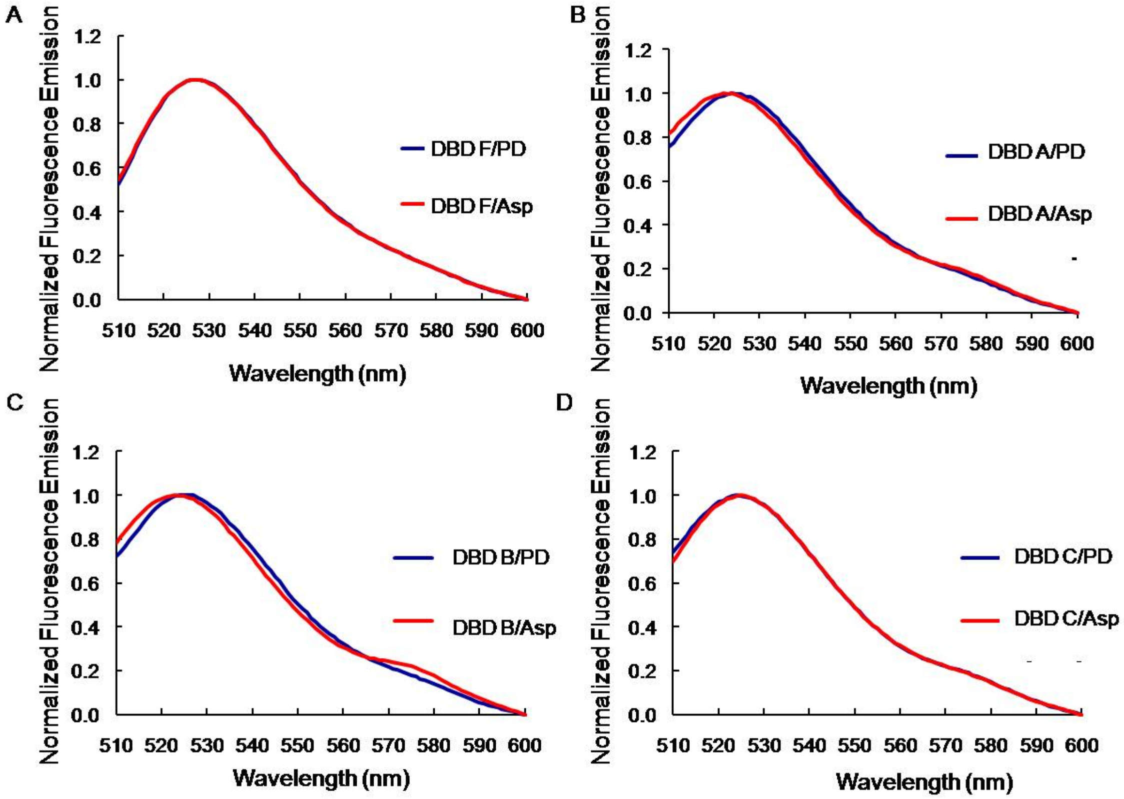
A
Normalized Fluorescence Emission
1.2
1.0
0.8
0.6
0.4
0.2
0.0
510 520 530 540 550 560 570 580 590 600
Wavelength (nm)
DBD F/PD
DBD F/Asp
B
Normalized Fluorescence Emission
1.2
1.0
0.8
0.6
0.4
0.2
0.0
510 520 530 540 550 560 570 580 590 600
Wavelength (nm)
DBD A/PD
DBD A/Asp
C
Normalized Fluorescence Emission
1.2
1.0
0.8
0.6
0.4
0.2
0.0
510 520 530 540 550 560 570 580 590 600
Wavelength (nm)
DBD B/PD
DBD B/Asp
D
Normalized Fluorescence Emission
1.2
1.0
0.8
0.6
0.4
0.2
0.0
510 520 530 540 550 560 570 580 590 600
Wavelength (nm)
DBD C/PD
DBD C/Asp

Figure A-3: Detection of purified RPA mutants labeled with FlAsH.

RPA mutants containing the FlAsH and ReAsH recognition sequence were purified over Affi-Gel Blue and Hydroxylapatite columns and labeled with FlAsH prior to electrophoresis on an 8-14% polyacrylamide gel. Labeled subunits were detected by illumination at 302 nm.

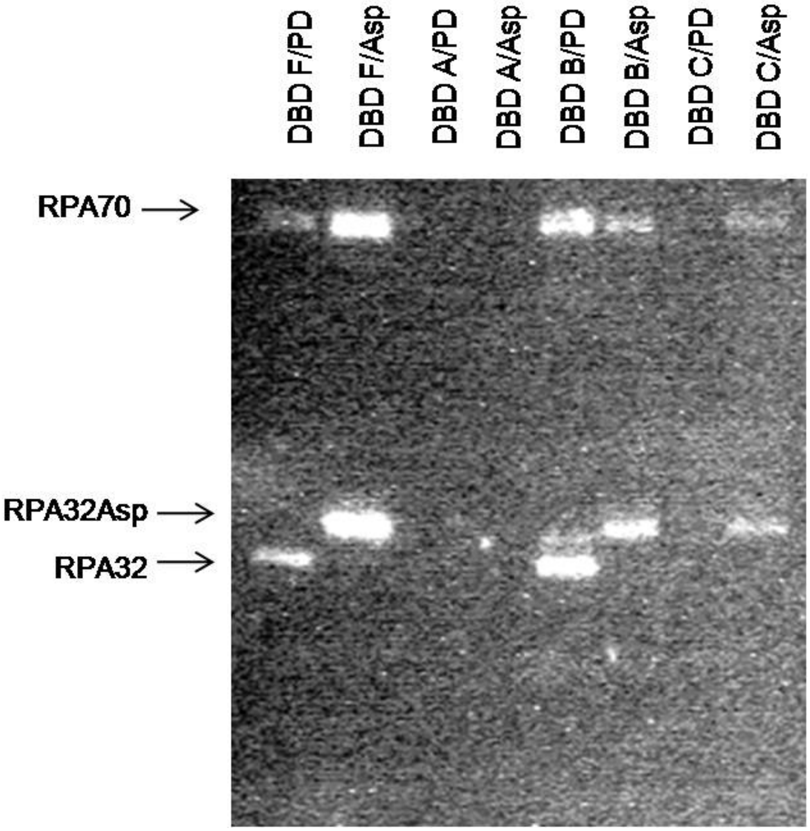
DBD F/PD
DBD F/Asp
DBD A/PD
DBD A/Asp
DBD B/PD
DBD B/Asp
DBD C/PD
DBD C/Asp
RPA70
RPA32Asp
RPA32

Figure A-4: FRET analysis of purified RPA mutants.

Indicated proteins were labeled with both FlAsH and ReAsH and monitored for FRET by excitation at 490 nm and emission monitored from 510 to 600 nm. Emission spectra were normalized where the highest signal was set to 1. (A) DBD F/PD (blue line) and DBD F/Asp (red line). (B) DBD B/PD (blue line) and DBD B/Asp (red line).

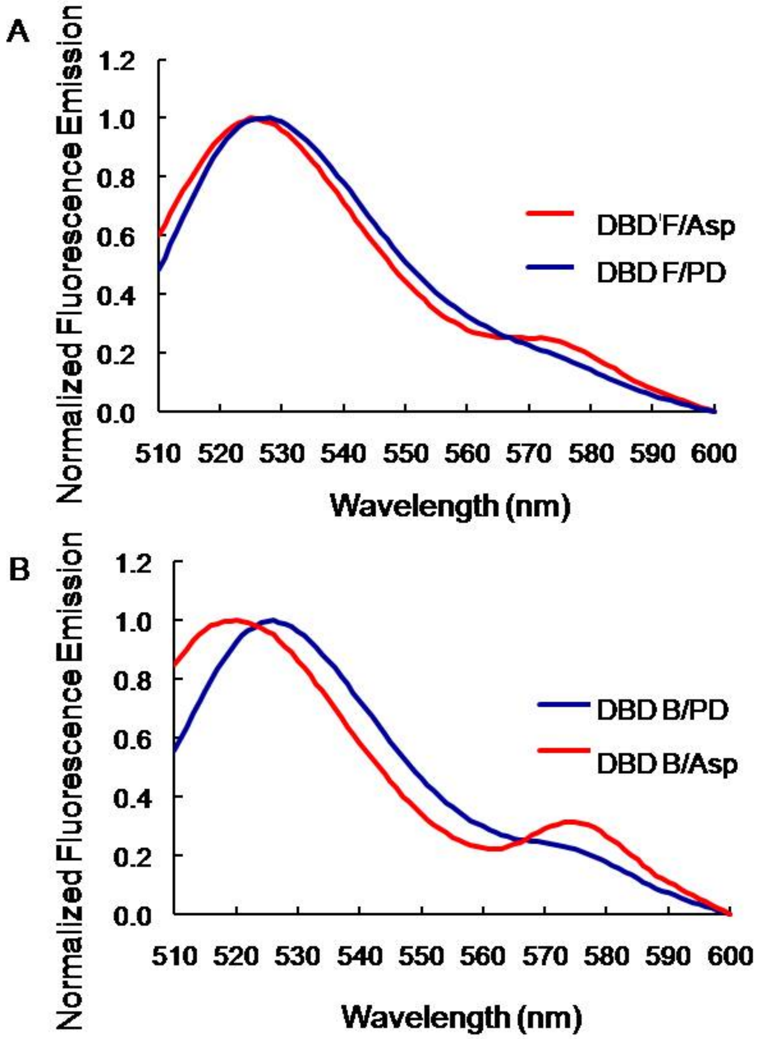
A
Normalized Fluorescence Emission
1.2
1.0
0.8
0.6
0.4
0.2
0.0
510 520 530 540 550 560 570 580 590 600
Wavelength (nm)
DBD F/Asp
DBD F/PD
B
Normalized Fluorescence Emission
1.2
1.0
0.8
0.6
0.4
0.2
0.0
510 520 530 540 550 560 570 580 590 600
Wavelength (nm)
DBD B/PD
DBD B/Asp

Figure A-5: Proteolysis of RPA does not decrease subunit interactions.

Indicated partially purified proteins were labeled with both FlAsH and ReAsH and monitored for FRET by excitation at 490 nm and emission monitored from 510 to 600 nm. RPA was proteolyzed to domain sized fragments by the addition of Subtilisin for 10 min. Emission spectra were normalized where the highest signal was set to 1. (A) DBD F/PD (black line) and DBD F/PD plus the addition of Subtilisin (orange line). (B) DBD F/Asp (black line) and DBD F/Asp plus the addition of Subtilisin (orange line). (C) DBD B/PD (black line) and DBD B/PD plus the addition of Subtilisin (orange line). (D) DBD B/Asp (black line) and DBD B/Asp plus the addition of Subtilisin (orange line).

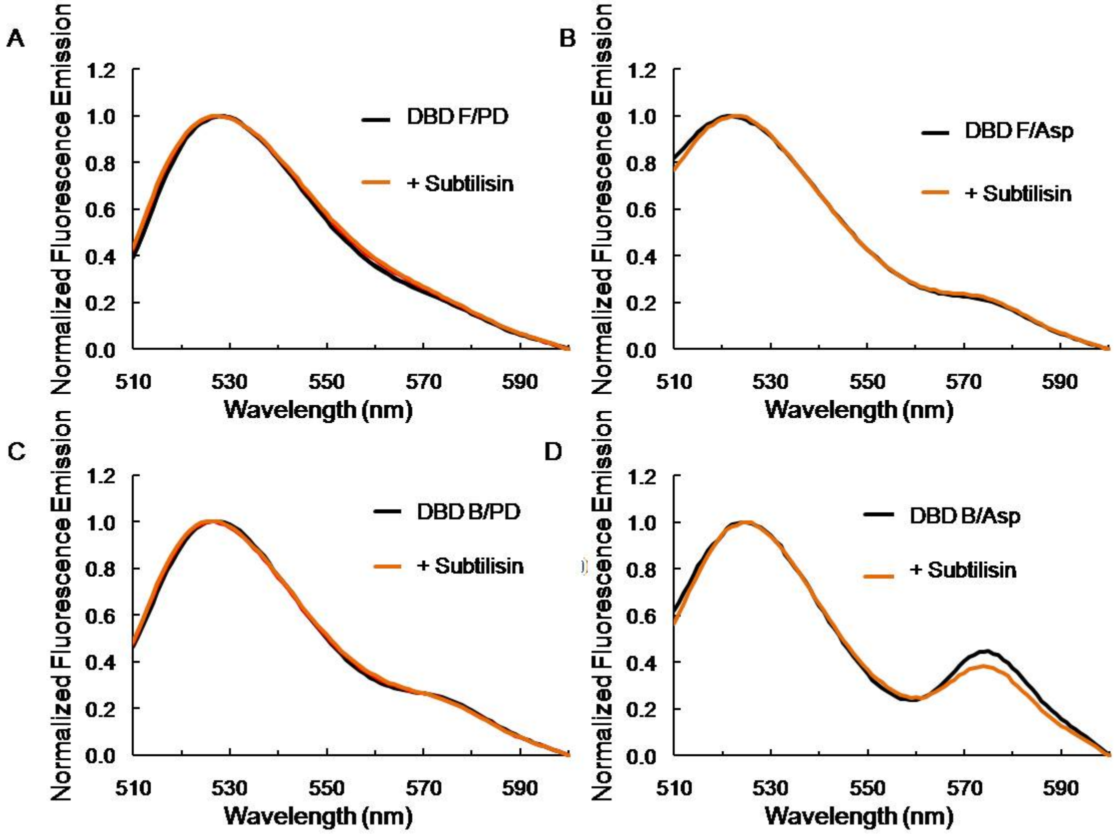
A
B
C
D
Normalized Fluorescence Emission
Wavelength (nm)
1.2
1.0
0.8
0.6
0.4
0.2
0.0
510
530
550
570
590
DBD F/PD
+ Subtilisin
DBD F/Asp
+ Subtilisin
DBD B/PD
+ Subtilisin
DBD B/Asp
+ Subtilisin

Figure A-6: Inter-molecular interactions between the phosphorylation mimetic, phosphorylation domain and DBDs of RPA1.

Indicated partially purified proteins were labeled with FlAsH and ReAsH separately and monitored for FRET by excitation at 490 nm and emission monitored from 510 to 600 nm. Emission spectra were normalized where the highest signal was set to 1. (A) DBD F/PD FlAsH labeled (black line) and plus the addition of DBD F/PD ReAsH labeled (red line). (B) DBD F/Asp FlAsH labeled (black line) and plus the addition of DBD F/Asp ReAsH labeled (red line). (C) DBD B/PD FlAsH (black line) and plus the addition of DBD B/PD ReAsH labeled (red line). (D) DBD B/Asp FlAsH labeled (black line) and plus the addition of DBD B/Asp ReAsH labeled (red line).

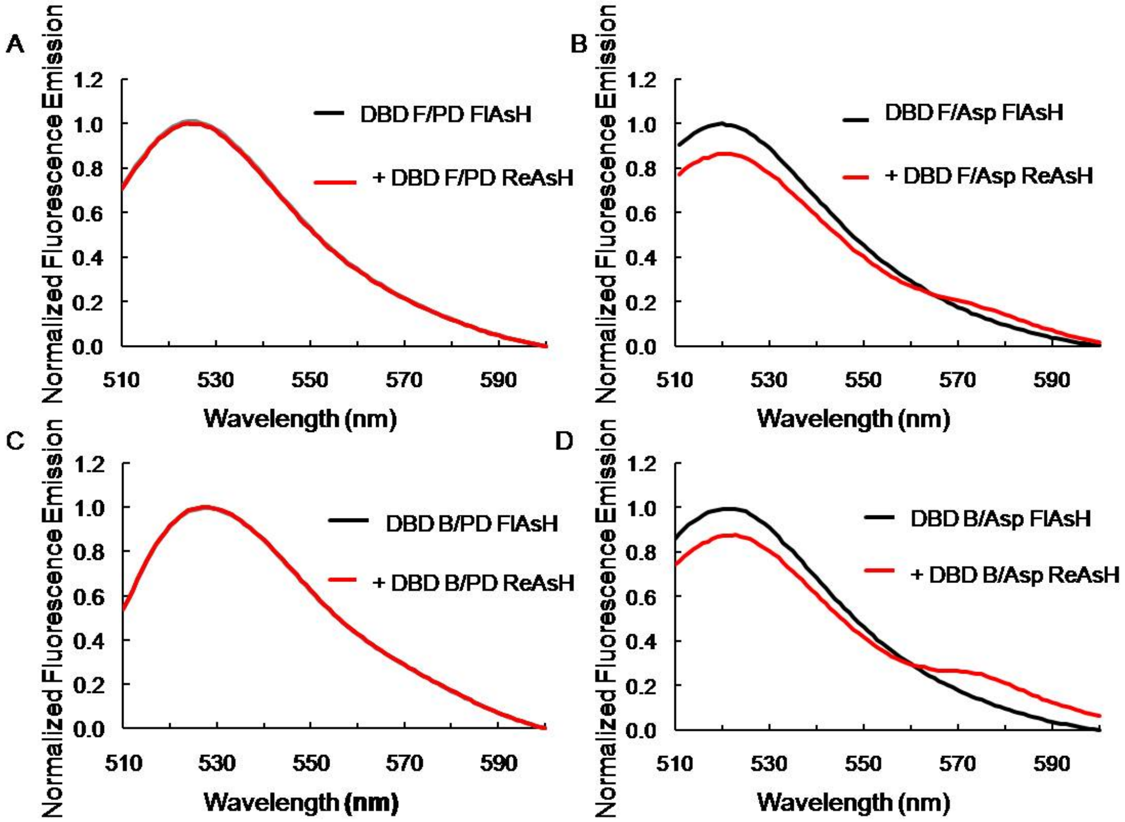
A
Normalized Fluorescence Emission
1.2
1.0
0.8
0.6
0.4
0.2
0.0
510
530
550
570
590
Wavelength (nm)
DBD F/PD FlAsH
+ DBD F/PD ReAsH
B
Normalized Fluorescence Emission
Wavelength (nm)
DBD F/Asp FlAsH
+ DBD F/Asp ReAsH
C
Normalized Fluorescence Emission
Wavelength (nm)
DBD B/PD FlAsH
+ DBD B/PD ReAsH
D
Normalized Fluorescence Emission
Wavelength (nm)
DBD B/Asp FlAsH
+ DBD B/Asp ReAsH

Figure A-7: Purified RPA2/3 and RPA-FAB.

^{15}N-RPA2/3 and ^{15}N-RPA-FAB were separated on 8-14% SDS-PAGE gels and visualized by silver staining.

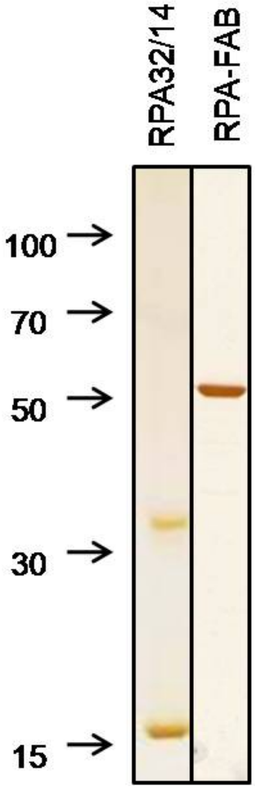
RPA32/14
RPA-FAB
100
70
50
30
15

Figure A-8: HSQC of ^{15}N labeled RPA2/3.

HSQC spectra of RPA2/3 with 313 resolvable cross peaks out of 425 expected cross peaks.

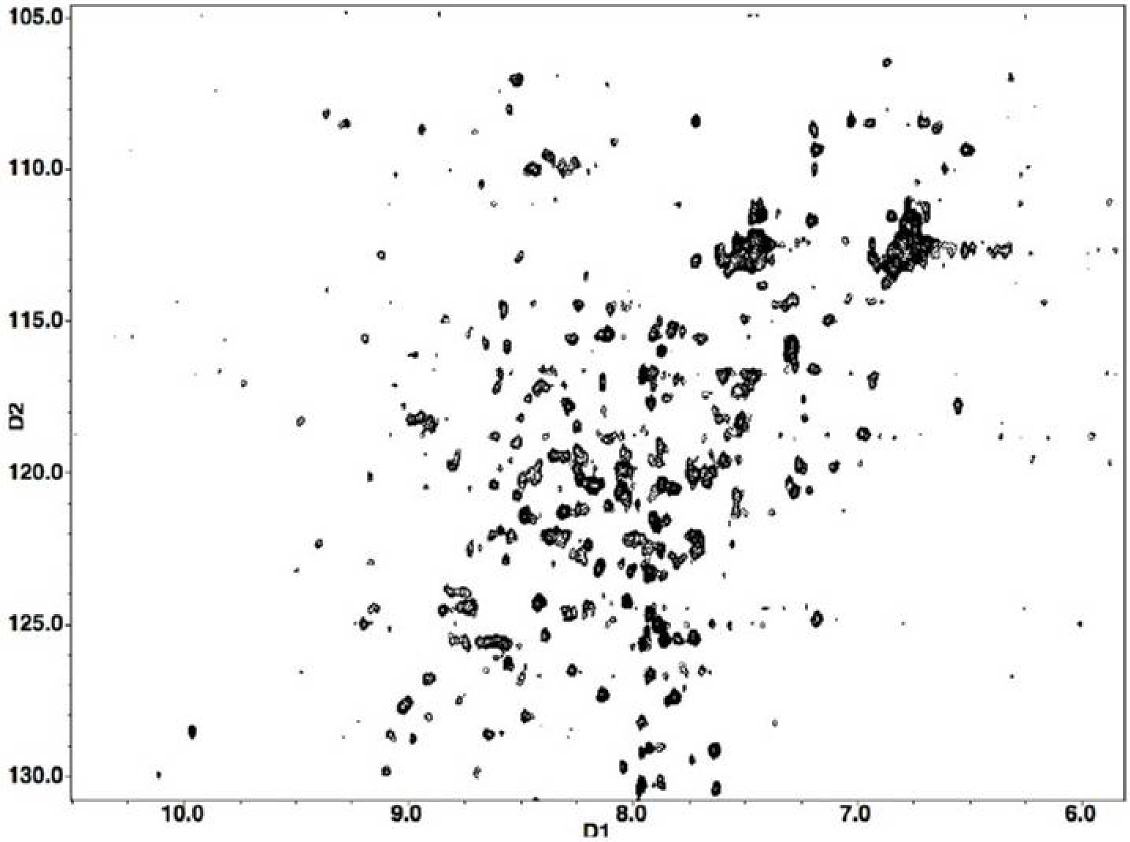
105.0
110.0
115.0
120.0
125.0
130.0
D2
10.0
9.0
8.0
7.0
6.0
D1

Figure A-9: HSQC of ^{15}N labeled RPA2/3Asp.

HSQC spectra of RPA2/3Asp with 283 resolvable cross peaks out of 425 expected cross peaks.

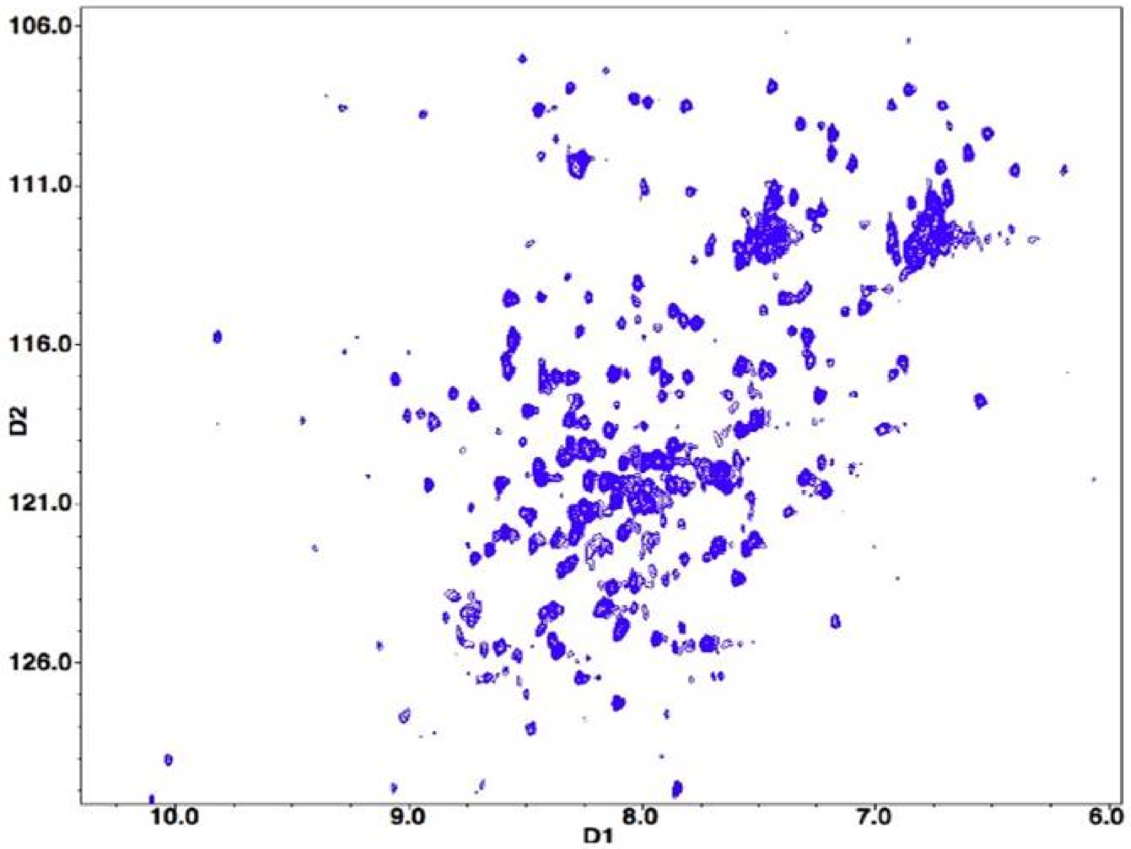
106.0
111.0
116.0
121.0
126.0
D2
10.0
9.0
8.0
7.0
6.0
D1

Figure A-10: Overlay of RPA2/3 and RPA2/3Asp HSPC spectra.

HSQC of RPA2/3 (black) and HSQC of RPA2/3Asp (blue).

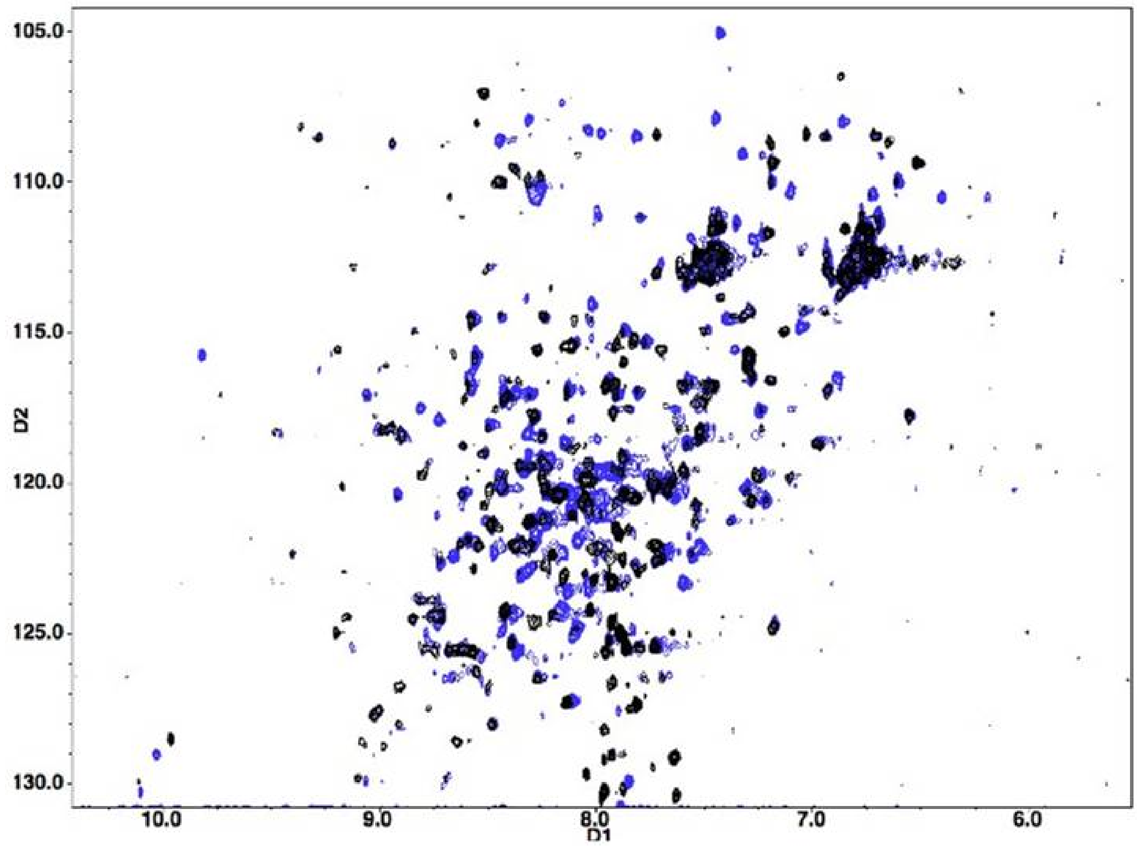
105.0
110.0
115.0
120.0
125.0
130.0
D2
10.0
9.0
8.0
7.0
6.0
D1

Figure A-11: DBD F causes peaks shifts in a distinct region of the RPA2/3Asp HSQC spectra.

(A) Overlay of RPA2/3 (black) and RPA2/3Asp (blue) HSQC spectra showing region ^{1}H: 8.5-7.7 ppm and ^{15}N: 108.2-111.3 ppm. (B) HSQC overlay of RPA2/3Asp (blue) and RPA2/3Asp plus unlabeled DBD F (red). (C) HSQC overlay of RPA2/3 (black) and RPA2/3 plus unlabeled DBD F (orange).

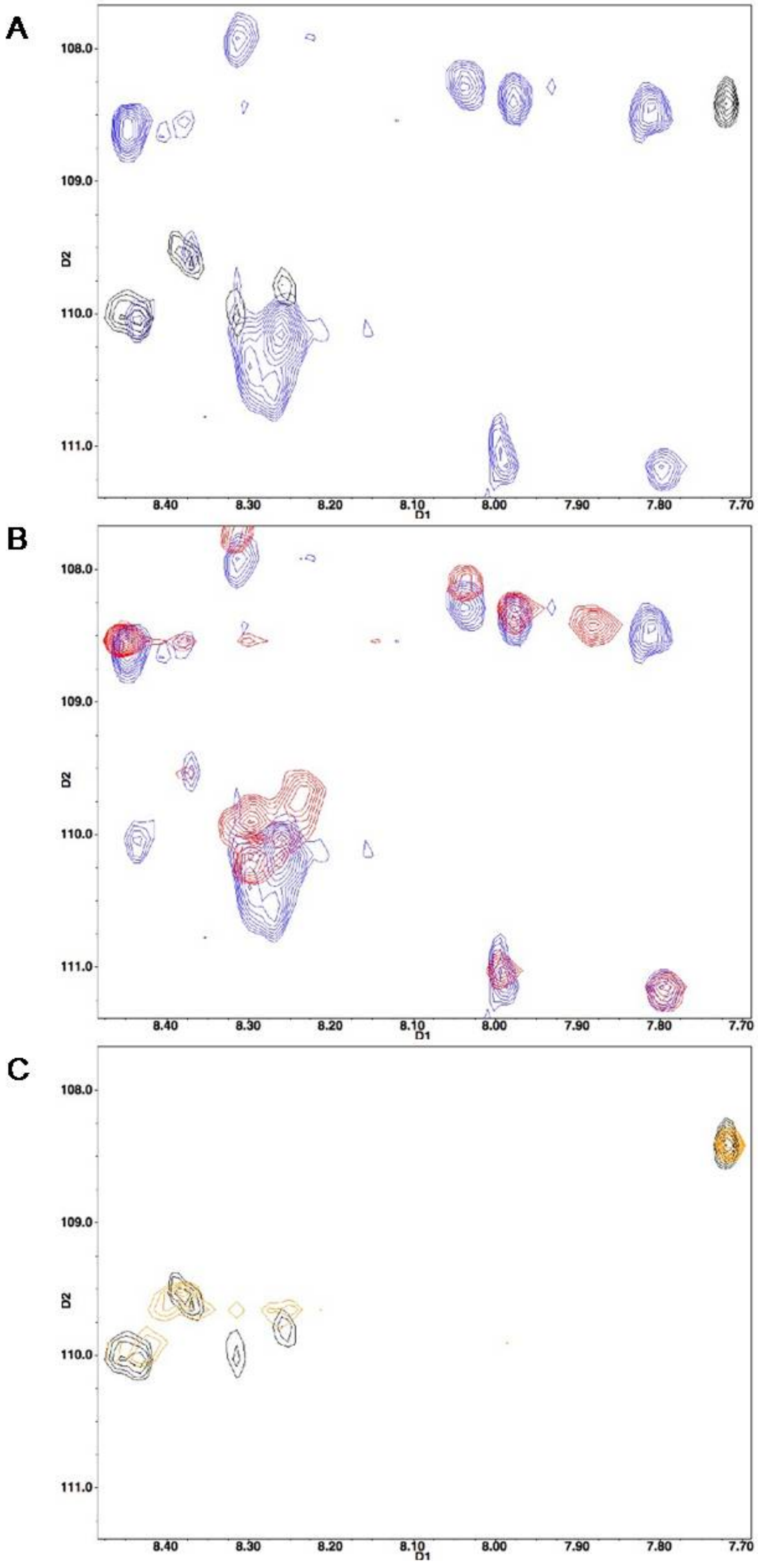
A
B
C
108.0
109.0
110.0
111.0
D2
8.40
8.30
8.20
8.10
8.00
7.90
7.80
7.70
D1

Figure A-12: TROSY spectrum of ^{15}N labeled RPA-FAB.

TROSY spectra of RPA-FAB with 434 resolvable cross peaks out of 520 expected cross peaks.

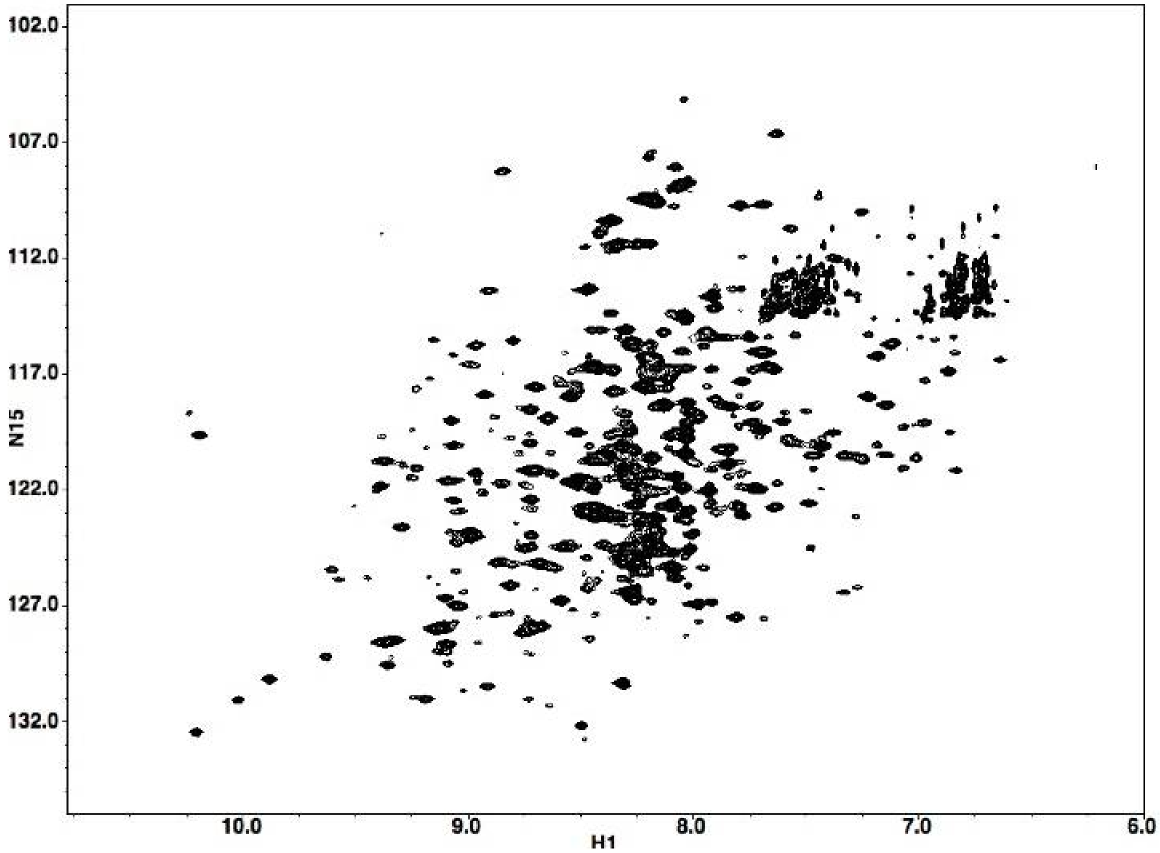
102.0
107.0
112.0
117.0
122.0
127.0
132.0
N15
10.0
9.0
8.0
7.0
6.0
H1

Figure A-13: Changes in TROSY spectra of RPA-FAB caused by phosphorylation mimetic peptide.

Selected region of TROSY spectra (^{1}H: 6.5-7.3 ppm, ^{15}N 107-113 ppm) of RPA-FAB (black) and RPA-FAB plus the addition of a hyper-phosphorylation mimetic peptide (pink) showing cross peak changes caused by the addition of the peptide.

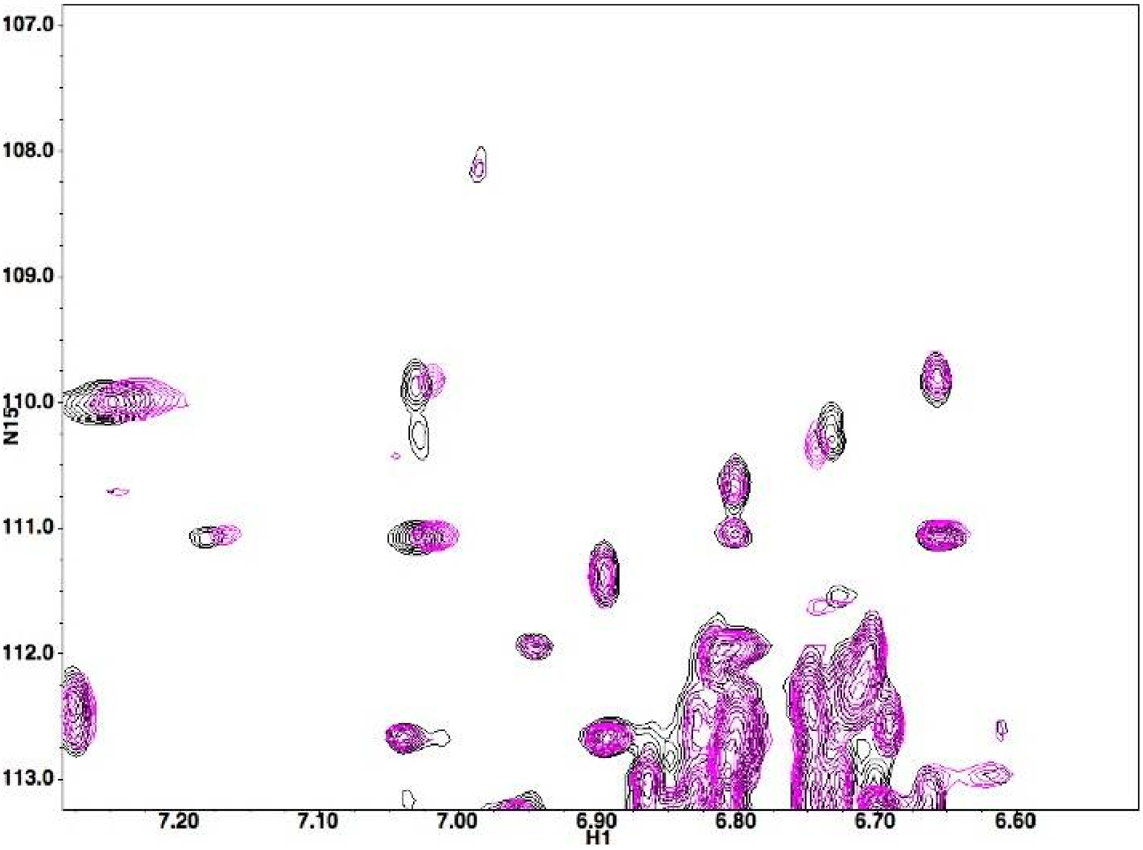
107.0
108.0
109.0
110.0
111.0
112.0
113.0
N15
7.20
7.10
7.00
6.90
6.80
6.70
6.60
H1

APPENDIX B

DEFINING THE DOMAINS OF RPA THAT INTERACT WITH DIFFERENT DNA STRUCTURES FOUND IN ESSENTIAL CELLULAR PROCESSES

Introduction

One of the main functions of RPA is to bind single-stranded DNA (ssDNA), which RPA does with high affinity and low specificity [119]. The literature favors a model of RPA binding to ssDNA that is defined by the length of the ssDNA and the number of DBDs contacting the DNA [35, 218, 219]. Single-stranded DNA is an intermediate in all DNA metabolic processes including replication, recombination, and DNA repair[17]. The size of the ssDNA region and the type of structure that surrounds the ssDNA vary. How RPA interacts with these various DNA intermediates remains to be determined.

The eight individual domains that comprise the RPA complex appear to form a flexible structure that interacts with DNA. Unfortunately, the overall structure of the trimeric complex remains unknown and little is known about how the individual DBDs interact with DNA. Furthermore, in the cell RPA does not interact with just one "type" of DNA but with multiple partially-duplex DNA structures. It is thus important to determine how RPA interacts with different DNA intermediates to understand the functionally important conformation(s) of RPA in the cell. These studies addressed the question by utilizing two general approaches. (A) Fluorescently labeled DNA was used to probe the specific interactions between RPA and partially-duplex DNA structures by examining changes in the fluorescence of the DNA. (B) Photochemical crosslinking was used to identify the specific domains of RPA that interacted with partially-duplex DNA structures.

Materials and Methods

DNA Substrates

Different DNA substrates were created by annealing shorter oligonucleotides to the following 70-mer DNAs with the indicated modified base: 70-mer 2-AP: 5’-GGAGGGACGTCAACTAGTAGTACCTTTCTCTTC(2-AP)CCTCCTTTGATGTTCTGACTCGAGGAGATCTGGAGC-3’ and 70-mer 4-thio-dT: 5’-GGAGGGACGTCAACTAGTAGTACCTTTCTTCTC(4-thio-dT)TCCTTTTTGATGTTCTGACTCGAGGAGATCTGGAGC-3’. A pseudo-replication fork was created by annealing 70-mer 4-thio-dT to 5’-TCTTGTAGTTTTCTCCACTTCTCTTTCCATCTACTAGTTGACGTCCCTCC-3’. A 5’ Overhang of 34 bases was created by annealing 70-mer 4-thio-dT or 70-mer 2-AP to 5’-GCTCCAGATCTCCTCGAGTCAGAACATCAAAAGAGG-3’. A 3’ Overhang of 37 bases was created by annealing 70-mer 4-thio-dT or 70-mer 2-AP to 5’-GAAGAGAAAGGTACTACTAGTTGACGTCCCTCC-3’. A 5’ Overhang of 50 bases was created by annealing 70-mer 4-thio-dT or 70-mer 2-AP to 5’-GCTCCAGATCTCCTCGAGTC-3’. A 3’ Overhang of 50 bases was created by annealing 70-mer 4-thio-dT or 70-mer 2-AP to 5’-CTACTAGTTGACGTCCCTCC-3’.

Protein

RPA-X_a was created using standard site directed mutagenesis procedures. tRPA-FSPN was used as the template for sequential rounds of mutagenesis. To create the Factor X_a recognition sequence at: *Sal I* 5’-CTGTGTTCCCCCAGAAGTCGAACGGCCCTCGATCGACAGGCTGGGACCTGCAGC-3’ and 5’-GCTGCAGGTCCCAGCCTGTCGATCGAGGGCCGTTCGACTTCTGGGGGAACACAG-3’, *Pml I* 5’-CGTGAAATCAAACTGAACCGTAGGCACACGGCCCTCGATGTGATGGTCGTCC

TCACAGGG-3’ and 5’-CCCTGTGAGGACGACCATCACATCGAGGGCCGTGTGCCTACGGTTCAGTTTGATTTCACG-3’, *Not I* 5’-GGTGTTACTCCCTCCGCGGCCACGGCCCTCGATGCCGCTCTTTAGATCAGAGATGG-3’ and 5’-CCATCTCTGATCTAAAGAGCGGCATCGAGGGCCGTGGCCGCGGAGGGAGTAACACC-3’. All mutations were verified by restriction endonuclease digestion and DNA sequencing. RPA-X_a was purified using the standard RPA purification procedure.

Fluorescence Assay

Fluorescence was monitored using a FluroLog 3 spectrofluorometer with excitation at 303 nm and emission from 345 to 420 nm with an integration time of 0.1 s. Samples contained 20 mM potassium phosphate (pH 7.5), KCl (100 mM), $MgCl_2$, RPA (25 or 150 nM) and DNA substrate (50 nM).

Photochemical Crosslinking Assay

Crosslinking reactions (20µl) contained 1X FBB, RPA-X_a (2.1µM) and DNA substrate (6µM). The DNA and RPA-X_a were incubated at 25°C for 15 minutes prior to crosslinking. The reactions were spotted on a piece of parafilm stretched over ice. The spotted solutions were then covered with a Pyrex Petri dish and illuminated with UV light using a Model UVGL-25 MINERALIGHT® LAMP (multi band UV-254/366nm 115 Volts) compact UV lamp (UVP, INC.). UV exposure times ranged from 4-8 hours.

Factor X_a Digestion

Factor X_a digestion was performed using 2µl of 1mg/ml solution of Factor X_a (Sigma) per 20µl crosslinking reaction. Reactions were incubated overnight at 4°C. Loading buffer containing SDS was used to quench the reaction when applicable.

Matrix Assisted Laser Desorption Ionization Time of Flight

C18 ZipTips (Millipore) were used to prepare the samples for mass spectrometry following the manufacture's protocol. Samples were spotted on a thin layer of cyano-4-hydroxycinnamic acid. The mode utilized for all MS experiments was BiFlex III. Data was collected in the linear positive direction. Data was analyzed using XMASS/XTOF software (Bruker).

Liquid Chromatography – Tandem Mass Spectroscopy

Following SDS-PAGE and coomassie blue staining, bands were excised from the gel and incubated in 25 mM NH_4HCO_3/50% acetonitrile overnight. Gel pieces were dehydrated in acetonitrile and air dried. Gel pieces were reduced with 10 mM dithiothreitol followed by incubation in 55 mM iodoacetamine at 65°C. Gel pieces were washed with 25 mM NH_4HCO_3 and dehydrated with acetonitrile. Protein was digested by the addition of 0.1 μg sequencing grade trypsin per 15 mm^3 of gel n 15 μL of 10 mM NH_4HCO_3. Samples were incubated overnight at 37°C. Gel pieces were extracted with 60% acetonitrile with 0.1% trifluoroacetic acid. Samples processed using standard LC/tandem mass spectroscopy procedures. Data was analyzed using XMASS/XTOF software (Bruker).

Results

To determine where on the DNA RPA interacts with various partially-duplexed DNA substates, a single 2-aminopurine (2-AP) was incorporated into DNA structures and changes in 2-AP fluorescence were monitored upon the addition of RPA. Initial studies showed that when RPA binds to DNA with 2-AP, the fluorescence from 2-AP increased. This was caused by the bases being twisted apart enough to disrupt base stacking with its neighbors. This disruption caused the fluorescence of 2-AP to increase upon RPA binding. Additional experiments showed RPA dependent differences in fluorescence depending on the DNA structures used (Figure B-1). There was a higher fluorescence change with ssDNA than with either a 5’ or 3’ overhang (Figure B-2). However, these changes could not be attributed to a specific position of RPA or region of RPA.

To determine what domains of RPA interact with partially-duplex DNA, photochemical crosslinking was used to crosslink RPA to the DNA at a specific base. The domains of RPA1 were separated by inserting the Factor Xa recognition sequence between the N-terminal linker and DBD A, DBD A and DBD B, DBD B and DBD C creating RPA-Xa. This form of RPA has been expressed and highly purified. Figure B-3 shows that after Factor Xa digestion of RPA-Xa and polyacrylamide gel electrophoresis, RPA was separated into fragments that contain the N-terminus, C-terminus, and core DNA binding domains of RPA1, DBD D, and DBD E. DNA binding studies indicated that the addition of the Factor Xa recognition sequences does not affect the binding of RPA to ssDNA.

Photochemical crosslinking experiments showed that RPA1 can be crosslinked to a 70-mer with 4-thio-dT placed in the middle of the oligonucleotide (Figure B-4). Different DNA structures were generated by annealing oligonucleotides to the 70-mer with the 4-thio-dT (Figure B-1). Crosslinking experiments with these structures showed they can also be crosslinked to RPA (Figure B-5, lane 2-5). Interestingly, there were multiple crosslinked species, which should only happen if two DNAs bind one RPA molecule. Alternatively, the different species could be different domains crosslinked to the DNA and this affected how they ran on a SDS polyacrylamide gel.

To analyze which domains were crosslinked to the DNA, matrix-assisted laser desorption/ionization – time of flight mass spectrometry (MALDI-TOF MS) was used. In the spectrum of a non-crosslinked Factor X_a digested sample of RPA-X_a, seven signals were detected and were attributed to Factor X_a, DBD A, DBD B, DBD C, DBD F-Linker, RPA2, and RPA3 (Figure B-6). After photochemical crosslinking to the 14nt-Gap DNA substrate and Factor X_a digestion, the spectrum was considerably different. Most significantly, there was a loss of signal were DBD A and DBD F-linker should have been

(Figure B-7). This suggests that these two domains were crosslinked to the DNA but were too negatively charged for analysis by mass spectrometry.

Given that the crosslinked DBD cannot be analyzed by MALDI TOF MS, liquid chromatography – tandem mass spectrometry (LC/MS/MS) was used to identify the trypsin proteolyzed region of RPA that was absent, indicating the crosslinked region. The result of the LC/MS/MS was a map of peptide fragments covering RPA1. However, there was incomplete coverage of the sequence when RPA was not crosslinked. Therefore, analysis of missing peptides was ambiguous.

Discussion

The fluorescent probe (2-aminopurine) that was chosen to be incorporated into the different DNA structures has properties that make interpreting the results difficult. When RPA was titrated with a DNA structure containing the fluorophore a change in fluorescence was observed. However, an increase and decrease in fluorescence was observed depending on the DNA structure used. These changes have not been attributed to a specific region of RPA.

RPA was successfully crosslinked to ssDNA using a 4-thio-dT incorporated into the ssDNA. However, the amount of crosslinked species was <10% of the input. This limited the amount of heteroconjugate that could be analyzed. Analysis of the heteroconjugate by mass spectrometry showed that the heteroconjugate does not fly in the mass spectrometer. Therefore, a loss of a signal would indicate a crosslinked region, but due to the limited amount of crosslinked product, the results were ambiguous.

Figure B-1: DNA substrates.

Various partially-duplex DNA substrates were created by annealing oligonucleotides to a common 70-mer that had either a centrally located 2-AP of 4-thio-dT. The red X indicates the position of either 2-AP of 4-thio-dT.

3′ Overhang

5′ GGAGGGACGTCAACTAGTAGTACCTTTCTTCTCXTCCTTTTTGATGTTCTGACTCGAGGAGATCTGGAGC 3′
CCTCCCTGCAGTTGATCATC

5′ Overhang

5′ GGAGGGACGTCAACTAGTAGTACCTTTCTTCTCXTCCTTTTTGATGTTCTGACTCGAGGAGATCTGGAGC 3′
CTGAGCTCCTCTAGACCTCG

Single Stranded Gap

5′ GGAGGGACGTCAACTAGTAGTACCTTTCTTCTCXTCCTTTTTGATGTTCTGACTCGAGGAGATCTGGAGC 3′
CCTCCCTGCAGTTGATCATC CTGAGCTCCTCTAGACCTCG

Replication Fork

5′ GGAGGGACGTCAACTAGTAGTACCTTTCTTCTCXTCCTTTTTGATGTTCTGACTCGAGGAGATCTGGAGC 3′
CCTCCCTGCAGTTGATCATCTACCTTTCTTCTCTTCCTTTTTGATGTTCT

X: 4-thio-dT or 2-AP

Figure B-2: RPA dependent changes in 2-AP fluorescence.

2-AP fluorescence from partially-duplex DNA substrates was monitored in the absence and presence of RPA. For the DNA substrates shown (from left to right), the 2-AP is positioned from the primer ends: no primer, 13 nucleotides 5’, 16 nucleotides 3’, 0 nucleotides 5’, 0 nucleotides 3’, 13 nucleotides 5’ and 13 nucleotides 5’/16 nucleotides 3’. Maximum fluorescence emission of the 2-AP DNA substrate in the absence of RPA was used to normalize the data.

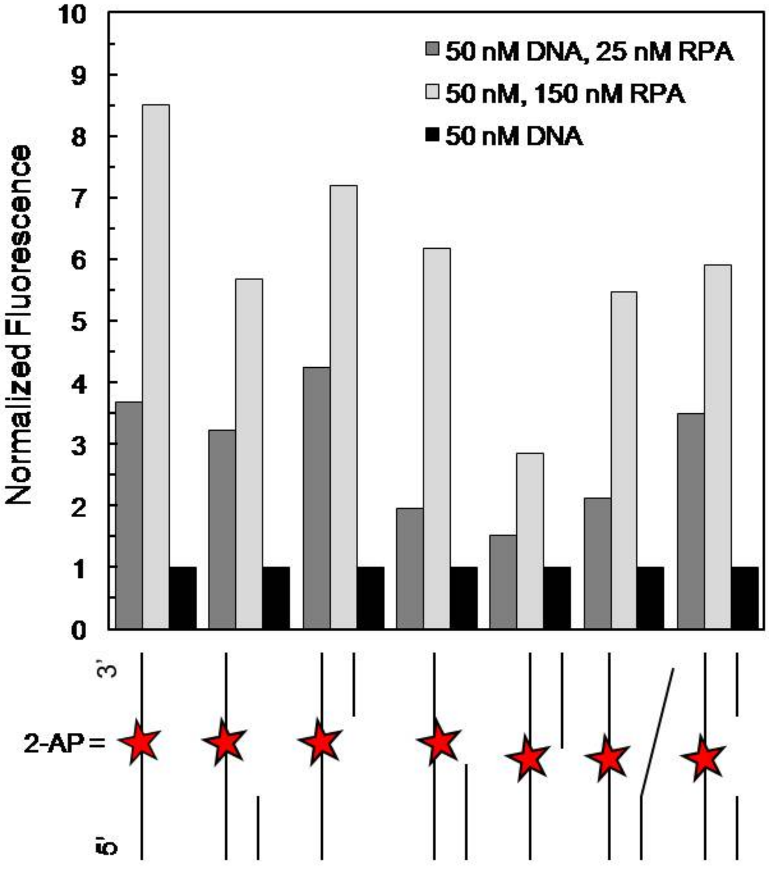

10
9
8
7
6
5
4
3
2
1
0
Normalized Fluorescence
50 nM DNA, 25 nM RPA
50 nM, 150 nM RPA
50 nM DNA
3'
2-AP =
5'

Figure B-3: Factor X_a digestion of RPA-X_a.

Silver stained SDS-PAGE gel of RPA-X_a before and after digestion with Factor X_a. 70, 32, and 14 kDa subunits are indicated along with proposed domain fragments after digestion.

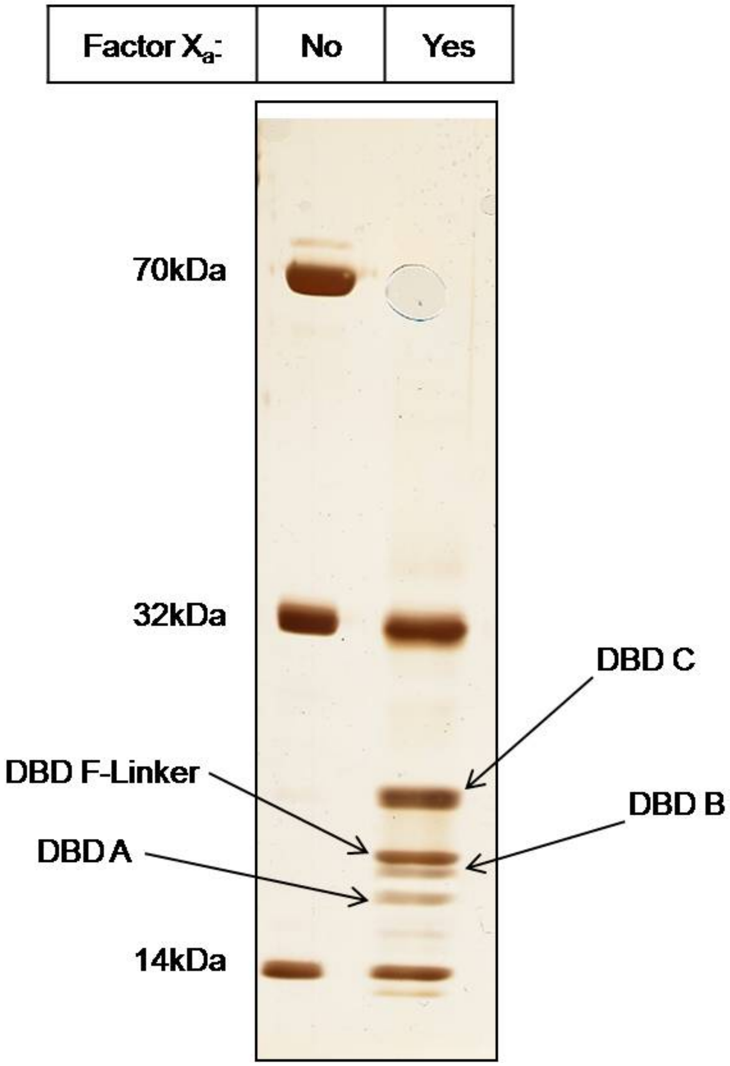
Factor Xa:
No
Yes
70kDa
32kDa
DBD C
DBD F-Linker
DBD B
DBD A
14kDa

Figure B-4: Photochemical crosslinking of RPA to ssDNA.

Silver stained SDS-PAGE gel of photochemical crosslinking reactions. 70, 32 and 14 kDa subunits are indicated along with RPA-DNA crosslink species

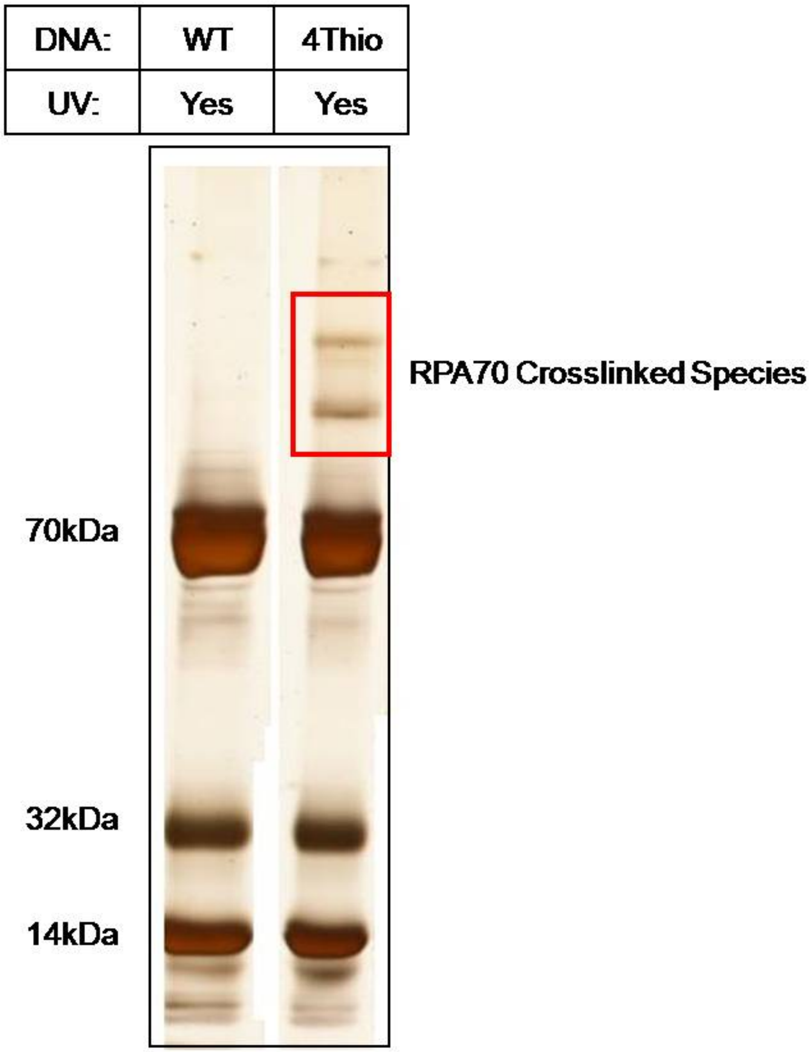
DNA:
WT
4Thio
UV:
Yes
Yes
RPA70 Crosslinked Species
70kDa
32kDa
14kDa

Figure B-5: Photochemical crosslinking of RPA to partially duplex DNA substrates.

Coomassie blue stained SDS-PAGE gel of photochemical crosslinking reactions to partially duplex DNA substrates depicted in Figure B-1. RPA-DNA crosslinked species are highlighted by the red box.

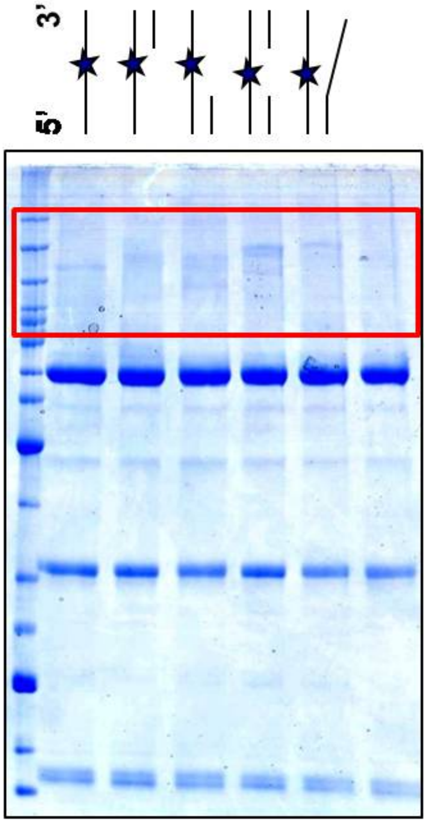
3'
5'

Figure B-6: MALDI-TOF MS analysis of RPA-X_a.

MALDI-TOF MS spectrum of RPA-X_a after digestion with Factor X_a. Seven distinct signals occur correlating to seven peptides. A mass to charge ratio of about 43 m/z corresponds to Factor X_a. At 30 m/z and 13.4 m/z are the signals corresponding to RPA2 and RPA3, respectively. A mass to charge ratio of 21.4, 18.7, 14.9 and 14.1 m/z are DBD C, DBD F-linker, DBD B and DBD A, respectively.

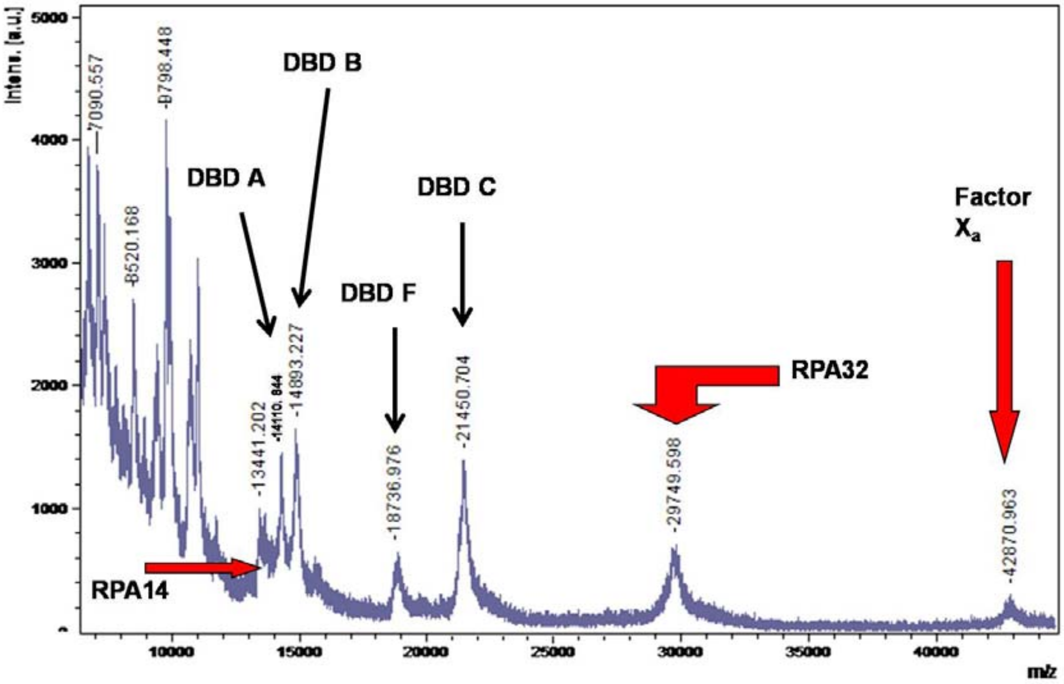
Intens. [a.u.]
5000
4000
3000
2000
1000
0
7090.557
8520.168
9798.448
DBD A
DBD B
13441.202
14110.844
14893.227
DBD F
18736.976
DBD C
21450.704
RPA32
29749.598
Factor X_a
42870.963
RPA14
10000
15000
20000
25000
30000
35000
40000
m/z

Figure B-7: MALDI-TOF MS analysis of RPA-X_a crosslinked to DNA.

MALDI-TOF MS spectrum of RPA-X_a crosslinked for eight hours followed by Factor X_a digestion. The signals for DBD C, DBD B, RPA 3, and RPA2 are indicated. There are no identifiable signals for Factor X_a, DBD A or DBD F-linker.

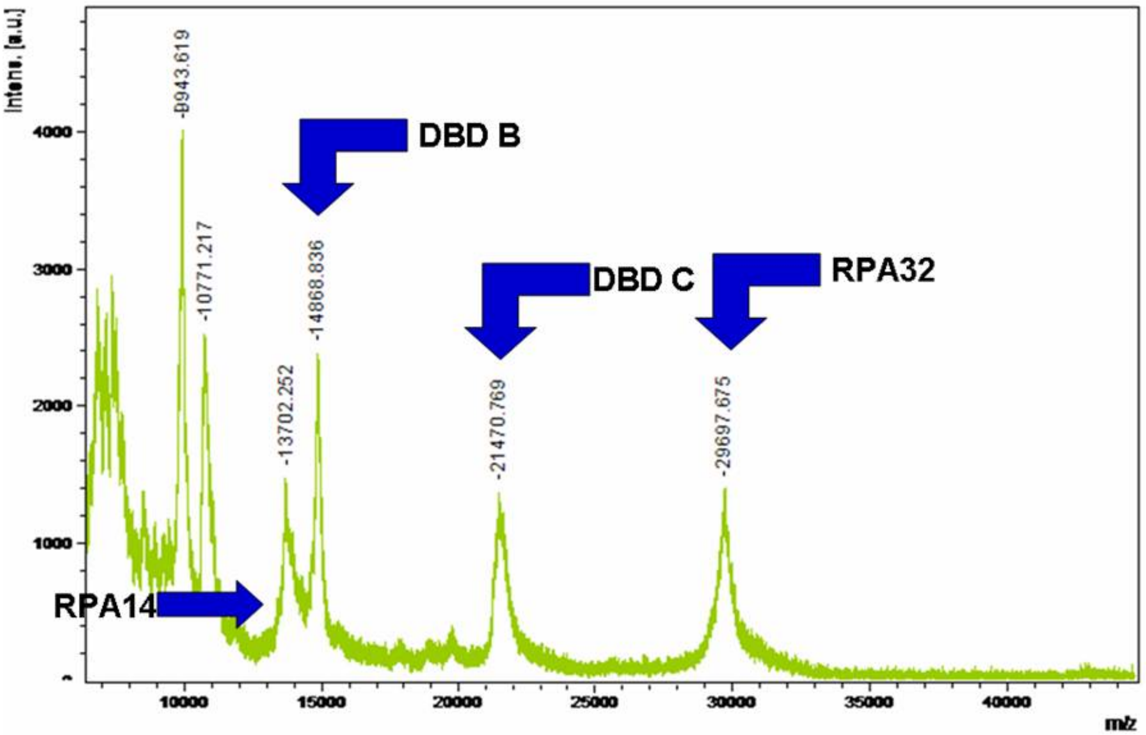
Intens. [a.u.]
4000
3000
2000
1000
0
-9943.619
-10771.217
-13702.252
-14868.836
-21470.769
-29697.675
DBD B
DBD C
RPA32
RPA14
10000
15000
20000
25000
30000
35000
40000
m/z

REFERENCES

1. Wold, M.S., *Replication Protein A: A heterotrimeric, single-stranded DNA-binding protein required for eukaryotic DNA metabolism.* Annu Rev Biochem 1997. **66**: p. 61-92.

2. Wold, M.S., et al., *Identification of cellular proteins required for simian virus 40 DNA replication.* J Biol Chem 1989. **264**: p. 2801-2809.

3. Kenny, M.K., S.-H. Lee, and J. Hurwitz, *Multiple functions of human single-stranded-DNA binding protein in simian virus 40 DNA replication: Single-strand stabilization and stimulation of DNA polymerases a and d.* Proc.Natl.Acad.Sci.USA, 1989. **86**: p. 9757-9761.

4. Seroussi, E. and S. Lavi, *Replication protein A is the major single-stranded DNA binding protein detected in mammalian cell extracts by gel retardation assays and UV cross-linking of long and short single-stranded DNA molecules.* J.Biol.Chem., 1993. **268**: p. 7147-7154.

5. Wang, Y., et al., *Mutation in Rpa1 results in defective DNA double-strand break repair, chromosomal instability and cancer in mice.* Nat Genet, 2005. **37**(7): p. 750-5.

6. Givalos, N., et al., *Replication protein A is an independent prognostic indicator with potential therapeutic implications in colon cancer.* Mod Pathol, 2007. **20**(2): p. 159-66.

7. Tomkiel, J.E., et al., *Autoimmunity to the M(r) 32,000 subunit of replication protein A in breast cancer.* Clin Cancer Res, 2002. **8**(3): p. 752-8.

8. Wold, M.S. and T. Kelly, *Purification and characterization of replication protein A, a cellular protein required for in vitro replication of simian virus 40 DNA.* Proc Natl Acad Sci USA, 1988. **85**: p. 2523-2527.

9. Wobbe, C.R., et al., *Replication of simian virus 40 origin-containing DNA in vitro with purified proteins.* Proc Natl Acad Sci U S A, 1987. **84**: p. 1834-1838.

10. Fairman, M.P. and B. Stillman, *Cellular factors required for multiple stages of SV40 DNA replication in vitro.* EMBO J., 1988. **7**: p. 1211-1218.

11. Coverley, D., et al., *Requirement for the replication protein SSB in human DNA excision repair.* Nature, 1991. **349**: p. 538-541.

12. Coverley, D., et al., *A role for the human single-stranded DNA binding protein HSSB/RPA in an early stage of nucleotide excision repair.* Nucleic Acids Res, 1992. **20**(15): p. 3873-80.

13. Heyer, W.-D., et al., *An essential Saccharomyces cerevisiae single-stranded DNA binding protein is homologous to the large subunit of human RP-A.* EMBO J., 1990. **9**: p. 2321-2329.

14. Moore, S.P., et al., *The human homologous pairing protein HPP-1 is specifically stimulated by the cognate single-stranded binding protein hRP-A.* Proc.Natl.Acad.Sci.USA, 1991. **88**: p. 9067-9071.

15. Dutta, A. and B. Stillman, *cdc2 family kinases phosphorylate a human cell DNA replication factor, RPA, and activate DNA replication.* Embo J, 1992. **11**(6): p. 2189-99.

16. Dutta, A., et al., *Inhibition of DNA replcation factor RPA by p53.* Nature, 1993. **365**: p. 79-82.

17. Zou, Y., et al., *Functions of human replication protein A (RPA): From DNA replication to DNA damage and stress responses.* J Cell Physiol, 2006. **208**(2): p. 267-73.

18. Fanning, E., V. Klimovich, and A.R. Nager, *A dynamic model for replication protein A (RPA) function in DNA processing pathways.* Nucleic Acids Res, 2006. **34**(15): p. 4126-37.

19. Iftode, C., Y. Daniely, and J.A. Borowiec, *Replication Protein A (RPA): The eukaryotic SSB.* CRC Critical Reviews in Biochemistry, 1999. **34**: p. 141-180.

20. Revzin, A.E., *The Biology of Nonspecific DNA-Protein Interactions*. 1 ed. 1990, Boca Raton: CRC Press.

21. Lohman, T.M. and M.E. Ferrari, *Escherichia coli single-stranded DNA-binding protein: Multiple DNA-binding modes and cooperativities.* Annu.Rev.Biochem., 1994. **63**: p. 527-570.

22. Murzin, A.G., *OB(oligonucleotide/oligosaccharide binding)-fold: common structural and functional solution for non-homologous sequences.* Embo J, 1993. **12**(3): p. 861-7.

23. Philipova, D., et al., *A hierachachy of SSB protomers in Replication Protein-A.* Genes Dev., 1996. **10**: p. 2222-2233.

24. Jacobs, D.M., et al., *Human replication protein A: Global fold of the N-terminal RPA-70 domain reveals a basic cleft and flexible C-terminal linker.* J Biomol NMR, 1999. **14**: p. 321-331.

25. Bochkarev, A., et al., *Structure of the single-stranded-DNA-binding domain of replication protein A bound to DNA.* Nature, 1997. **385**: p. 176-181.

26. Bochkarev, A., et al., *The crystal structure of the complex of replication protein A subunits RPA32 and RPA14 reveals a mechanism for single-stranded DNA binding.* EMBO J, 1999. **18**: p. 4498-4504.

27. Walther, A.P., et al., *Replication Protein A interactions with DNA: I. Analysis of the high affinity DNA-binding domain of the 70-kDa subunit.* Biochemistry, 1999. **38**: p. 3963-3973.

28. Lao, Y., et al., *Replication protein A interactions with DNA. III. Molecular basis of recognition of damaged DNA.* Biochemistry, 2000. **39**: p. 850-859.

29. Lao, Y., C.G. Lee, and M.S. Wold, *Replication protein A interactions with DNA. 2. Characterization of double-stranded DNA-binding/helix-destabilization activities and the role of the zinc-finger domain in DNA interactions.* Biochemistry, 1999. **38**: p. 3974-3984.

30. Bochkareva, E., S. Korolev, and A. Bochkarev, *The role for zinc in replication protein A.* J Biol Chem 2000. **275**: p. 27332-27338.

31. Sibenaller, Z.A., B.R. Sorensen, and M.S. Wold, *The 32- and 14-kDa subunits of Replication Protein A are responsible for species-specific interactions with ssDNA.* Biochemistry, 1998. **37**: p. 12496-12506.

32. Bochkareva, E., et al., *The RPA32 subunit of human replication protein A contains a single-stranded DNA-binding domain.* J Biol Chem 1998. **273**: p. 3932-3936.

33. Binz, S.K., A.M. Sheehan, and M.S. Wold, *Replication protein A phosphorylation and the cellular response to DNA damage.* DNA Repair (Amst), 2004. **3**(8-9): p. 1015-24.

34. Bochkareva, E., et al., *Single-stranded DNA mimicry in the p53 transactivation domain interaction with replication protein A.* Proc Natl Acad Sci U S A, 2005. **102**(43): p. 15412-7.

35. Bochkareva, E., et al., *Structure of the RPA trimerization core and its role in the multistep DNA-binding mechanism of RPA.* EMBO J, 2002. **21**(7): p. 1855-63.

36. Gao H, C.R., Mandell EK, Otero JH, Lundblad V., *RPA-like proteins mediate yeast telomere function.* Nat Struct Mol Biol, 2007. **14**(3): p. 208-214.

37. Habel, J.E., J.F. Ohren, and G.E.O. Borgstahl, *Dynamic light-scattering analysis of full-length human RPA14/32 dimer: purification, crystallization and self-association.* Acta Crystallographica.Section.D-Biological.Crystallography.57(Part.2):254-259,.2001.Feb., 2001: p. 254-259.

38. Deng, X., et al., *Structure of the full-length human RPA14/32 complex gives insights into the mechanism of DNA binding and complex formation.* J Mol Biol, 2007. **374**(4): p. 865-76.

39. Kim, C., R.O. Snyder, and M.S. Wold, *Binding properties of replication protein A from human and yeast cells.* Mol Cell Biol 1992. **12**: p. 3050-3059.

40. Carmichael, E.P., J.M. Roome, and A.F. Wahl, *Binding of a sequence-specific single-stranded DNA-binding factor to the simian virus 40 core origin inverted repeat domain is cell cycle regulated.* Mol.Cell.Biol., 1993. **13**: p. 408-420.

41. Iftode, C. and J.A. Borowiec, *5' --> 3' molecular polarity of human replication protein A (hRPA) binding to pseudo-origin DNA substrates.* Biochemistry, 2000. **39**: p. 11970-11981.

42. De Laat, W.L., et al., *DNA-binding polarity of human replication protein A positions nucleases in nucleotide excision repair.* Genes Dev., 1998. **12**: p. 2598-2609.

43. Wyka, I.M., et al., *Replication Protein A Interactions with DNA: Differential Binding of the Core Domains and Analysis of the DNA Interaction Surface.* Biochemistry, 2003. **42**: p. 12909-12918.

44. Pfuetzner, R.A., et al., *Replication protein A - Characterization and crystallization of the DNA binding domain.* J Biol Chem, 1997. **272**: p. 430-434.

45. Fanning, E. and K. Zhao, *SV40 DNA replication: from the A gene to a nanomachine.* Virology, 2009. **384**(2): p. 352-9.

46. Taneja, P., et al., *Timed interactions between viral and cellular replication factors during the initiation of SV40 in vitro DNA replication.* Biochem J, 2007. **407**(2): p. 313-20.

47. Wold, M.S., J.J. Li, and T.J. Kelly, *Initiation of simian virus 40 DNA replication in vitro: large-tumor-antigen- and origin-dependent unwinding of the template.* Proc Natl Acad Sci USA, 1987. **84**: p. 3643-3647.

48. Weisshart, K., P. Taneja, and E. Fanning, *The replication protein A binding site in simian virus 40 (SV40) T antigen and its role in the initial steps of SV40 DNA replication.* J.Virol., 1998. **72**: p. 9771-9781.

49. Melendy, T. and B. Stillman, *An interaction between replication protein A and SV40 T antigen appears essential for primosome assembly during SV40 DNA replication.* J.Biol.Chem., 1993. **268**: p. 3389-3395.

50. Smith, R.W., et al., *Species specificity of simian virus 40 DNA replication in vitro requires multiple functions of human DNA polymerase alpha.* J Biol Chem, 2002. **277**(23): p. 20541-8.

51. Maga, G., et al., *Replication protein a as a "fidelity clamp" for DNA polymerase alpha.* J Biol Chem, 2001. **276**(21): p. 18235-18242.

52. Burgers, P.M., *Polymerase dynamics at the eukaryotic DNA replication fork.* J Biol Chem, 2009. **284**(7): p. 4041-5.

53. Yuzhakov, A., et al., *Multiple competition reactions for RPA order the assembly of the DNA polymerase delta holoenzyme.* EMBO J, 1999. **18**(21): p. 6189-99.

54. Walther, A.P., M.P. Bjerke, and M.S. Wold, *A novel assay for examining the molecular reactions at the eukaryotic replication fork: Activities of Replication Protein A required during elongation.* Nucleic Acids Res, 1999. **27**: p. 656-664.

55. Bell, S.P. and A. Dutta, *DNA replication in eukaryotic cells.* Annu Rev Biochem, 2002. **71**: p. 333-74.

56. Dimitrova, D.S., et al., *Mcm2, but not RPA, is a component of the mammalian early G1-phase prereplication complex.* J.Cell Biol., 1999. **146**: p. 709-722.

57. Zou, L. and B. Stillman, *Assembly of a complex containing Cdc45p, replication protein A, and Mcm2p at replication origins controlled by S-phase cyclin-dependent kinases and Cdc7p-Dbf4p kinase.* Mol.Cell.Biol., 2000. **20**: p. 3086-3096.

58. Lei, M. and B.K. Tye, *Initiating DNA synthesis: from recruiting to activating the MCM complex [Review].* Journal.of.Cell Science.114(8):1447-1454,.2001.Apr., 2001: p. 1447-1454.

59. Walter, J. and J. Newport, *Initiation of eukaryotic DNA replication: origin unwinding and sequential chromatin association of Cdc45, RPA, and DNA polymerase alpha.* Mol Cell, 2000. **5**(4): p. 617-27.

60. San Filippo, J., P. Sung, and H. Klein, *Mechanism of eukaryotic homologous recombination.* Annu Rev Biochem, 2008. **77**: p. 229-57.

61. West, S.C., *Molecular views of recombination proteins and their control.* Nat Rev Mol Cell Biol, 2003. **4**(6): p. 435-45.

62. Valerie, K. and L.F. Povirk, *Regulation and mechanisms of mammalian double-strand break repair.* Oncogene, 2003. **22**(37): p. 5792-812.

63. Golub, E.I., et al., *Interaction of human Rad51 recombination protein with single-stranded DNA binding protein, RPA.* Nucleic Acids Res, 1998. **26**: p. 5388-5393.

64. Park, M.S., et al., *Physical interaction between human RAD52 and RPA is required for homologous recombination in mammalian cells.* J Biol Chem 1996. **271**: p. 18996-19000.

65. Jackson, D., et al., *Analysis of the human replication protein A:Rad52 complex: evidence for crosstalk between RPA32, RPA70, Rad52 and DNA.* J Mol Biol, 2002. **321**(1): p. 133-48.

66. Sung, P. and H. Klein, *Mechanism of homologous recombination: mediators and helicases take on regulatory functions.* Nat Rev Mol Cell Biol, 2006. **7**(10): p. 739-50.

67. Hickson, I.D., et al., *Role of the Bloom's syndrome helicase in maintenance of genome stability.* Biochem Soc Trans, 2001. **29**(Pt 2): p. 201-4.

68. Ahn, B., et al., *Mechanism of Werner DNA helicase: POT1 and RPA stimulates WRN to unwind beyond gaps in the translocating strand.* PLoS ONE, 2009. **4**(3): p. e4673.

69. Doherty, K.M., et al., *Physical and functional mapping of the replication protein a interaction domain of the werner and bloom syndrome helicases.* J Biol Chem, 2005. **280**(33): p. 29494-505.

70. Sancar, A., *DNA excision repair.* Annu.Rev.Biochem., 1996. **65**: p. 43-81.

71. Wood, R.D., *Nucleotide excision repair in mammalian cells.* J.Biol.Chem., 1997. **272**: p. 23465-23468.

72. Reardon, J.T. and A. Sancar, *Nucleotide excision repair.* Prog Nucleic Acid Res Mol Biol, 2005. **79**: p. 183-235.

73. Mu, D., et al., *Reconstitution of human DNA repair excision nuclease in a highly defined system.* J.Biol.Chem., 1995. **270**: p. 2415-2418.

74. Mu, D., D.S. Hsu, and A. Sancar, *Reaction mechanism of human DNA repair excision nuclease.* J.Biol.Chem., 1996. **271**: p. 8285-8294.

75. Evans, E., et al., *Mechanism of open complex and dual incision formation by human nucleotide excision repair factors.* EMBO J., 1997. **16**: p. 6559-6573.

76. Reardon, J.T. and A. Sancar, *Recognition and repair of the cyclobutane thymine dimer, a major cause of skin cancers, by the human excision nuclease.* Genes Dev, 2003. **17**(20): p. 2539-51.

77. Wang, M., A. Mahrenholz, and S.H. Lee, *RPA stabilizes the XPA-damaged DNA complex through protein-protein interaction.* Biochemistry, 2000. **39**: p. 6433-6439.

78. He, Z., et al., *RPA involvement in the damage-recognition and incision steps of nucleotide excision repair.* Nature, 1995. **374**: p. 566-569.

79. Matsuda, T., et al., *DNA repair protein XPA binds replication protein A (RPA).* J.Biol.Chem., 1995. **270**: p. 4152-4157.

80. Li, L., et al., *An interaction between the DNA repair factor XPA and replication protein a appears essential for nucleotide excision repair.* Mol.Cell.Biol., 1995. **15**: p. 5396-5402.

81. Stigger, E., R. Drissi, and S.H. Lee, *Functional analysis of human replication protein a in nucleotide excision repair.* J.Biol.Chem., 1998. **273**: p. 9337-9343.

82. Miyamoto, I., et al., *Mutational analysis of the structure and function of the xeroderma pigmentosum group A complementing protein. Identification of essential domains for nuclear localization and DNA excision repair.* J Biol Chem, 1992. **267**(17): p. 12182-7.

83. Wakasugi, M. and A. Sancar, *Order of assembly of human DNA repair excision nuclease.* J.Biol.Chem., 1999. **274**: p. 18759-18768.

84. Wakasugi, M. and A. Sancar, *Assembly, subunit composition, and footprint of human DNA repair excision nuclease.* Proc.Natl.Acad.Sci.USA, 1998. **95**: p. 6669-6674.

85. Patrick, S.M. and J.J. Turchi, *Replication protein A (RPA) binding to duplex cisplatin-damaged DNA is mediated through the generation of single-stranded DNA.* J.Biol.Chem., 1999. **274**: p. 14972-14978.

86. Matsunaga, T., et al., *Replication protein A confers structure-specific endonuclease activities to the XPF-ERCC1 and XPG subunits of human DNA repair excision nucleases.* J.Biol.Chem., 1996. **271**: p. 11047-11050.

87. Bessho, T., et al., *Reconstitution of human excision nuclease with recombinant XPF-ERCC1 complex.* J.Biol.Chem., 1997. **272**: p. 3833-3837.

88. Shivji, M.K.K., et al., *Nucleotide excision repair DNA synthesis by DNA polymerase Œ in the presence of PCNA, RFC, and RPA.* Biochemistry, 1995. **34**: p. 5011-5017.

89. Dalhus, B., et al., *DNA base repair--recognition and initiation of catalysis.* FEMS Microbiol Rev, 2009. **33**(6): p. 1044-78.

90. Baute, J. and A. Depicker, *Base excision repair and its role in maintaining genome stability.* Crit Rev Biochem Mol Biol, 2008. **43**(4): p. 239-76.

91. Nagelhus, T.A., et al., *A sequence in the N-terminal region of human uracil-DNA glycosylase with homology to XPA interacts with the c-terminal part of the 34-kDa subunit of replication protein A.* J.Biol.Chem., 1997. **272**: p. 6561-6566.

92. DeMott, M.S., S. Zigman, and R.A. Bambara, *Replication protein A stimulates long patch DNA base excision repair.* J.Biol.Chem., 1998. **273**: p. 27492-27498.

93. Li, G.M., *Mechanisms and functions of DNA mismatch repair.* Cell Res, 2008. **18**(1): p. 85-98.

94. Ramilo, C., et al., *Partial reconstitution of human DNA mismatch repair in vitro: characterization of the role of human replication protein A.* Mol Cell Biol, 2002. **22**(7): p. 2037-46.

95. Guo, S., et al., *Regulation of replication protein A functions in DNA mismatch repair by phosphorylation.* J Biol Chem, 2006. **281**(31): p. 21607-16.

96. Cimprich, K.A. and D. Cortez, *ATR: an essential regulator of genome integrity.* Nat Rev Mol Cell Biol, 2008. **9**(8): p. 616-27.

97. Nyberg, K.A., et al., *Toward maintaining the genome: DNA damage and replication checkpoints.* Annu Rev Genet, 2002. **36**: p. 617-56.

98. Jazayeri, A., et al., *ATM- and cell cycle-dependent regulation of ATR in response to DNA double-strand breaks.* Nat Cell Biol, 2006. **8**(1): p. 37-45.

99. Mahaney, P.E., et al., *Structure-activity relationships of the 1-amino-3-(1H-indol-1-yl)-3-phenylpropan-2-ol series of monoamine reuptake inhibitors.* Bioorg Med Chem Lett, 2009. **19**(19): p. 5807-10.

100. Zou, L. and S.J. Elledge, *Sensing DNA damage through ATRIP recognition of RPA-ssDNA complexes.* Science, 2003. **300**(5625): p. 1542-8.

101. Xu, X., et al., *The basic cleft of RPA70N binds multiple checkpoint proteins including RAD9 to regulate ATR signaling.* Mol Cell Biol, 2008. **28**(24): p. 7345-53.

102. Olson, E., et al., *The Mre11 complex mediates the S-phase checkpoint through an interaction with replication protein A.* Mol Cell Biol, 2007. **27**(17): p. 6053-67.

103. Lee, J.H. and T.T. Paull, *Activation and regulation of ATM kinase activity in response to DNA double-strand breaks.* Oncogene, 2007. **26**(56): p. 7741-8.

104. Ishibashi, T., et al., *Two types of replication protein A 70 kDa subunit in rice, Oryza sativa: molecular cloning, characterization, and cellular & tissue distribution.* Gene, 2001. **272**(1-2): p. 335-43.

105. Ishibashi, T., S. Kimura, and K. Sakaguchi, *A Higher Plant Has Three Different Types of RPA Heterotrimeric Complex.* J Biochem (Tokyo), 2006. **139**(1): p. 99-104.

106. Ishibashi, T., et al., *Two types of replication protein A in seed plants.* Febs J, 2005. **272**(13): p. 3270-81.

107. Sakaguchi, K., et al., *The multi-replication protein A (RPA) system - a new perspective.* Febs J, 2009.

108. Millership, J.J. and G. Zhu, *Heterogeneous expression and functional analysis of two distinct replication protein A large subunits from Cryptosporidium parvum.* Int J Parasitol, 2002. **32**(12): p. 1477-85.

109. Keshav, K.F., C. Chen, and A. Dutta, *Rpa4, a homolog of the 34-kilodalton subunit of the replication protein A complex.* Mol.Cell.Biol., 1995. **15**: p. 3119-3128.

110. Haring, S.J. and M.S. Wold, *A naturally occurring human RPA subunit homologue that prevents DNA replication and cell cycle progression.* submitted.

111. Haring, S.J., T.D. Humphreys, and M.S. Wold, *A naturally occurring human RPA subunit homolog does not support DNA replication or cell-cycle progression.* Nucleic Acids Res, 2010. **38**(3): p. 846-58.

112. Higgs, H.N., *Formin proteins: a domain-based approach.* Trends Biochem Sci, 2005. **30**(6): p. 342-53.

113. Humphreys, T.D.a.W., Marc S, *Eukaryotic Replication Protein A*, in *Encyclopedia of Life Sciences*. January 2010, John Wiley & Sons, Ltd.

114. Poirot, O., E. O'Toole, and C. Notredame, *Tcoffee@igs: A web server for computing, evaluating and combining multiple sequence alignments.* Nucleic Acids Res, 2003. **31**(13): p. 3503-6.

115. Zhang, D., et al., *Human RPA (hSSB) interacts with EBNA1, the latent origin binding protein of Epstein-Barr virus.* Nucleic Acids Res., 1998. **26**: p. 631-637.

116. Henricksen, L.A., C.B. Umbricht, and M.S. Wold, *Recombinant replication protein A: Expression, complex formation, and functional characterization.* J Biol Chem 1994. **269**: p. 11121-11132.

117. Binz, S.K., et al., *Functional assays for replication protein A (RPA).* Methods Enzymol, 2006. **409**: p. 11-38.

118. Dickson, A.M., et al., *Essential functions of the 32-kDa subunit of yeast Replication Protein A.* Nucleic Acids Res, 2009. **submitted**.

119. Kim, C., B.F. Paulus, and M.S. Wold, *Interactions of Human Replication Protein A with Oligonucleotides.* Biochemistry, 1994. **33**: p. 14197-14206.

120. Brush, G.S., T.J. Kelly, and B. Stillman, *Identification of eukaryotic DNA replication proteins using simian virus 40 in vitro replication system.* Methods Enzymol., 1995. **262**: p. 522-548.

121. Gomes, X.V. and M.S. Wold, *Functional domains of the 70-kDa subunit of human Replication Protein A.* Biochemistry, 1996. **35**: p. 10558-10568.

122. Walther, A.P., et al., *Replication protein A interactions with DNA. 1. Functions of the DNA-binding and zinc-finger domains of the 70-kDa subunit.* Biochemistry, 1999. **38**: p. 3963-3973.

123. Kowalczykowski, S.C., et al., *Interactions of bacteriophage T4-coded gene 32 protein with nucleic acids. I. Characterization of the binding interactions.* J.Mol.Biol., 1981. **145**: p. 75-104.

124. Bujalowski, W. and T.M. Lohman, *Limited co-operativity in protein-nucleic acid interactions. A thermodynamic model for the interactions of Escherichia coli single strand binding protein with single-stranded nucleic acids in the "beaded?, (SSB)65 mode.* J.Mol.Biol., 1987. **195**: p. 897-907.

125. Kelly, T.J., *SV40 DNA replication.* J.Biol.Chem., 1988. **263**: p. 17889-17892.

126. Arunkumar, A.I., et al., *Insights into hRPA32 C-terminal domain--mediated assembly of the simian virus 40 replisome.* Nat Struct Mol Biol, 2005. **12**(4): p. 332-9.

127. Collins, K.L. and T.J. Kelly, *Effects of T antigen and replication protein A on the initiation of DNA synthesis by DNA polymerase a-primase.* Mol.Cell.Biol., 1991. **11**: p. 2108-2115.

128. Murakami, Y., T. Eki, and J. Hurwitz, *Studies on the initiation of simian virus 40 replication in vitro: RNA primer synthesis and its elongation.* Proc.Natl.Acad.Sci.USA, 1992. **89**: p. 952-956.

129. Braun, K.A., et al., *Role of protein-protein interactions in the function of Replication Protein A (RPA): RPA modulates the activity of DNA polymerase a by multiple mechanisms.* Biochemistry, 1997. **36**: p. 8443-8454.

130. Richard, D.J., et al., *Single-stranded DNA-binding protein hSSB1 is critical for genomic stability.* Nature, 2008.

131. Simmons, D.T., et al., *Assembly of the replication initiation complex on SV40 origin DNA.* Nucleic Acids Res, 2004. **32**(3): p. 1103-12.

132. Yuzhakov, A., et al., *Multiple competition reactions for RPA order the assembly of the DNA polymerase d holoenzyme.* EMBO J., 1999. **18**: p. 6189-6199.

133. Siegal, L.M. and K.J. Monty, *Determination of molecular weights and frictional ratios of proteins in impure systems by use of gel filtration and density gradient centrifugation. Application to crude preparations of sulfite and hydroxylamine reductases.* Biochim.Biophys.Acta, 1966. **112**: p. 346-362.

134. Harlow, E., et al., *Monoclonal antibodies specific for simian virus 40 tumor antigens.* J Virol, 1981. **39**: p. 861-869.

135. Sugiyama, T. and S.C. Kowalczykowski, *Rad52 protein associates with replication protein A (RPA)-single-stranded DNA to accelerate Rad51-mediated displacement of RPA and presynaptic complex formation.* J Biol Chem, 2002. **277**(35): p. 31663-72.

136. Eggler, A.L., R.B. Inman, and M.M. Cox, *The Rad51-dependent Pairing of Long DNA Substrates Is Stabilized by Replication Protein A.* J Biol Chem, 2002. **277**(42): p. 39280-39288.

137. Sugiyama, T. and N. Kantake, *Dynamic Regulatory Interactions of Rad51, Rad52, and Replication Protein-A in Recombination Intermediates.* J Mol Biol, 2009.

138. Mason, A.C., et al., *An alternative form of replication protein A prevents viral replication in vitro.* J Biol Chem, 2009. **284**: p. 5324-5331.

139. Reardon, J.T. and A. Sancar, *Purification and characterization of Escherichia coli and human nucleotide excision repair enzyme systems.* Methods Enzymol, 2006. **408**: p. 189-213.

140. Carreira, A., et al., *The BRC repeats of BRCA2 modulate the DNA-binding selectivity of RAD51.* Cell, 2009. **136**(6): p. 1032-43.

141. Pfaffl, M.W., *A new mathematical model for relative quantification in real-time RT-PCR.* Nucleic Acids Res, 2001. **29**(9): p. e45.

142. Huang, J.C., et al., *Human nucleotide excision nuclease removes thymine dimers from DNA by incising the 22nd phosphodiester bond 5' and the 6th phosphodiester bond 3' to the photodimer.* Proc Natl Acad Sci U S A, 1992. **89**(8): p. 3664-8.

143. Bugreev, D.V. and A.V. Mazin, *Ca2+ activates human homologous recombination protein Rad51 by modulating its ATPase activity.* Proc Natl Acad Sci U S A, 2004. **101**(27): p. 9988-93.

144. Potten, C.S. and M. Loeffler, *Stem cells: attributes, cycles, spirals, pitfalls and uncertainties. Lessons for and from the crypt.* Development, 1990. **110**(4): p. 1001-20.

145. Stauffer, M.E. and W.J. Chazin, *Physical interaction between replication protein A and Rad51 promotes exchange on single-stranded DNA.* J Biol Chem, 2004. **279**(24): p. 25638-45.

146. Sugiyama, T., E.M. Zaitseva, and S.C. Kowalczykowski, *A single-stranded DNA-binding protein is needed for efficient presynaptic complex formation by the Saccharomyces cerevisiae Rad51 protein.* J.Biol.Chem., 1997. **272**: p. 7940-7945.

147. Kemp, M.G., et al., *An alternative form of replication protein a expressed in normal human tissues supports DNA repair.* J Biol Chem, 2010. **285**(7): p. 4788-97.

148. Shuck, S.C., E.A. Short, and J.J. Turchi, *Eukaryotic nucleotide excision repair: from understanding mechanisms to influencing biology.* Cell Res, 2008. **18**(1): p. 64-72.

149. Mer, G., et al., *Structural basis for the recognition of DNA repair proteins UNG2, XPA, and RAD52 by replication factor RPA.* Cell, 2000. **103**(3): p. 449-456.

150. Sancar, A., et al., *Molecular mechanisms of mammalian DNA repair and the DNA damage checkpoints.* Annu Rev Biochem, 2004. **73**: p. 39-85.

151. Bullock, P.A., *The initiation of Simian Virus 40 DNA replication in vitro.* Crit.Rev.Biochem.Mol.Biol., 1997. **32**: p. 503-568.

152. Huang, S.G., et al., *Stoichiometry and mechanism of assembly of SV40 T antigen complexes with the viral origin of DNA replication and DNA polymerase a-primase.* Biochemistry, 1998. **37**: p. 15345-15352.

153. Simmons, D.T., P.W. Trowbridge, and R. Roy, *Topoisomerase I stimulates SV40 T antigen-mediated DNA replication and inhibits T antigen's ability to unwind DNA at nonorigin sites.* Virology, 1998. **242**: p. 435-443.

154. Nick McElhinny, S.A., et al., *Division of labor at the eukaryotic replication fork.* Mol Cell, 2008. **30**(2): p. 137-44.

155. Zlotkin, T., et al., *DNA polymerase epsilon may be dispensable for SV40- but not cellular-DNA replication.* EMBO J., 1996. **15**: p. 2298-2305.

156. Kunkel, T.A. and P.M. Burgers, *Dividing the workload at a eukaryotic replication fork.* Trends Cell Biol, 2008. **18**(11): p. 521-7.

157. Simmons, D.T., *SV40 large T antigen functions in DNA replication and transformation.* Adv Virus Res, 2000. **55**: p. 75-134.

158. Khopde, S. and D.T. Simmons, *Simian virus 40 DNA replication is dependent on an interaction between topoisomerase I and the C-terminal end of T antigen.* J Virol, 2008. **82**(3): p. 1136-45.

159. Khopde, S., R. Roy, and D.T. Simmons, *The binding of topoisomerase I to T antigen enhances the synthesis of RNA-DNA primers during simian virus 40 DNA replication.* Biochemistry, 2008. **47**(36): p. 9653-60.

160. Waga, S. and B. Stillman, *Anatomy of a DNA replication fork revealed by reconstitution of SV40 DNA replication in vitro.* Nature, 1994. **369**: p. 207-212.

161. Masuda, Y., et al., *Dynamics of human replication factors in the elongation phase of DNA replication.* Nucleic Acids Res, 2007. **35**(20): p. 6904-16.

162. Fazlieva, R., et al., *Proofreading exonuclease activity of human DNA polymerase delta and its effects on lesion-bypass DNA synthesis.* Nucleic Acids Res, 2009. **37**(9): p. 2854-66.

163. Hohn, K.T. and F. Grosse, *Processivity of the DNA polymerase alpha-primase complex from calf thymus.* Biochemistry, 1987. **26**: p. 2870-2878.

164. Mason, A.C., et al., *An alternative form of replication protein a prevents viral replication in vitro.* J Biol Chem, 2009. **284**(8): p. 5324-31.

165. Burgers, P.M.J., *Saccharomyces cerevisiae replication factor C. II. Formation and activity of complexes with the proliferating cell nuclear antigen and with DNA polymerases d and Œ.* J.Biol.Chem., 1991. **266**: p. 22698-22706.

166. Podust, V.N., et al., *Reconstitution of human DNA polymerase delta using recombinant baculoviruses: the p12 subunit potentiates DNA polymerizing activity of the four-subunit enzyme.* J Biol Chem, 2002. **277**(6): p. 3894-901.

167. Chilkova, O., et al., *The eukaryotic leading and lagging strand DNA polymerases are loaded onto primer-ends via separate mechanisms but have comparable processivity in the presence of PCNA.* Nucleic Acids Res, 2007. **35**(19): p. 6588-97.

168. Shivji, M.K., et al., *Nucleotide excision repair DNA synthesis by DNA polymerase epsilon in the presence of PCNA, RFC, and RPA.* Biochemistry, 1995. **34**(15): p. 5011-7.

169. Dornreiter, I., et al., *Interaction of DNA polymerase a-primase with cellular replication protein A and SV40 T antigen.* EMBO J., 1992. **11**: p. 769-776.

170. Maga, G., et al., *DNA elongation by the human DNA polymerase lambda polymerase and terminal transferase activities are differentially coordinated by proliferating cell nuclear antigen and replication protein A.* J Biol Chem, 2005. **280**(3): p. 1971-81.

171. Haracska, L., et al., *Stimulation of DNA synthesis activity of human DNA polymerase kappa by PCNA.* Mol Cell Biol, 2002. **22**(3): p. 784-91.

172. Saeki, H., et al., *Suppression of the DNA repair defects of BRCA2-deficient cells with heterologous protein fusions.* Proc Natl Acad Sci U S A, 2006. **103**(23): p. 8768-73.

173. Bochkarev, A. and E. Bochkareva, *From RPA to BRCA2: lessons from single-stranded DNA binding by the OB-fold.* Curr Opin Struct Biol, 2004. **14**(1): p. 36-42.

174. Casteel, D.E., et al., *A DNA polymerase-{alpha}{middle dot}primase cofactor with homology to replication protein A-32 regulates DNA replication in mammalian cells.* J Biol Chem, 2009. **284**(9): p. 5807-18.

175. Miyake, Y., et al., *RPA-like mammalian Ctc1-Stn1-Ten1 complex binds to single-stranded DNA and protects telomeres independently of the Pot1 pathway.* Mol Cell, 2009. **36**(2): p. 193-206.

176. Sun, J., et al., *Stn1-Ten1 is an Rpa2-Rpa3-like complex at telomeres.* Genes Dev, 2009. **23**(24): p. 2900-14.

177. Surovtseva, Y.V., et al., *Conserved telomere maintenance component 1 interacts with STN1 and maintains chromosome ends in higher eukaryotes.* Mol Cell, 2009. **36**(2): p. 207-18.

178. Li, Y., et al., *HSSB1 and hSSB2 form similar multiprotein complexes that participate in DNA damage response.* J Biol Chem, 2009. **284**(35): p. 23525-31.

179. Sakaguchi, K., et al., *The multi-replication protein A (RPA) system--a new perspective.* Febs J, 2009. **276**(4): p. 943-63.

180. Sukhodolets, K.E., et al., *The 32-kilodalton subunit of replication protein A interacts with menin, the product of the MEN1 tumor suppressor gene.* Mol Cell Biol, 2003. **23**(2): p. 493-509.

181. Nagelhus, T.A., et al., *A sequence in the N-terminal region of human uracil-DNA glycosylase with homology to XPA interacts with the C-terminal part of the 34-kDa subunit of replication protein A.* J Biol Chem, 1997. **272**(10): p. 6561-6.

182. Bouziane, M., et al., *Promoter structure and cell cycle dependent expression of the human methylpurine-DNA glycosylase gene.* Mutat Res, 2000. **461**(1): p. 15-29.

183. MacNeill, S.A., *Structure and function of the GINS complex, a key component of the eukaryotic replisome.* Biochem J, 2010. **425**(3): p. 489-500.

184. De Marco, V., et al., *Quaternary structure of the human Cdt1-Geminin complex regulates DNA replication licensing.* Proc Natl Acad Sci U S A, 2009. **106**(47): p. 19807-12.

185. Walter, J. and J. Newport, *Initiation of eukaryotic DNA replication: Origin unwinding and sequential chromatin association of Cdc45, RPA, and DNA polymerase a.* Mol.Cell, 2000. **5**: p. 617-627.

186. Byun, T.S., et al., *Functional uncoupling of MCM helicase and DNA polymerase activities activates the ATR-dependent checkpoint.* Genes Dev, 2005. **19**(9): p. 1040-52.

187. Cortez, D., *Unwind and slow down: checkpoint activation by helicase and polymerase uncoupling.* Genes Dev, 2005. **19**(9): p. 1007-12.

188. Tamura, T., et al., *Minichromosome maintenance-7 and geminin are reliable prognostic markers in patients with oral squamous cell carcinoma: immunohistochemical study.* J Oral Pathol Med, 2010.

189. Gonzalez, M.A., et al., *Control of DNA replication and its potential clinical exploitation.* Nat Rev Cancer, 2005. **5**(2): p. 135-41.

190. Arentson, E., et al., *Oncogenic potential of the DNA replication licensing protein CDT1.* Oncogene, 2002. **21**(8): p. 1150-8.

191. Menezo, Y., Jr., et al., *Expression profile of genes coding for DNA repair in human oocytes using pangenomic microarrays, with a special focus on ROS linked decays.* J Assist Reprod Genet, 2007. **24**(11): p. 513-20.

192. Anantha, R.W. and J.A. Borowiec, *Mitotic crisis: the unmasking of a novel role for RPA.* Cell Cycle, 2009. **8**(3): p. 357-61.

193. Anantha, R.W. and J.A. Borowiec, *Mitotic crisis: The unmasking of a novel role for RPA.* Cell Cycle, 2009. **8**(3).

194. DePamphilis, M.L., *DNA replication and human disease*. Cold Spring Harbor monograph series 46. 2006, Cold Spring Harbor, N.Y.: Cold Spring Harbor Laboratory Press. xvii, 814 p.

195. Basilion, J.P., et al., *Selective killing of cancer cells based on loss of heterozygosity and normal variation in the human genome: a new paradigm for anticancer drug therapy.* Mol Pharmacol, 1999. **56**(2): p. 359-69.

196. Andrews, B.J. and J.J. Turchi, *Development of a high-throughput screen for inhibitors of replication protein A and its role in nucleotide excision repair.* Mol Cancer Ther, 2004. **3**(4): p. 385-91.

197. Toll-Riera, M., et al., *Evolution of primate orphan proteins.* Biochem Soc Trans, 2009. **37**(Pt 4): p. 778-82.

198. Toll-Riera, M., et al., *Origin of primate orphan genes: a comparative genomics approach.* Mol Biol Evol, 2009. **26**(3): p. 603-12.

199. Schittek, B., et al., *Dermcidin: a novel human antibiotic peptide secreted by sweat glands.* Nat Immunol, 2001. **2**(12): p. 1133-7.

200. Digweed, M., et al., *Irreversible repression of DNA synthesis in Fanconi anemia cells is alleviated by the product of a novel cyclin-related gene.* Mol Cell Biol, 1995. **15**(1): p. 305-14.

201. Martinez-Garay, I., et al., *A new gene family (FAM9) of low-copy repeats in Xp22.3 expressed exclusively in testis: implications for recombinations in this region.* Genomics, 2002. **80**(3): p. 259-67.

202. Tay, S.K., J. Blythe, and L. Lipovich, *Global discovery of primate-specific genes in the human genome.* Proc Natl Acad Sci U S A, 2009. **106**(29): p. 12019-24.

203. Adams, J.M., et al., *Resource utilization among neonatologists in a university children's hospital.* Pediatrics, 1997. **99**(6): p. E2.

204. Potrzebowski, L., N. Vinckenbosch, and H. Kaessmann, *The emergence of new genes on the young therian X.* Trends Genet, 2010. **26**(1): p. 1-4.

205. Binz, S.K., et al., *The Phosphorylation Domain of the 32-kDa Subunit of Replication Protein A (RPA) Modulates RPA-DNA Interactions: Evidence for an intersubunit interaction.* J Biol Chem, 2003. **278**(37): p. 35584-91.

206. Block, W.D., Y. Yu, and S.P. Lees-Miller, *Phosphatidyl inositol 3-kinase-like serine/threonine protein kinases (PIKKs) are required for DNA damage-induced phosphorylation of the 32 kDa subunit of replication protein A at threonine 21.* Nucleic Acids Res, 2004. **32**(3): p. 997-1005.

207. Oakley, G.G., et al., *RPA phosphorylation in mitosis alters DNA binding and protein-protein interactions.* Biochemistry, 2003. **42**(11): p. 3255-3264.

208. Fang, F. and J.W. Newport, *Distinct roles of cdk2 and cdc2 in RP-A phosphorylation during the cell cycle.* J.Cell Sci., 1993. **106**: p. 983-994.

209. Zernik-Kobak, M., et al., *Sites of UV-induced phosphorylation of the p34 subunit of Replication Protein A from HeLa cells.* J Biol Chem 1997. **272**: p. 23896-23904.

210. Dutta, A. and B. Stillman, *cdc2 Family kinases phosphorylate a human cell DNA replication factor, RPA, and activate DNA replication.* EMBO J., 1992. **11**: p. 2189-2199.

211. Din, S., et al., *Cell-cycle-regulated phosphorylation of DNA replication factor A from human and yeast cells.* Genes & Development, 1990. **4**: p. 968-977.

212. Sakasai, R., et al., *Differential involvement of phosphatidylinositol 3-kinase-related protein kinases in hyperphosphorylation of replication protein A2 in response to replication-mediated DNA double-strand breaks.* Genes Cells, 2006. **11**(3): p. 237-46.

213. Patrick, S.M., et al., *DNA Damage Induced Hyperphosphorylation of Replication Protein A. 2. Characterization of DNA Binding Activity, Protein Interactions, and Activity in DNA Replication and Repair.* Biochemistry, 2005. **44**(23): p. 8438-8448.

214. Nuss, J.E., et al., *DNA damage induced hyperphosphorylation of replication protein a. 1. Identification of novel sites of phosphorylation in response to DNA damage.* Biochemistry, 2005. **44**(23): p. 8428-37.

215. Liu, Y., et al., *Modulation of replication protein A function by its hyperphosphorylation-induced conformational change involving DNA binding domain B.* J Biol Chem, 2005. **280**(38): p. 32775-83.

216. Chen, B., Cao, H., Yan, P., Mayer, M.U., Squier, T.C., *Identification of an orthogonal peptide binding motif for biarsenical multiuse affinity probes.* Bioconjug Chem, 2007. **18**(4): p. 1259-1265.

217. Anantha, R.W., Vassin, V.M., Borowiec, J.A., *Sequential and synergistic modification of human RPA stimulates chromosomal DNA repair.* J Biol Chem, 2007. **282**(49): p. 35910-35923.

218. Bastin-Shanower, S.A. and S.J. Brill, *Functional analysis of the four DNA binding domains of replication protein A - The role of RPA2 in ssDNA binding.* J Biol Chem, 2001(276): p. 36446-36453.

219. Bochkareva, E., et al., *Structure of the major single-stranded DNA-binding domain of replication protein A suggests a dynamic mechanism for DNA binding.* EMBO J, 2001. **20**(3): p. 612-618.